8. SITE 592: LORD HOWE RISE, 36°S[1]

Shipboard Scientific Party[2]

HOLE 592

Date occupied: 25 December 1982

Date departed: 27 December 1982

Time on hole: 46.5 hr.

Position: 36°28.40′S; 165°26.53′E

Water depth (sea level; corrected m, echo-sounding): 1088 m

Water depth (rig floor; corrected m, echo-sounding): 1098 m

Bottom felt (m, drill pipe): 1099

Penetration (m): 388.5

Number of cores: 41

Total length of cored section (m): 388.5

Total core recovered (m): 340.12

Core recovery (%): 87.5

Oldest sediment cored:
Depth sub-bottom (m): 388.5
Nature: Nannofossil chalk
Age: Middle late Eocene (Kaiatan Stage of New Zealand)
Measured velocity (km/s): 1.807 km/s at 383 m
Shear strength: 350 g/cm^2 at 353 m; greater values below

Basement: Not reached

Principal results: Site 592, drilled on the southern Lord Howe Rise (36°28.40′S; 164°26.92′E) in relatively shallow water (1088 m from sea level), consists of one hole cored continuously with the hydraulic piston cored (HPC) from 0 to 234.9 m sub-bottom and then with the extended core barrel (XCB) from 234.9 to 388.5 m. The section recovered consists of a single lithostratigraphic unit that varies from foraminifer-bearing nannofossil ooze (chalk) to nannofossil ooze (chalk). The age of the section is from middle late Eocene (42 m.y.) to Quaternary. The bottom of the hole consists of 83.5 m of Paleogene ooze and chalk ranging in age from the late Eocene to the early Oligocene (35 m.y. ago). The regional unconformity of the southwest Pacific separates the lower Oligocene sediments from immediately overlying middle lower Miocene sediments 18.5 m.y. old. The section is represented by a section of high-quality cores with almost complete recovery from the middle Miocene to Quaternary using the HPC, and a less complete but still excellent section recovered at greater depths using the extended core barrel. A paleomagnetic polarity stratigraphy has been identified down to the late Gauss Chron (2.5 m.y. ago).

The section has been divided into five subunits: Subunit IA represents a veneer (0.0–0.3 m) of pale orange to pinkish gray foraminifer-bearing nannofossil ooze within the oxidized zone near the seafloor. Subunits IB to IE are differentiated by degree of lithification. There is good foraminifer preservation in the Neogene and Oligocene, whereas the nannofossils are only well preserved in the late Neogene and Oligocene. Radiolarians are present in small amounts only in the Eocene. The biostratigraphic sequences seem to be complete except for that part missing in the regional unconformity. Sedimentation rates range from lowest values (7 m/m.y.) in the late Eocene to highest value (92.5 m/m.y.) in the late early Pliocene. In general, sedimentation rates are much lower at Site 592 than in sites both to the north and south.

Of particular interest at this site is a fine complete boundary section between the Eocene and the Oligocene in Cores 592-36 and 592-37. The hiatus present in all other South Pacific sites except Site 277 in the subantarctic area south of New Zealand is not found at Site 592. A distinct lithologic change occurs near the level of extinction of *Globigerinatheka index*, which is the foraminifer marker for the boundary in south temperate latitudes. The late Eocene is represented by nannofossil chalks containing siliceous microfossils such as radiolarians and sponge spicules, the Oligocene by surprisingly soft nannofossil ooze lacking biosiliceous materials. The section provides good opportunities for high-resolution stratigraphy across the boundary.

Volcanic ash layers or altered laminae occur in the Quaternary, early late Miocene (10 m.y.), and through the Paleogene.

Good benthic foraminifer and ostracode assemblages occur throughout much of the sequence and exhibit changes at a number of levels associated with paleoceanographic events.

BACKGROUND AND OBJECTIVES

Site 592 (SW-2) is located near the southern end of Lord Howe Rise, about 60 km north of Site 207 (Fig. 1), and was selected from the *Glomar Challenger* Leg 21 profile recorded at 1900 hr., 15 December 1971.

Site 207 was located in an area of thin (360 m) sediment cover overlying a basement high composed of rhyolite. At Site 207, the upper 142 m of sediment cover consists of a thin middle Miocene to Quaternary sequence of foraminifer–nannofossil ooze, which is unconformably underlain by siliceous calcareous and calcareous oozes of Eocene age. The Neogene sediments clearly were winnowed at Site 207, judging by the low sedimentation rates and relatively high proportion of foraminifers. The basement high upon which Site 207 is located had focused bottom currents during the Cenozoic.

[1] Kennett, J. P., von der Borch, C. C., et al., *Init. Repts. DSDP*, 90: Washington (U.S. Govt. Printing Office).

[2] James P. Kennett (Co-Chief Scientist), Graduate School of Oceanography, University of Rhode Island, Narragansett, RI 02882; Christopher C. von der Borch (Co-Chief Scientist), School of Earth Sciences, Flinders University of South Australia, Bedford Park, South Australia 5042; Paul A. Baker, Department of Geology, Duke University, Durham, NC 27708; Charles E. Barton, Graduate School of Oceanography, University of Rhode Island, Narragansett, RI 02882 (present address: Bureau of Mineral Resources, Geology, and Geophysics, P.O. Box 378, Canberra, A.C.T., Australia); Anne Boersma, Microclimates, Inc., 404 RR1, Stony Point, NY 10980; Jean-Pierre Caulet, Laboratoire de Géologie, Muséum National d'Histoire Naturelle, 43 Rue Buffon, 75005, Paris, France; Walter C. Dudley, Jr., Natural Sciences Division, College of Arts and Sciences, University of Hawaii at Hilo, Hilo, Hawaii 96720; James V. Gardner, Pacific-Arctic Branch of Marine Geology, U.S. Geological Survey, 345 Middlefield Rd., Menlo Park, CA 94025; D. Graham Jenkins, Department of Earth Sciences, Open University, Walton Hall, Milton Keynes, MK7 6AA, Buckinghamshire, United Kingdom; William H. Lohman, Marathon Oil Co., Denver Research Center, P.O. Box 269, Littleton, CO 80160; Erlend Martini, Geologisch-Paläontologisches Institut, Johann-Wolfgang-Goethe Universität, Senckenberg-Anlage 32-34, D-6000 Frankfurt am Main, Federal Republic of Germany; Russell B. Merrill, Deep Sea Drilling Project A031, Scripps Institution of Oceanography, La Jolla, CA 92093 (present address: Ocean Drilling Project, Texas A&M University, College Station, TX 77843-3469); Roger Morin, Department of Earth and Planetary Sciences, Massachusetts Institute of Technology, Cambridge, MA 02139 (present address: U.S. Geological Survey, Denver Federal Center, Denver, CO 80225); Campbell S. Nelson, Department of Earth Sciences, University of Waikato, Private Bag, Hamilton, New Zealand; Christian Robert, Laboratoire de Géologie Marine, Centre Universitaire de Luminy, Case 901, 13288 Marseille Cedex 09, France; M. S. Srinivasan, Department of Geology, Banaras Hindu University, Varanasi 221 005, India; Rüdiger Stein, Geologisch-Paläontologisches Institut, Universität Kiel, 2300 Kiel, Federal Republic of Germany (present address: Institute of Petroleum and Organic Geochemistry (ICH-5), Kernforschungslage Jülich GmbH, P.O. Box 1913, 5170 Jülich, Federal Republic of Germany); Akira Takeuchi, Department of Earth Sciences, Faculty of Science, Toyama University, Gohuku 3190, Toyama 930, Japan.

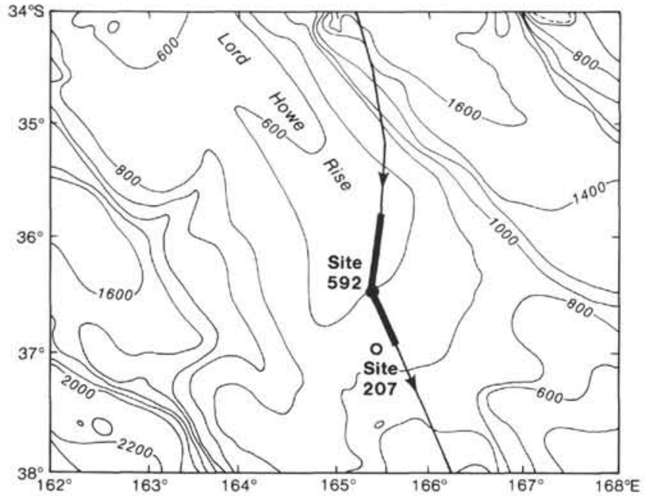

Figure 1. Regional bathymetry (fathoms) around Site 592, after Mammerickx et al., 1974. *Glomar Challenger* Leg 90 track shown; heavy portion locates water gun seismic profile illustrated in Fig. 2.

Since the primary objectives of Leg 90 were related to paleoceanographic history, rather than to basement problems, a site was chosen in an area of thick (600 m) sediment cover close to Site 207. The seismic profile (Fig. 2) shows that this location is represented by relatively transparent sediments that probably are not complicated by bottom current activity.

Site 592 was proposed by the JOIDES Paleoenvironmental Panel as a secondary objective because it lies in the same cool-temperate water mass as Leg 29, Site 284. Precruise calculations indicated that there would be time for only one site located in the cool-temperate water mass. Since Site 284 was in thicker Neogene sediments, it was designated the primary site (SW-2). However, the discovery during Leg 90 of spectacularly high rates of calcareous biogenic sedimentation during the Pliocene in the area of Sites 590 and 591 (about 31°S) led to much interest in determining if these are of local nature or if they extend further south to the area of Site 592. We had already determined that such high sedimentation rates do not seem to occur in the northern Lord Howe Rise area (Site 588).

A total of only two days could be budgeted toward the drilling of Site 592. Nevertheless, we believed that if we managed to determine sedimentation rates for the Pliocene Epoch only it would be a successful use of the two days assigned for this experiment. A total of two days on the site would allow time for only one HPC hole and perhaps a short sequence using the extended core barrel.

The objectives for drilling Site 592 were much the same as for the other sites drilled near the crest of Lord Howe Rise. In particular, a sequence was needed for the following studies:

1. To compare and contrast rates of calcareous biogenic sedimentation between other Lord Howe Rise sites and Site 592, in an area with much less evidence of winnowing than at Site 207.
2. To provide another late Neogene sequence intermediate in latitude between Sites 590 and 593. This should help in cross-latitudinal correlation.
3. To provide another Neogene sequence of shallower-water benthic foraminifers for studies of possible north-south biogeographic differences in assemblages at similar water depths. There are few data available to show whether faunas within the same intermediate water masses exhibit changes with changing latitude. The general assumption is that little biogeographic change does occur within the same deeper-water masses in the oceans.
4. To provide a longer Neogene and perhaps Paleogene sedimentary record than was available at Site 207.

OPERATIONS

Site 591 to Site 592

A combination of good average speed between sites, very few mechanical breakdowns, little time lost waiting on weather, and no drilling problems all combined at this point in the voyage to indicate that operations were well ahead of schedule. Continued use of the XCB and continuation of the excellent vessel speed was expected to further improve the schedule. Given all this, enough

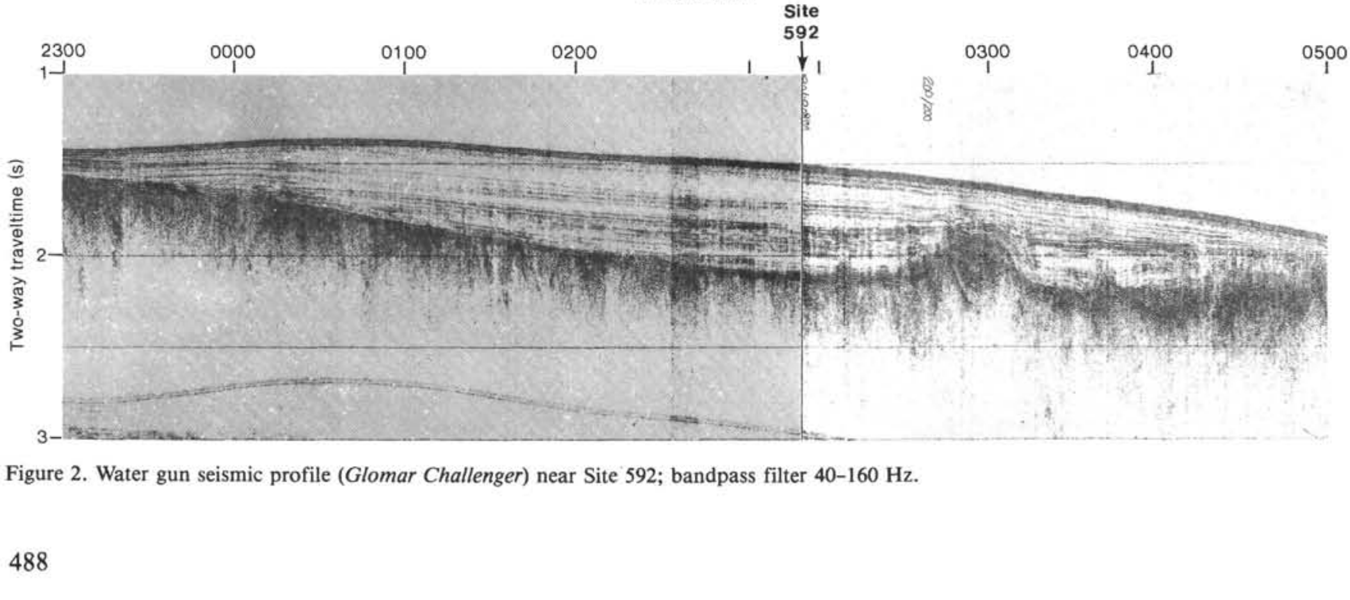

Figure 2. Water gun seismic profile (*Glomar Challenger*) near Site 592; bandpass filter 40–160 Hz.

extra time was anticipated to allow coring contingency Site SW-3.

The vessel made its way south to the chosen site coordinates without incident. The beacon (16.0 kHz, D.L.) was dropped on the first pass at 1416 hr., 25 December 1982.

Site 592 (SW-3): Southern Lord Howe Rise

The operating plan for the site was to obtain a good piston-cored sequence through the Neogene sediments to refusal and then to deploy the XCB, in order to test it under modified operational practices and, if possible, to core into stiffer sediments as far as the Oligocene/Eocene boundary. The time on site was to be limited to 48 hr.

Although weather conditions were not good, the vessel was able to be positioned with her bow into the prevailing wind and swell so that positioning in automatic with tolerable roll and pitch was relatively easy.

A combination XCB/variable length (VL) HPC bottom-hole assembly was made up as before and run to the height chosen for the mud line core attempt. Hole 592 was spudded at 2035 hr. with a VLHPC mud line core (Table 1), which established the water depth to be 1099.7 m by drill pipe measurement.

A rig floor failure of a small threaded connection caused the loss of the lower portion of the Kuster orientation tool pressure case just prior to running in for the second piston core. This was the only weather-related mishap at the site. Fortunately the plan had been to deploy the Kuster tool starting with the third core so the tool itself was not installed at that time.

Piston coring with the 9.5-m VLHPC using two shear pins continued smoothly despite blustery weather. Full stroke was achieved on all cores. Core quality was not up to normal VLHPC standards, mainly because of the vessel's significant heave. At the 25th VLHPC core, an overpull of 25,000 lb. was required while inching the tool free. Piston coring was then terminated and the sinker bars were changed in preparation for XCB coring. The first XCB was deployed without problems and recovered a good core. The second XCB was initially stuck at the top of the BHA, and then jarred loose.

It was clear that the XCB latch was still causing problems, so the remainder of the hole was cored by running the XCB in on the wire line. One other XCB barrel, Core 592-36, did become stuck. It was dislodged by hammering with the deplugger barrel on the wire line. Core 592-36 suffered some disturbance as a by-product of the unjamming procedure.

The hole was cored to its full scientific objective plus two or three extra cores and was terminated to allow the pipe to be pulled and the ship to get under way within the original 48-hr. time limit.

Table 1. Coring summary, Site 592.

Core No.	Date (Dec. 1982)	Time	Depth from drill floor (m) Top Bottom	Depth below seafloor (m) Top Bottom	Length cored (m)	Length recovered (m)	Percentage recovered
1	25	2105	1099.7-1104.2	0.0-4.5	4.5	4.45	98.8
2	25	2230	1104.2-1113.8	4.5-14.1	9.6	9.52	99.1
3	25	2330	1113.8-1123.4	14.1-23.7	9.6	9.41	98.0
4	26	0025	1123.4-1133.0	23.7-33.3	9.6	9.43	98.2
5	26	0100	1133.0-1142.6	33.3-42.9	9.6	9.54	99.3
6	26	0145	1142.6-1152.2	42.9-52.5	9.6	9.31	97.0
7	26	0225	1152.2-1161.8	52.5-62.1	9.6	9.32	97.0
8	26	0310	1161.8-1171.4	62.1-71.7	9.6	9.01	93.8
9	26	0355	1171.4-1181.0	71.7-81.3	9.6	9.30	96.9
10	26	0450	1181.0-1190.6	81.3-90.9	9.6	9.50	98.9
11	26	0535	1190.6-1200.2	90.9-100.5	9.6	8.02	83.3
12	26	0610	1200.2-1209.8	100.5-110.1	9.6	9.71	100+
13	26	0700	1209.8-1219.4	110.1-119.7	9.6	8.59	89.4
14	26	0745	1219.4-1229.0	119.7-129.3	9.6	9.70	100+
15	26	0815	1229.0-1238.6	129.3-138.9	9.6	9.18	95.6
16	26	0900	1238.6-1248.2	138.9-148.5	9.6	9.69	100+
17	26	0930	1248.2-1257.8	148.5-158.1	9.6	8.48	88.3
18	26	1015	1257.8-1267.4	158.1-167.7	9.6	9.66	100+
19	26	1100	1267.4-1277.0	167.7-177.3	9.6	8.76	91.2
20	26	1150	1277.0-1286.6	177.3-186.9	9.6	9.68	100+
21	26	1235	1286.6-1296.2	186.9-196.5	9.6	9.60	100+
22	26	1330	1296.2-1305.8	196.5-206.1	9.6	9.42	98.1
23	26	1420	1305.8-1315.4	206.1-215.7	9.6	9.69	100+
24	26	1520	1315.4-1328.0	215.7-225.3	9.6	9.08	94.5
25	26	1615	1328.0-1334.6	225.3-234.9	9.6	9.77	100+
26	26	1735	1334.6-1344.2	234.9-244.5	9.6	9.50	99.9
27	26	1845	1344.2-1353.8	244.5-254.1	9.6	0.0	0
28	26	2145	1353.8-1363.4	254.1-263.7	9.6	9.58	99.8
29	26	2240	1363.4-1373.0	263.7-273.3	9.6	8.67	90.3
30	26	2340	1373.0-1382.6	273.3-282.9	9.6	8.44	87.9
31	27	0010	1382.6-1392.2	282.9-292.5	9.6	7.94	82.7
32	27	0100	1392.2-1401.8	292.5-302.1	9.6	8.03	83.6
33	27	0140	1401.8-1411.4	302.1-311.7	9.6	7.05	74.4
34	27	0205	1411.4-1421.0	311.7-321.3	9.6	6.31	65.7
35	27	0300	1421.0-1430.6	321.3-330.9	9.6	8.13	84.6
36	27	0510	1430.6-1440.2	330.9-340.5	9.6	4.78	79.6
37	27	0600	1440.2-1449.8	340.5-350.1	9.6	5.44	56.6
38	27	0645	1449.8-1459.4	350.1-359.7	9.6	9.05	94.2
39	27	0730	1459.4-1469.0	359.7-369.3	9.6	5.52	57.5
40	27	0830	1469.0-1478.6	369.3-378.9	9.6	6.83	71.1
41	27	0910	1478.6-1488.2	378.9-388.5	9.6	9.03	94.0
					388.5	340.12	87.5

LITHOSTRATIGRAPHY

Site 592 consists of one hole cored continuously with the HPC from 0–234.9 m sub-bottom and then with the XCB from 234.9–388.5 m sub-bottom. Although the hole was cored continuously, recovery is not complete and decreases below 240 m sub-bottom in the rotary-cored sequence. Cores 592-29 to 592-33 are moderately disturbed by drilling and are broken into separated biscuits. The sequence recovered consists of one lithostratigraphic unit that varies from foraminifer-bearing nannofossil ooze (chalk) to nannofossil ooze (chalk). The unit is divided into five subunits (Table 2). Subunit IA (0–0.3 m) is distinguished from Subunit IB by its very pale orange to pinkish gray color. This uppermost part of the site, which corresponds to Subunit IA in most other sites drilled during Leg 90, is the oxidized zone of the sediment section. The upper part of Subunit IB, between 0.3 and 33.3 m, is marked by alternating layers ranging in color from pale olive to white and very light gray

Table 2. Lithostratigraphy at Site 592.

Lithological subunits	Cores	Sub-bottom depth (m)	Description	Age
IA	1	0–0.3	Very pale orange to pinkish gray foraminifer-bearing nannofossil ooze	late Quaternary
IB	1–29	0.3–273.3	White to light gray foraminifer-bearing nannofossil ooze to nannofossil ooze	late Quaternary to early Miocene
IC	30–33	273.3–305.8	White to very light greenish gray foraminifer-bearing nannofossil chalk to nannofossil chalk	early Miocene
ID	33–37	305.8–350.1	White to very light gray nannofossil ooze	early Oligocene to late Eocene
IE	38–41	350.1–388.5	White to very light gray nannofossil chalk	late Eocene

(Cores 592-1 to 592-4; Pleistocene to upper Pliocene). White to very light gray dominate from 33.3 to 302.1 m. Subunit IC (273.3–305.8 m) is a chalk. The sediment from 305.8–350.1 m sub-bottom (Subunit ID), just below the early Miocene/early Oligocene unconformity, is an ooze. The white to very light colored sediment sequence contains numerous pale green laminae (Fig. 3). The lower part of Subunit ID is marked by a chert nodule surrounded by a 15-cm-thick layer of lithified limestone. The transition zone between Subunits ID and IE, from an ooze to a firm recrystallized chalk, occurs between 350 and 369 m. Light gray to medium gray blebs, pockets, and laminae are rare to occasional in Cores 592-1 to 592-16 and 592-22 to 592-37, and moderate in 592-17 to 592-21 and 592-38 to 592-41.

Calcareous nannofossils are the dominant component (about 75%) of the entire sediment sequence. Foraminifers vary from less than 5 to 25% (Fig. 4). Beds containing numerous 1–4-cm-sized molluscan (*Ostrea*) fragments occur in Section 592-34-3. Chert nodules are present in Cores 592-36-3 and 592-41-5. Noncarbonate components occur only in trace abundances (Fig. 4): volcanic glass and pyrite occur throughout the entire sequence, whereas quartz, feldspar, and heavy minerals are found only occasionally. Biogenic opal is absent except at the top of Core 592-1 and in the Eocene section (Cores 592-37 to 592-41), where radiolarians and sponge spicules occur in trace amounts (Fig. 4).

Some pale olive intervals in the upper part and some grayish green to pale green pockets in the lower part of the sediment sequence are characterized by more common volcanic glass (Fig. 4). The pale olive intervals in the Quaternary–upper Pliocene sediments and the pale green laminae in the lower Oligocene–upper Eocene sed-

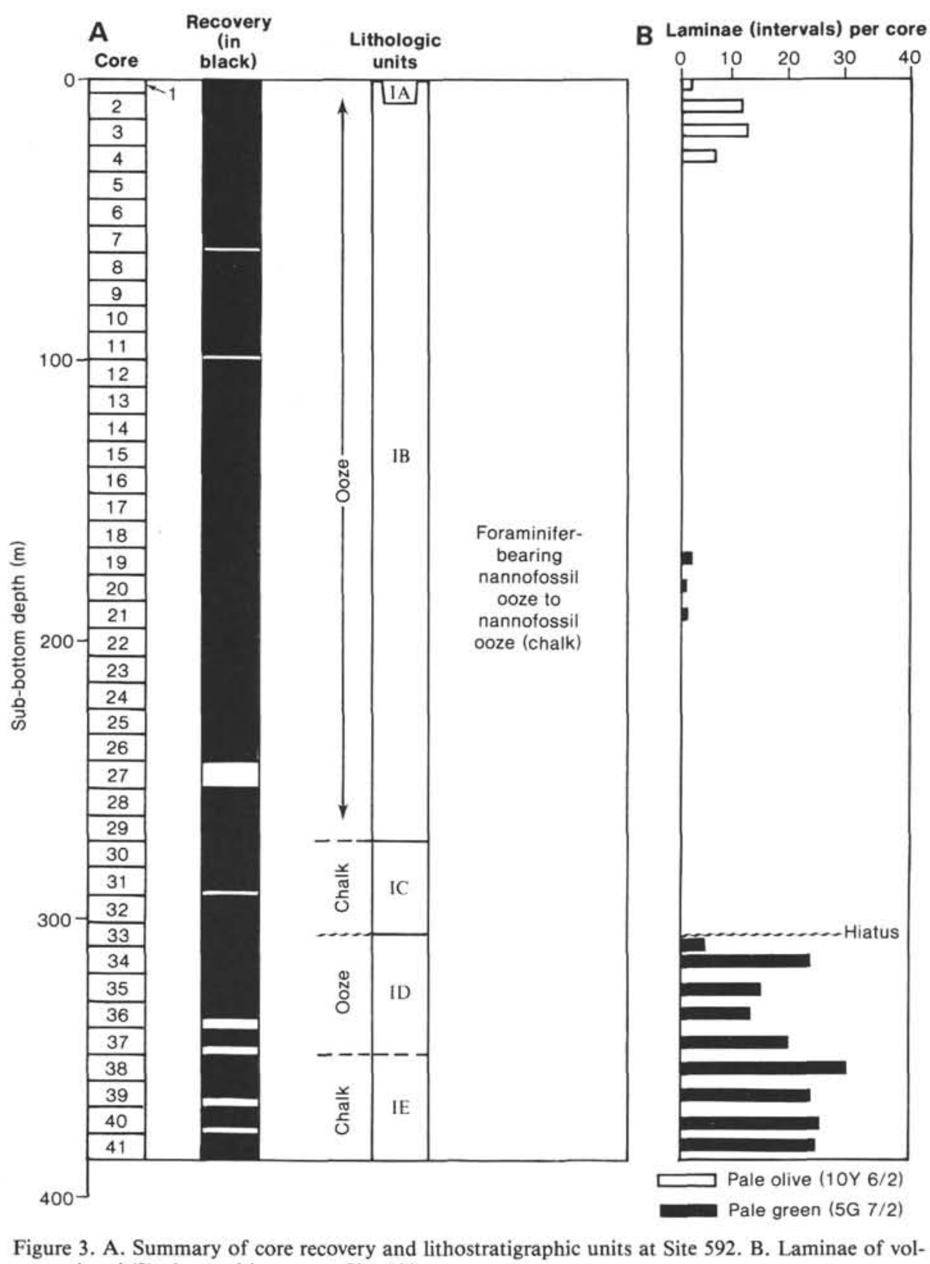

Figure 3. A. Summary of core recovery and lithostratigraphic units at Site 592. B. Laminae of volcanic ash(?) observed in core at Site 592.

iments (Fig. 3) may represent periods of increased volcanic ash supply.

Bioturbation is rare in the upper part of the sequence (Cores 592-1 to 592-30). Burrows are occasionally observed as pale olive to yellowish gray mottles and blebs. Cores 592-31 to 592-41 are moderately bioturbated with Zoophycos, Planolites and Chrondrites all evident.

PHYSICAL PROPERTIES

Site 592 provided 388 m of sediment recovery. The standard suite of gravimetric, acoustic velocity, and shear strength measurements was performed at prescribed intervals and the continuous scanning GRAPE apparatus was employed on selected cores (see Introduction for details of specific methods). A full discussion of the physical properties results for Site 592 is presented by Morin (this volume).

The GRAPE porosity results (points) are plotted versus depth in Figure 5A. These data were derived directly from the GRAPE wet-bulk densities by assuming a grain density of 2.691 g/cm^3. A mean porosity is determined across each meter of depth and these averages are plotted as the solid line. Porosity does not show the usual signs of gradual decline with increasing lithostatic load, but remains relatively constant over several hundred meters (90–290 m).

The results of the compressional wave velocity and shear strength measurements performed on split cores, parallel to bedding, are shown in Figure 5B and C, respectively. Both graphs show a coincident increase in each property at a depth of approximately 260 m, followed by an equally sharp decline at 290 m. This spike corresponds to the onset of chalk at the former depth, followed by a reintroduction of calcareous ooze. The ooze layer quickly undergoes a transition to chalk again at a depth of approximately 320 m. This behavior is reflected in increases in the matrix modulus properties at the appropriate depth. Below 355 m, the sediment shear strength is beyond the range of the miniature vane shear apparatus.

The GRAPE porosity data are combined with the compressional velocity results in order to develop a relationship between porosity and velocity (Fig. 5D). A similar analysis yields a relationship between porosity and shear strength (Fig. 5E). The shear strength is seen to rise sharply as a declining porosity approaches 52%. The velocity data are also correlated with the GRAPE wet-bulk density profile, and a record of acoustic impedance versus depth is established (Fig. 5F). Fluctuating values of impedance at a depth of about 300 m correspond to the ooze-to-chalk transitions observed at this level.

SEISMIC STRATIGRAPHY

Figure 6A illustrates a portion of the shipboard water gun seismic profile collected during the approach to Site 592. Figure 6B is a line-drawing of the profile. Three acoustic units have been identified (A, B, and C) and these are compared in part with the lithology of the site (lithostratigraphic Units IA–IE).

Acoustic Unit A incorporates a relatively transparent zone with numerous laterally continuous low-amplitude reflectors. In the region of Site 592 these reflectors are parallel to the sediment/water interface, suggesting that the area is not undergoing erosion. About 90 km to the north, however, upper reflectors of Unit A have been truncated by erosion over a broad basement high.

Acoustic Unit B marks a zone of parallel reflectors with somewhat higher amplitude. These reflectors are parallel to those of Unit A.

Acoustic Unit C incorporates a well-defined series of relatively high amplitude parallel reflectors. Subtle truncation of reflectors immediately below the top of Unit C by base of Unit B, visible immediately north of Site 592 (Fig. 6B), suggests minor erosional truncation of strata at the upper limit of Unit C. In addition, all reflectors of Unit C can be seen to onlap the strong basement reflector when traced to the north.

Acoustic basement in the region is very smooth.

Lithostratigraphic Units IA, IB, IC and ID comprise a visually monotonous sequence of foraminifer-bearing nannofossil ooze to nannofossil ooze, ranging in age from Quaternary to the late Eocene. Within this section, gradational boundaries between ooze and chalk occur at about 272 and 345 m sub-bottom. The upper chalk horizon actually reverts to ooze at 306 m sub-bottom before becoming chalky again between 345 m and the bottom of the hole. A distinct hiatus was shown to exist at 306 m sub-bottom, separating the late early Miocene from the early Oligocene. Below this a continuous sequence was cored across the Oligocene/Eocene boundary.

In matching the lithology with the seismic profile at Site 592 we tentatively assume an interval velocity of 1700 m/s, averaged from shipboard velocimeter measurements. Comparisons suggest that the boundary between acoustic Units A and B does not coincide with the onset of chalkiness, as hypothesized at earlier sites. Rather, it appears due to a subtle and undetermined change in acoustic impedance which is not obvious from the lithology or physical properties. The strong reflector marking the upper limit of Unit C may be correlated with the top of lithostratigraphic Unit IC, at which level chalk is first observed. This level also coincides with the low-angle truncation surface already described.

Lithostratigraphic Unit ID, an ooze which is sandwiched between two chalk horizons (IC and IE), appears to correlate with a slightly more transparent zone within acoustic Unit C, and the top of lithostratigraphic Unit IE appears to match a strong reflector within acoustic Unit C.

BIOSTRATIGRAPHY

Site 592 was drilled on the southern end of the Lord Howe Rise, at latitude 36°28.40′S, longitude 165°26.35′E in a water depth of 1088 m below sea level; this is just north of DSDP Site 207, drilled on Leg 21. The nannofossil preservation and planktonic foraminiferal zones of Site 592 are shown in Figure 7.

The preservation and abundance of planktonic foraminifers were good for the Neogene and Oligocene but deteriorated in the Eocene; the benthic foraminifers are well preserved down to the upper Miocene, then deteriorate in the lower Miocene, improve in the Oligocene, and again deteriorated in the upper Eocene. Nannoplankton preservation is good for the Quaternary and Plio-

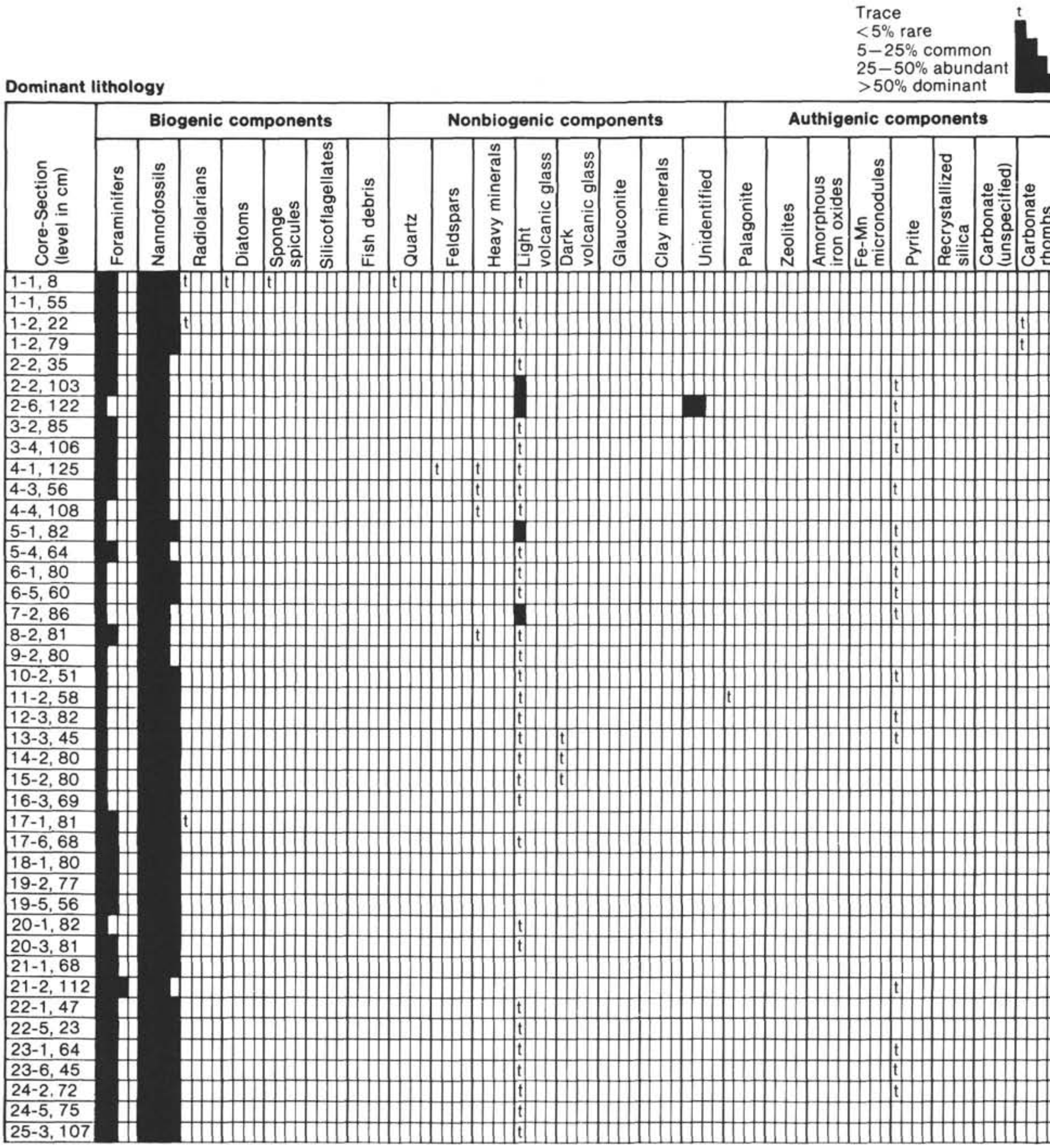

Figure 4. Smear slide summary, Site 592.

cene but deteriorates in the Miocene, and is better below the unconformity in the Oligocene, but again deteriorates in the Eocene.

Radiolarians were found to be present only in the Paleogene deposits, whereas diatoms and silicoflagellates were missing throughout. Shell fragments were noted in Core 592-34, and a more complete specimen from Section 4 was identified as *Ostrea* sp.

In terms of planktonic foraminiferal zones, the unconformity at Site 592 occurs between the lower part of the *Globigerinoides trilobus* Zone and the upper part of the *Globigerina angiporoides* Zone (i.e., between 18–19 and 31–32± m.y. ago). In terms of nannoplankton zones, the unconformity occurs between the NN2 and NP22 Zones (i.e., between 19.5 and 35 m.y. ago).

The major boundary of interest at Site 592 is the Eocene/Oligocene boundary and, following the practice in New Zealand, this was placed at the extinction of *Globigerinatheka index*, which was noted in Section 592-36-3 between 90 and 64 cm. According to the nannoplankton, the boundary at the extinction of *Discoaster saipanensis* is in Core 592-37-2, between 5–6 and 33–34 cm. A similar sequence of extinctions for the two taxa was recorded at DSDP Site 277, drilled south of New Zealand.

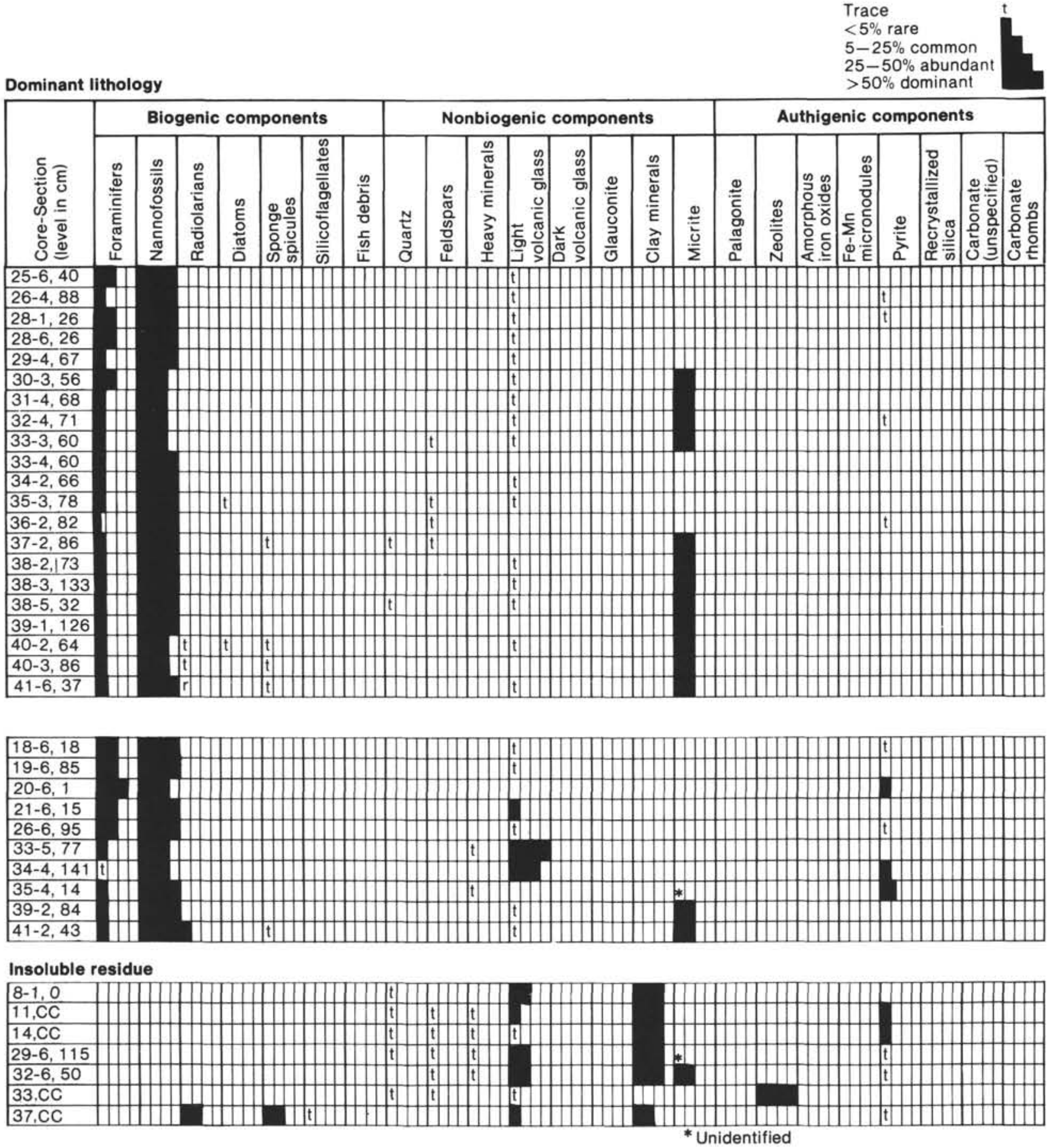

Figure 4. (Continued).

Planktonic Foraminifers

Zones

The following zones were identified at Site 592; the zonal boundary markers are shown below:

Globorotalia truncatulinoides Zone
L. A. *G. tosaensis*
Globorotalia truncatulinoides–G. tosaensis Zone
I. A. *G. truncatulinoides*
Globorotalia inflata Zone
I. A. *G. inflata*
Globorotalia crassaformis Zone
I. A. *G. crassaformis*
Globorotalia puncticulata Zone
I. A. *G. puncticulata*
Globorotalia sphericomiozea Zone
L. A. *G. conomiozea*
Globorotalia conomiozea Zone
I. A. *G. conomiozea*
Globorotalia miotumida Zone
L. A. *N. continuosa*
Neogloboquadrina continuosa Zone
L. A. *G. mayeri*

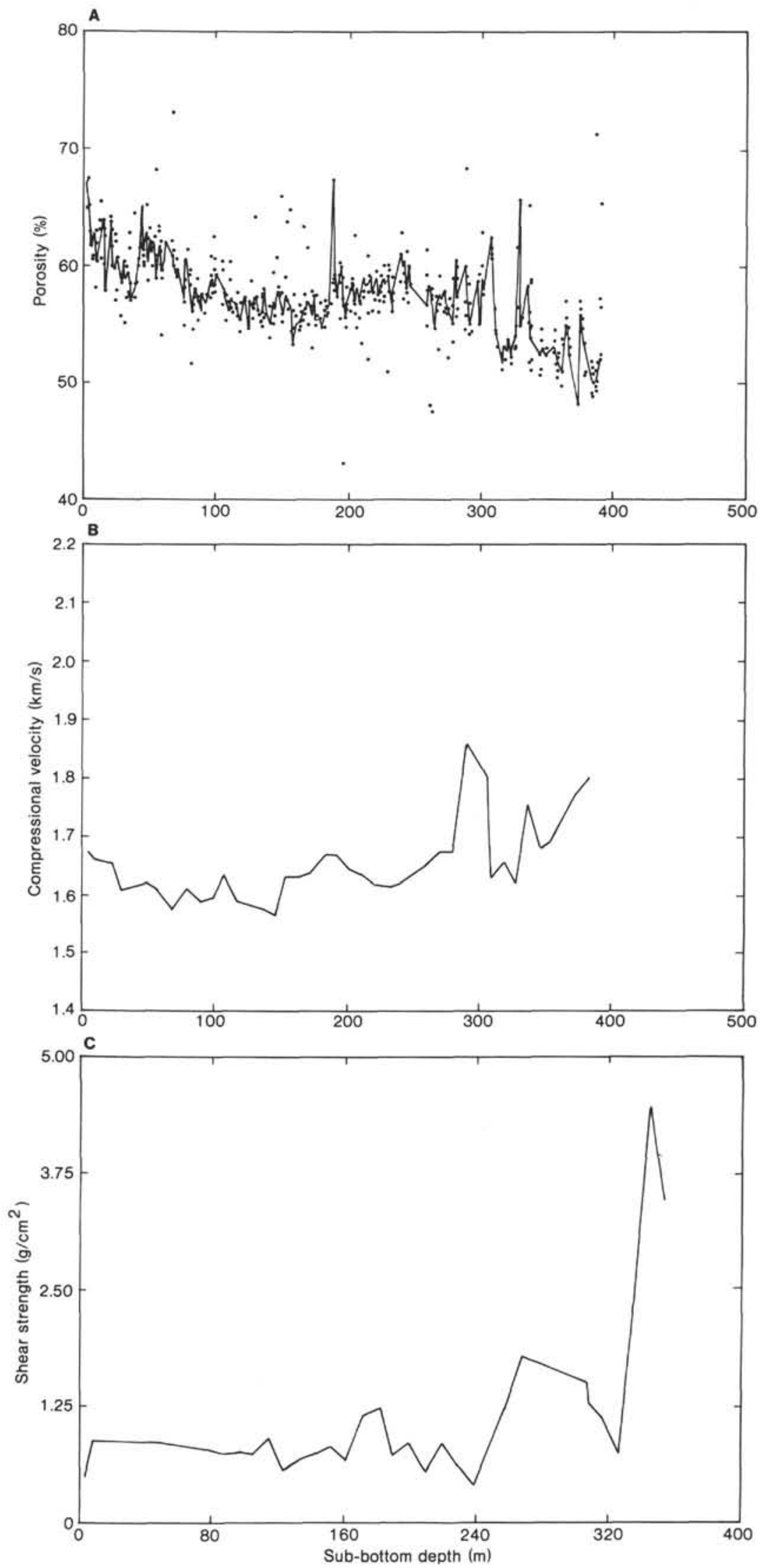

Figure 5. A. GRAPE porosity versus sub-bottom depth for Site 592. B. Compressional velocity versus sub-bottom depth for Site 592. C. Shear strength versus sub-bottom depth for Site 592. D. Porosity versus compressional velocity for Site 592. E. Porosity versus shear strength for Site 592. F. Acoustic impedance versus sub-bottom depth for Site 592.

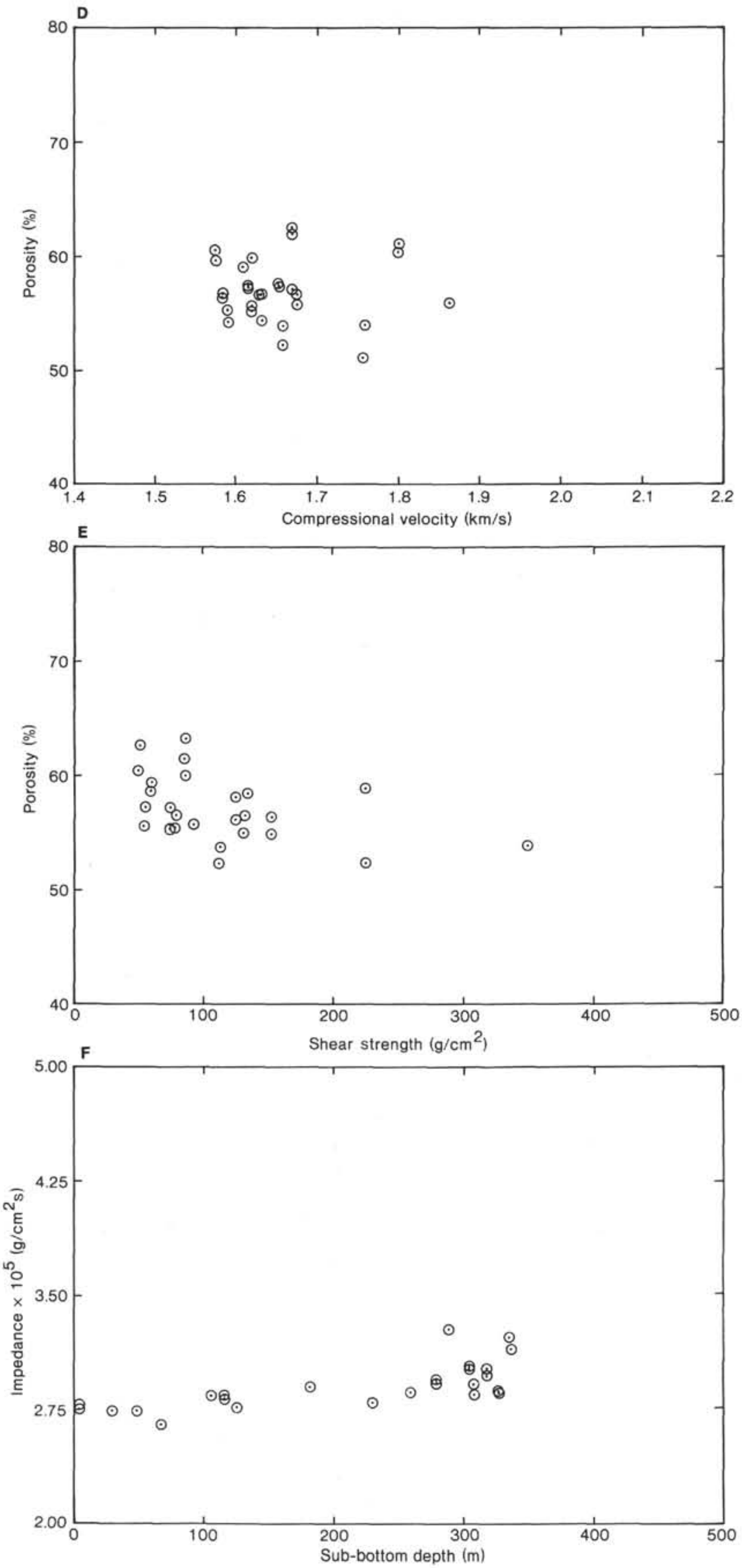

Figure 5. (Continued).

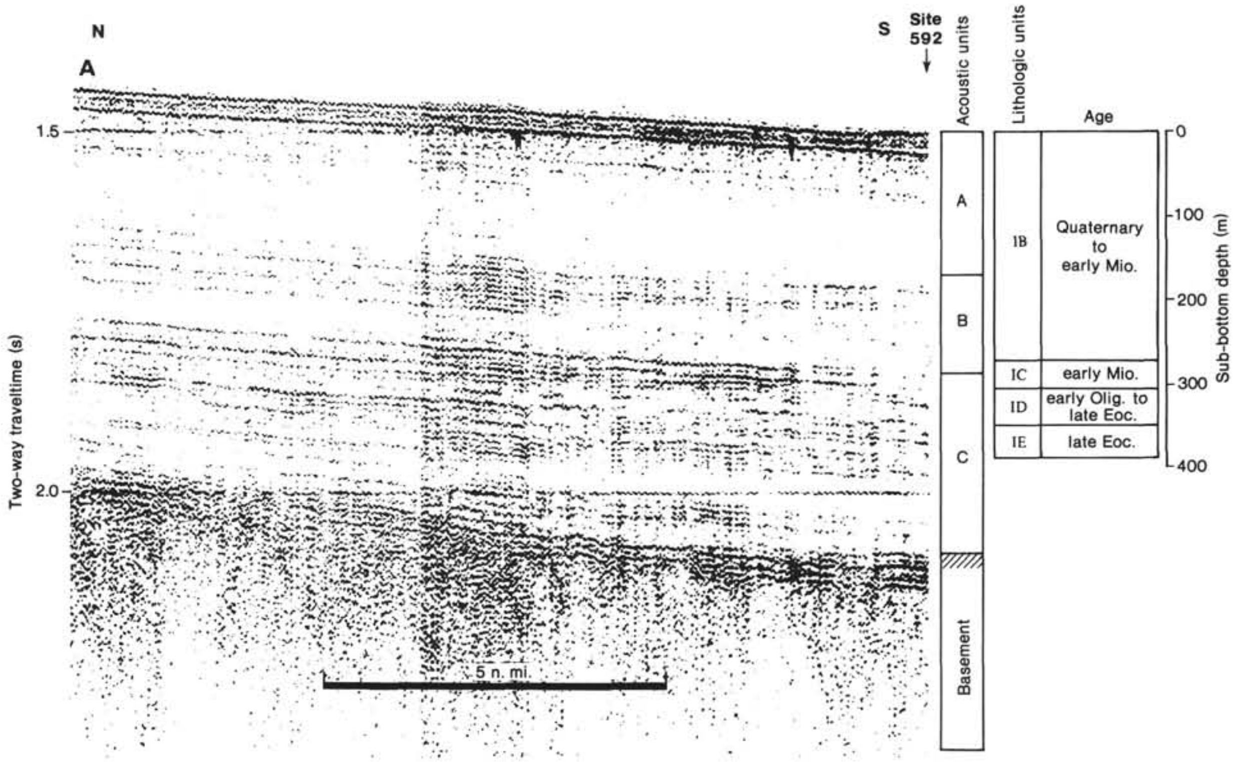

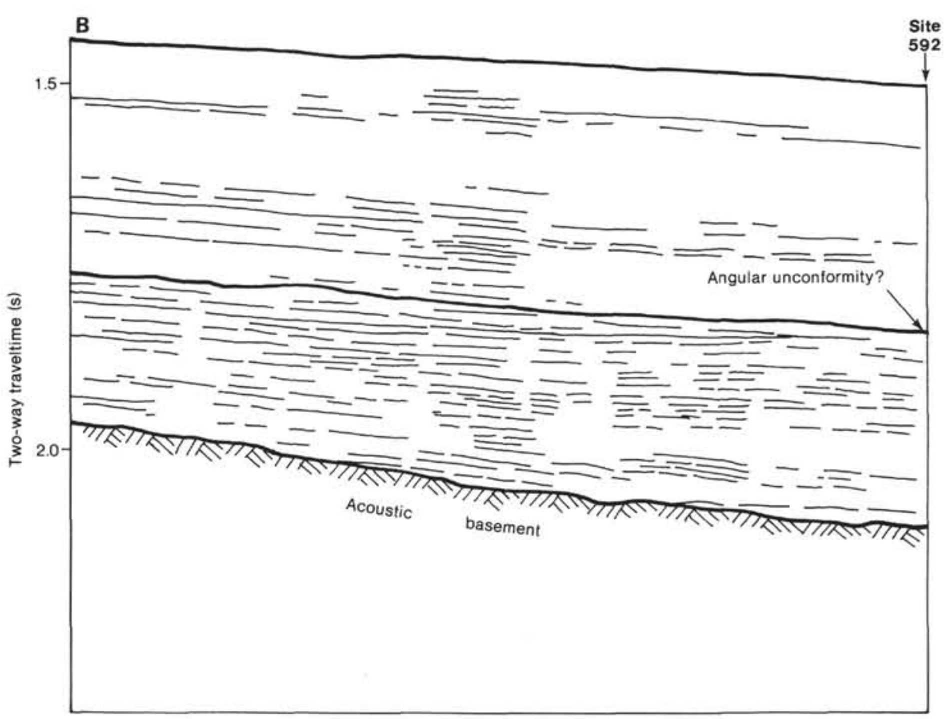

Figure 6. A. Comparison of acoustic Units A–C with lithostratigraphic Units IA (not shown), IB, IC, ID, and IE cored at Site 592; shipboard water gun seismic profile, collected during site approach; depths in meters estimated by assuming a sediment sound velocity of 1700 m/s. B. Line drawing of seismic profile shown in A; note subtle angular unconformity, with truncation of strata of probable early Oligocene age.

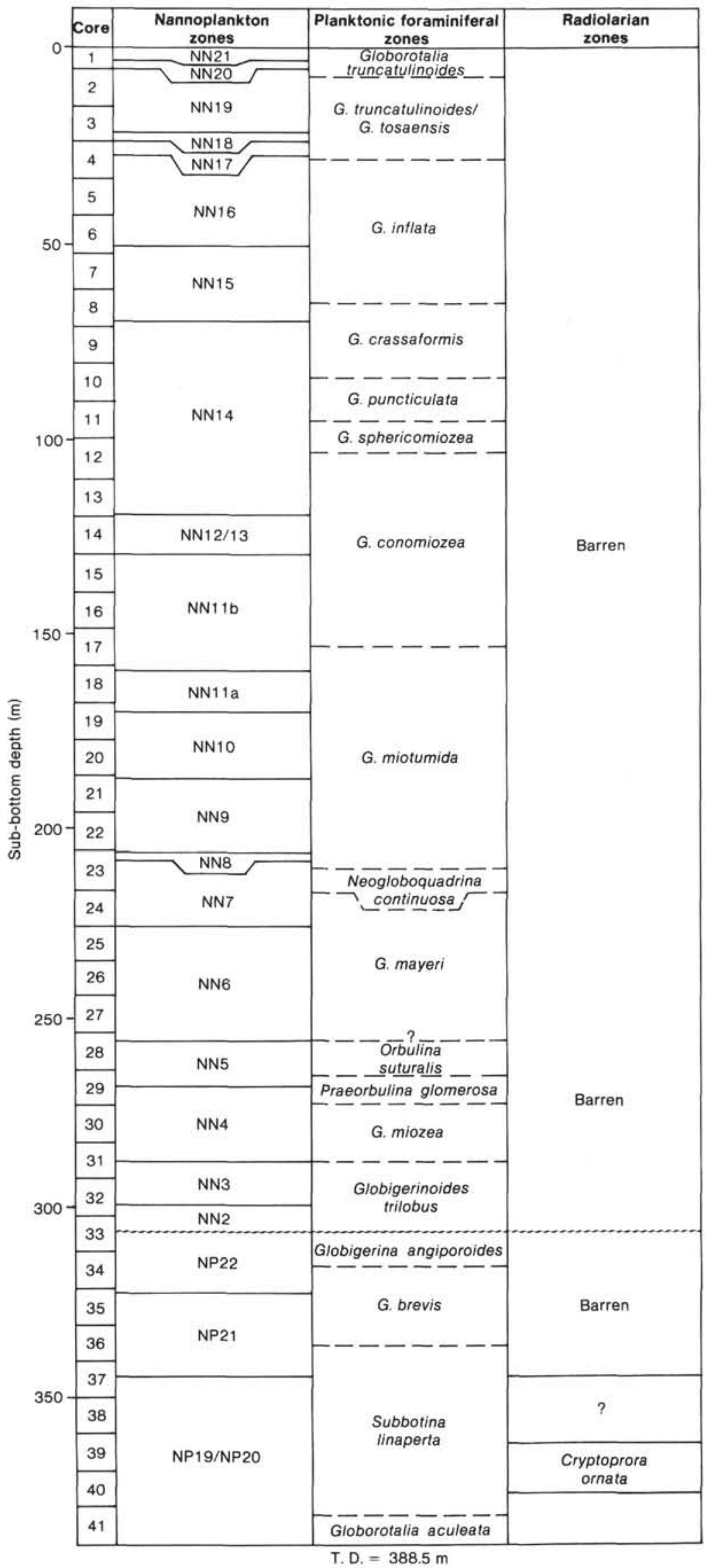

Figure 7. Comparison between calcareous nannoplankton, foraminiferal, and radiolarian zones at Site 592.

Globorotalia mayeri Zone
I. A. *G. mayeri*
Orbulina suturalis Zone
I. A. *O. suturalis*
Praeorbulina glomerosa curva Zone
I. A. *P. glomerosa*
Globorotalia miozea Zone
I. A. *G. miozea*
Globigerinoides trilobus Zone
——— UNCONFORMITY ———
Globigerina angiporoides Zone
L. A. *G. brevis*
Globigerina brevis Zone
I. A. *G. brevis*
Subbotina linaperta Zone
L. A. *G. aculeata*
Globorotalia aculeata Zone

The missing zones represented by the unconformity, in descending order, are *Globigerina connecta* Zone; *G. woodi* Zone; *G. dehiscens* Zone; *G. euapertura* Zone; *G. angiporoides* Zone (upper part only).

There were a few problems in recognizing some of the zones in the more northern sites; for example, the *Globorotalia tosaensis* Zone was not detected in the late Pliocene. The best explanation for its absence below the first appearance of *G. truncatulinoides* is that *G. tosaensis* evolved from *G. crassaformis* to the north of Site 592 and later spread southward with *G. truncatulinoides*; there is no hiatus.

The *N. continuosa* Zone is based on the range of the zonal marker after the extinction of *G. mayeri*. It is not a satisfactory zone because *N. continuosa* is rare and it is not known whether the extinction level is diachronous. The *G. fohsi* s.1. Zone was not recognized at Site 592 because *Fohsella* species are missing at this site.

Faunas

The planktonic foraminifers are abundant and well preserved from the Pleistocene to the Oligocene, but there is a marked deterioration in preservation in the late Eocene.

The Neogene faunas indicate temperate conditions with a few incursions of warmer water from the north; such warm incursions were detected in Samples 592-6,CC, 592-8,CC, 592-10,CC, 592-16,CC, and 592-17,CC. Because of the cooler-water conditions none of the following taxa were found: *Pulleniatina, Globorotalia menardii, Sphaeroidinella dehiscens, Catapsydrax dissimilis,* and *C. stainforthi: G. margaritae* is rare. The cooler-water species *G. conica* was present in the *G. mayeri* Zone; its northern paleogeographic limit is probably close to Site 592.

The Paleogene faunas are similar to those found in New Zealand and Victoria, Australia. The relatively low diversity in some of the late Eocene samples is due mainly to poor preservation, but the low diversity in the Oligocene is due to the cool-water conditions which prevailed at that time.

Unconformity and Major Boundaries

The unconformity between the *Globigerina angiporoides* Zone and the *Globigerinoides trilobus* Zone is a regional hiatus and was first detected in the Tasman Sea by the scientists of DSDP Leg 21 (Burns, Andrews, et al., 1973). The uppermost samples below the unconformity contained both *Globorotalia munda* and *Chiloquembelina cubensis, Globorotaloides testarugosa,* and *Globigerina ampliapertura,* which suggests that this is in the upper part of the *G. angiporoides* Zone. The extinction of *C. cubensis* slightly later in the late Oligocene has been dated by Berggren (1972) at about 30 m.y.

The lowermost lower Miocene above the unconformity is within the *Globigerinoides trilobus* Zone, above the local extinction of *Catapsydrax dissimilis*. An estimated age for this part of the zone is about 18–19 m.y. ago (Berggren et al., in press).

The unconformity at Site 592 is closer in stratigraphic position to that at Site 206 than to Site 207 drilled during Leg 21 (Fig. 8). This unconformity could be related to the initiation of the Circum-Antarctic Current, which occurred at about 29–30 m.y. ago (Jenkins, 1974; Kennett et al., 1972).

Other major boundaries noted include the following:

Pliocene/Pleistocene:	first occurrence of *Globorotalia truncatulinoides*;
Miocene/Pliocene:	extinction of *G. conomiozea*;
Eocene/Oligocene:	extinction of *Globigerinatheka index* (in Section 592-36-3, between 64 and 90 cm).

Benthic Foraminifers

Benthic foraminifers were examined in the fraction >63 μm from all core catchers taken at Site 592. Several additional samples were studied in Cores 37 and 36 across the Eocene/Oligocene boundary. Benthics are well preserved in the top of the section down to Core 23 (*Globorotalia miotumida* Zone), in which recrystallization becomes evident and faunal diversity drops markedly. Preservation worsens slightly through the lower Miocene, but improves in the lower Oligocene (Cores 592-33 to 592-36). Uppermost Eocene sediments resemble those of the lower Miocene, except that a large and diverse foraminiferal fauna was recovered.

Throughout the section, benthic faunas are dominated by species of the genera *Cibicidoides, Cibicides,* and *Bolivina*. Also common are *Melonis barleeanum, Sigmoilopsis schlumbergeri,* and, in the Paleogene, species of *Anomalinoides*. The number of New Zealand endemic species increases in the Paleogene, including such forms as *Vaginulinopsis hochstetteri, Cibicidoides molestus,* and *Rotaliatina sulcigera*. In the Neogene, species named in New Zealand are less frequent and are the same as those found at Site 591 farther to the north.

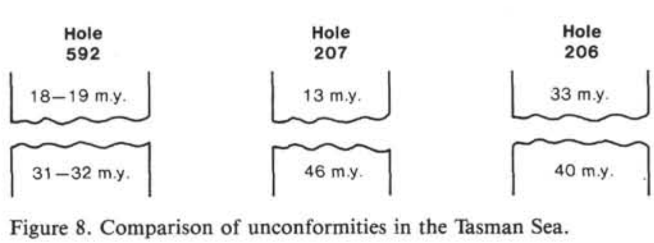

Figure 8. Comparison of unconformities in the Tasman Sea.

Downslope transport of shallower-water materials does not appear to be common at this site; exceptions are Cores 592-4, 592-22 and 592-23, which contain uncommon specimens of large, abraded, shallow-water species of *Spiroloculina* and *Ammonia*.

Typical Eocene faunas (Cores 592-41 and 592-36) contain abundant benthic individuals; common species are *C. molestus*, *Uvigerina bortotara* (= *U. spinicostata*, *U. havanensis*, and *U. rippensis*), *C. io*, *A. semiteres*, *Stilostomella nuttali*, and *Globocassidulina subglobosa*. *Vaginulinopsis* spp. are present in all Eocene samples, but disappear at the Eocene/Oligocene boundary, which is located between Cores 592-36-3, 88 cm and 592-36-2, 119 cm. Species common for the first time above the boundary include the spinose stilostomellids, *Valvulineria* sp., *Sphaeroidina bulloides*, *C. lobatulus* and the bolivinids. The more ornate cibicidids, with limbate sutures, become less common above the boundary.

Lower Oligocene faunas (Cores 592-36 to 592-33) resemble those of the upper Eocene, except for the larger proportions of *A. semiteres*, *C. io*, *Cibicides lobatulus*, and the striate bolivinids.

Lower to middle Miocene sediments are the least well preserved, but are better than those at the other sites drilled during Leg 90. The faunas are considered dissolution-residue faunas, but are relatively large and contain increased percentages of orbulinids from the *Globigerinoides trilobus* to the *Orbulina suturalis* Zone (Cores 592-32 to 592-28). Above this level a new fauna, still the result of dissolution, is marked by the abundant presence of *Bolivina anastomosa* (Cores 592-27 to 592-21, *Globorotalia mayeri–G. miotumida* zones).

The last change in benthic faunas of the Miocene occurs in the lower *G. conomiozea* Zone (Core 592-15), when there is an increase in the abundance of miliolids which is possibly due to better preservation and when *Anomalina semipunctata* first appears. These events occur earlier in Site 592 than in sites to the north.

A major change in sedimentation and in the diversity and abundance of benthic faunas occurs in the lower Pliocene *G. sphericomiozea–G. puncticulata* interval (Cores 592-11 and 592-10). Through the remainder of the section the abundance of benthics increases dramatically, diversity is consistently higher, but few new forms are found.

At the *G. crassaformis*/*G. inflata* change, which is considered to represent in the Northern Hemisphere the change to glacial conditions, the faunas change in two ways. First, *Cibicides lobatulus* increases dramatically in abundance and dominates all faunas through the remainder of the Pliocene and Quaternary. The numbers of other cibicidids and of the bolivinids also increase markedly. In addition, there is an increase in the proportion of uvigerinids, and a change in the types of uvigerinids from a *Uvigerina hispida–U. hispido-costata* assemblage below, to one dominated by the *U. peregrina* plexus, including forms tending to *U. mediterranea* and, in one sample, *U. spinulosa*. These morphotypes were not seen at the more northerly sites.

The *U. peregrina* plexus then disappears during the *G. tosaensis* interval, when miliolids again become more common in the benthic faunas; but it reappears in the Quaternary (Cores 592-2 to 592-1).

Calcareous Nannoplankton

Core-catcher samples and sufficient additional samples to determine zonal boundaries were examined for calcareous nannoplankton. All of the zonal indicators are present with the exception of *Helicosphaera ampliaperta* and *Sphenolithus pseudoradians*. The upper boundary of the *Helicosphaera ampliaperta* Zone (NN4) is determined instead by the first occurrence of *Discoaster exilis*, and the *Isthmolithus recurvus* Zone/*Sphenolithus pseudoradians* Zone (NP19/NP20) are combined. Calcareous nannoplankton are abundant throughout the section at Site 592. Preservation is good in the Quaternary and Pliocene. In the Miocene, preservation deteriorates from moderate to poor, and in particular most of the discoasters are heavily overgrown. A major unconformity between the early Miocene (~19.5 m.y.) and early Oligocene (~35.0 m.y.) is based upon the absence of Zones NN1 to NP23. In the lower Oligocene, preservation is somewhat improved, but is poor again in the upper Eocene, where most specimens are overgrown by calcite.

Quaternary

The presence of *Emiliania huxleyi* in Samples 592-1-1, 3–4 cm and 592-1-3, 3–4 cm places these samples in the late Pleistocene *Emiliania huxleyi* Zone (NN21). Sample 592-1,CC, above the last occurrence of *E. ovata* in Sample 592-2-1, 3–4 cm, is placed in the late Pleistocene *Gephyrocapsa oceanica* Zone (NN20). The interval from Samples 592-2-1, 3–4 cm to 592-3-1, 3–4 cm, above the last occurrence of *Calcidiscus macintyrei* in Sample 592-3-2, 2–3 cm, is placed in the upper subzone of the early Pleistocene *E. ovata* Zone (NN19b). The lower subzone of this zone (NN19a) includes Samples 592-3-2, 3–4 cm (the last occurrence of *C. macintyrei*), and 592-3-5, 3–4 cm.

Pliocene

The presence of *Discoaster brouweri* and the absence of *D. pentaradiatrus* in Samples 592-3-6, 3–4 cm to 592-4-1, 3–4 cm places these samples in the late Pliocene *Discoaster brouweri* Zone (NN18). Sample 592-4-2, 3–4 cm includes both *D. brouweri* and *D. pentaradiatus* and is placed in the late Pliocene *D. pentaradiatus* Zone (NN17). The addition of *D. surculus* in Samples 592-4-3, 3–4 cm places the interval from this sample to Sample 592-6-3, 3–4 cm in the late Pliocene *D. surculus* Zone (NN16).

The interval from the last occurrence of *Reticulofenestra pseudoumbilica* in Samples 592-6,CC to 592-8-5, 3–4 cm is placed in the early Pliocene *Reticulofenestra pseudoumbilica* Zone (NN15). The interval from the last occurrence of *Amaurolithus tricorniculatus* in Sample 592-8,CC to the first occurrence of *D. asymmetricus* in Sample 592-13,CC is placed in the early Pliocene *D. asymmetricus* Zone (NN14).

The boundary between the early Pliocene Zones NN12 and NN13 cannot be determined because *Ceratolithus rugosus* is not present at this site. Therefore the interval from Samples 592-14-1, 3–4 cm to 592-14,CC, above the last occurrence of *D. quinqueramus*, is placed in the combined NN12/NN13 Zone.

Miocene

The co-occurrence of *Amaurolithus primus* and *D. quinqueramus* in Samples 592-15-1, 3–4 cm to 592-17,CC places these samples in the upper subzone of the late Miocene *D. quinqueramus* Zone (NN11b). The lower subzone of this zone (NN11a) includes Samples 592-18-1, 3–4 cm to 592-19-1, 3–4 cm. The interval between the first occurrence of *D. quinqueramus* and the last occurrence of *D. hamatus* (Samples 592-19-3, 3–4 cm to 592-20,CC) is placed in the late Miocene *D. calcaris* Zone (NN10). The range of *D. hamatus*, Samples 592-21-1, 3–4 cm to 592-22,CC, defines the middle Miocene *D. hamatus* Zone (NN9). The first occurrence of *Catinaster coalitus* in Sample 592-23-1, 3–4 cm places this sample in the middle Miocene *Catinaster coalitus* Zone (NN8). The interval below the first occurrence of *C. coalitus*, Sample 592-23-3, 3–4 cm, to the first occurrence of *D. kugleri* in Sample 592-24,CC, is placed in the middle Miocene *D. kugleri* Zone (NN7).

The middle Miocene *D. exilis* Zone (NN6) includes Samples 592-25-1, 3–4 cm to 592-28-1, 3–4 cm, above the last occurrence of *Sphenolithus heteromorphus*. The middle Miocene *Sphenolithus heteromorphus* Zone (NN5) includes Sample 592-28-3, 3–4 cm, the last occurrence of *S. heteromorphus*, to the first occurrence of *D. exilis* in Sample 592-29-3, 3–4 cm. Samples 592-29-5, 3–4 cm to 592-31-3, 3–4 cm, above the last occurrence of *S. belemnos* in Sample 592-31-5, 3–4 cm, are placed in the early Miocene *Helicosphaera ampliaperta* Zone (NN4). The interval from Samples 592-31-5, 3–4 cm to 592-32-3, 3–4 cm, above the last occurrence of *Triquetrorhabdulus carinatus* in Sample 592-32-5, 3–4 cm, is placed in the early Miocene *S. belemnos* Zone (NN3).

An unconformity exists between Samples 592-33-3, 5–6 cm and 70 cm. All of the early Miocene *Triquetrorhabdulus carinatus* Zone (NN1) and possibly part of the overlying *D. druggii* Zone (NN2) as well as all of the late and middle Oligocene Zones (NP23 to NP25) and part of the early Oligocene *H. reticulata* Zone (NP22) are missing.

Oligocene

The interval from Samples 592-33-3, 70 cm to 592-34,CC is placed in the early Oligocene *H. reticulata* Zone (NP22). The early Oligocene *Ericsonia subdisticha* Zone (NP21) includes Samples 592-35-1, 3–4 cm to 592-37-2, 5–6 cm.

Eocene

The last occurrence of *D. saipanensis* in Sample 592-37-2, 33–34 cm and the first occurrence of *Isthmolithus recurvus* in Sample 592-41,CC places this interval in the combined late Eocene *Isthmolithus recurvus–S. pseudoradians* Zone (NP19/NP20). Sample 592-40,CC to 591-41,CC contain reworked species from the late middle and early upper Eocene such as *Neococcolithus dubius* and *Chiasmolithus solitus*, similar to the approximate interval at Site 593. The presence of abundant *Zygrhablithus bijugatus* and some *Braarudosphaera bigelowi* in the late Eocene–early Oligocene indicates shallow-water conditions during that interval.

Radiolaria, Diatoms, and Silicoflagellates

In Site 592, Radiolaria are present only in part of the late Eocene. Samples available for radiolarian studies range from Section 592-37-1 to 592-40-5. Well-preserved radiolarian faunas are present in Sections 592-40-4, 592-40-3, 592-40-2, 592-40-1, 592-39-4, and 592-39-3. Very rare specimens are present in Cores 592-37-4 and 592-37-3. Cores 592-37-1 and 592-37-2 contain only some fragments.

As radiolarian assemblages are different in tropical and polar areas, dating of temperate-latitude sediments by the use of either the low-latitude or high-latitude radiolarian biostratigraphy is often unsuccessful. Fortunately, late Eocene radiolarian assemblages from Site 592 are not very different from tropical faunas and thus the classic biostratigraphy of Riedel and Sanfilippo (1977) can be used.

Radiolarian abundances were roughly estimated from the density of radiolarians on strewn-slides, from counts of 2000 to 5000 well-preserved shells for each sample.

The classification used in this report is after Riedel (1967) except for the taxonomy of Trissocyclidae and Lophophaenidae, which is from Petrushevskaya (1971). Some new morphotypes need to be described. A large number of morphotypes have been encountered, but only 39 well-known forms are tabulated (see Caulet, this volume).

Only one radiolarian zone is recognized in Site 592: the *Cryptoprora ornata* Zone in Sections 592-39-3 to 592-40-4. The *C. ornata* Zone, top of the former *Thyrsocyrtis bromia* Zone Riedel and Sanfilippo, emended by Maurrasse and Glass (1976) and Saunders et al. (in press), is the uppermost radiolarian zone of the Eocene.

Since no radiolarian forms were found from the *Theocyrtis tuberosa* Zone of early Oligocene age, the Eocene/Oligocene radiolarian boundary cannot be located at Site 592.

Late Eocene radiolarian assemblages from Site 592 are similar to tropical faunas but lack some typical morphotypes like the *Lithocyclia* group. Other tropical species like *Thyrsocyrtis bromia* appear to be rare and restricted to the upper part of the radiolarian zone. However, their skeletons are somewhat different from the tropical forms. Tests of *Cyclampterium*(?) *milowi* are frequent but the test outline is narrower in the mid-latitude assemblages. Some forms like *Lychnocanoma amphitrite* and *Lithapium mitra* are more frequent than in tropical assemblages. As shown by Chen (1975), high-latitude radiolarian assemblages "are similar to but less diverse than the late middle Eocene to late Eocene low-latitude assemblages previously described by Riedel and Sanfilippo (1971) and Foreman (1973)."

Petrushevskaya (1975) reported that Eocene radiolarian faunas from the South Pacific sector of the Southern Ocean (DSDP, Leg 29) are more similar to the Californian Eocene assemblages than those from the Caribbean. This is also the case for Eocene radiolarians from Site 592.

The preservation of the tests is good only in Sections 592-40-2, 592-40-3 and 592-40-4, where the diversity of morphotypes is higher and diatoms are more abundant. In Sample 592-39-3 the siliceous fraction is represented only by broken radiolarian tests. In Samples 592-37-3 and 592-37-4, the number of the forms found is low and their state of preservation poor.

It may be concluded that the deposition of radiolarians and other siliceous microfossils ceased at Site 592 before the very end of the late Eocene and that reworking processed are responsible for the rare latest Eocene siliceous accumulations occurring near the Eocene/Oligocene boundary.

Silicoflagellates have not been found in the Site 592 material.

PALEOMAGNETISM

Sediments from this site were characterized by a thinner and less prominent surficial high-intensity zone and generally very high directional scatter. A magnetic polarity stratigraphy can be traced back to about 3 m.y. ago.

Both the HPC and the XCB cores were subsampled at three specimens per section. Kuster-tool orientation data was obtained for only 25% of the HPC cores recovered. Laboratory NRM and low-field susceptibility measurements have been completed on most specimens. Hole mean statistics are:

Geometric mean intensity (μG)	-0.056
Scalar mean inclination ($\pm$ s.d.)	$-5.8 \pm 41.9°$
Axial dipole inclination	$-55.9°$
Mean angular difference between repeats	10.2° (20 repeats)

The sediments gave very weak low-field magnetic susceptibilities (less than a few μG/Oe) which were predominantly negative—that is diamagnetic (Table 3). Pure diamagnetic materials do not retain a magnetic remanence. However, in sediments such as these, the diamagnetism of the bulk of the material could easily swamp a weak positive-susceptibility contribution from grains capable of retaining a magnetic remanence.

The usual high-intensity, oxidized zone occurs at the top of the section, but here it was weaker (-0.03 to 1.0 μG) and thinner (~ 3 m) than at previous sites. Below this zone intensities showed considerable scatter, generally within the range 0.01 to 0.1 μG, which is indicative of very variable conditions of sedimentation. An exception to this rule is a region of higher intensity (~ 1.0 μG) from Cores 592-29 through 592-32, spanning the early Miocene and the start of the middle Miocene. The onset of this region is gradual, but its termination at the top of Core 592-29 is abrupt. It probably correlates and has a similar origin to the high-intensity zones observed in the middle Miocene at Sites 588 and 593, although it is less pronounced.

Relatively high intensity spikes in Hole 592 are noted in Table 4.

The upper sediments were difficult to subsample without causing distortion. This is reflected in an increase in directional scatter, but is not sufficient to mask the polarity stratigraphy, which could be traced down to the end of the Gauss Chron about 3 m.y. ago (Fig. 9). Be-

Table 3. Magnetic susceptibilities at Site 592.

Core-Section (level in cm)	Depth	Susceptibility
592-1-1, 25	0.25	
		Very weak negative (diamagnetic)
592-29-1, 27	264.45	
		Very weak positive
592-30-1, 25	273.55	
		Very weak negative (diamagnetic)
592-30-6, 25	281.05	
592-31-1, 44	283.34	
		Very weak positive
592-32-4, 77	297.77	
		Very weak negative (diamagnetic)
592-41-6, 75	387.15	

Table 4. Magnetic intensity spikes in Hole 592.

Core-Section (level in cm)	Depth (m)	Intensity (μG)
2-6, 75	12.75	0.264
12-2, 25	102.25	1.754
12-5, 25	106.75	0.876
13-1, 75	110.85	2.449
15-1, 25	129.55	0.236
15-3, 75	133.05	0.260
16-1, 25	139.15	0.302
16-1, 125	140.15	0.355
17-5, 25	154.75	0.921
18-2, 25	159.85	1.042
18-4, 125	163.85	0.291
19-4, 25	172.45	0.368
20-3, 75	181.05	0.490
26-4, 125	240.65	0.981
34-2, 75	315.45	0.580
35-1, 75	322.05	0.452
38-4, 25	354.85	1.480
40-4, 75	374.55	1.027

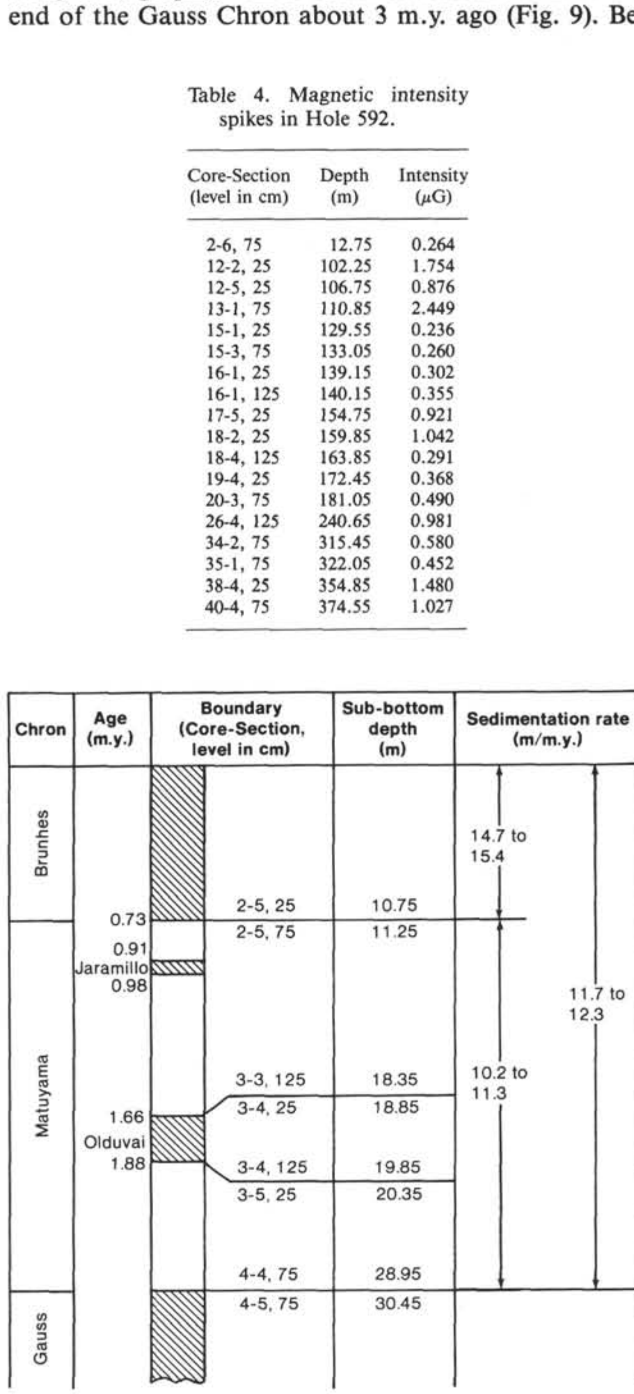

Figure 9. Magnetic polarity stratigraphy for the upper part of Site 592.

low this (apart from the higher-intensity zone just mentioned), directions were more scattered than for previous sites, with a high percentage of intermediate directions. The scatter is particularly bad between 100 and 190 m sub-bottom depth. Since the laboratory measurements were repeatable (mean angle between repeats = 10.2°), this cannot be attributed to instrumental noise and must be an intrinsic property of the sediments. It is not yet known if the scatter can be reduced by AF cleaning.

SEDIMENTATION RATES

Sedimentation rates are calculated as outlined for the previous sites, but the intervals used are subdivided where necessary, especially in the Pliocene and late Miocene (Fig. 10).

The late Eocene sedimentation rate (7.0 m/m.y.; nannoplankton Zones NP19/NP20) in indurated calcareous sediments with trace amounts of siliceous material (radiolarians, sponge spicules, volcanic glass) seems similar to that of the early Oligocene. In the early Oligocene (Zones NP21 and NP22), the sedimentation rate is 19.0 m/m.y. in a calcareous ooze, calculated on the basis of two datum levels.

The sedimentation rate drops in the early to middle Miocene interval (Zones NN2 top to NN7 top) to 13.6 m/m.y. in a foraminifer-bearing nannofossil ooze.

For the late Miocene (nannoplankton Zone NN11) it drops further to 7.5 m/m.y., and then increases again to 24.8 m/m.y. during the early Pliocene. In the late early Pliocene (Zones NN14 and NN15) a major increase of the sedimentation rate occurs, to 92.5 m/m.y., similar to the even higher value at Site 591. In the late Pliocene (Zones NN16 to NN18) it decreases again, and calculated on the basis of four datum levels is 21.2 m/m.y. Finally, in the Quaternary the sedimentation rate is reduced to only 9.8 m/m.y.

Compared with Site 591, there is a considerable drop in the sedimentation rate throughout the Miocene to Recent, although the rate is still high in the late early Pliocene.

SUMMARY AND CONCLUSIONS

Site 592 is located near the southern end of Lord Howe Rise at 36°28.4′S, 165°26.53′E, at a water depth of 1098 m. Although Site 592 (originally SW-2) was assigned as a secondary objective during Leg 90, it was possible to budget two days for drilling at this location. Of particular interest was the determination of calcareous biogenic sedimentation rates during the Neogene to compare and contrast with sites both to the north and south. The coring would also provide another valuable site for the north-south paleoceanographic traverse to study both surface and intermediate water mass changes through the Neogene.

Site 592 is located about 60 km north of Site 207, which was located in an area of thin (360 m) sediment cover overlying a basement high composed of rhyolite. At Site 207, the upper 142 m of sediment cover consists of a thin middle Miocene to Quaternary sequence of foraminifer-nannofossil ooze that is unconformably underlain by siliceous calcareous and calcareous oozes of Eocene age. At Site 207 the Neogene sediments clearly were winnowed, judging from low sedimentation rates and the relatively high proportion of foraminifers. The basement high upon which Site 207 is located focused bottom currents during the Cenozoic.

Since the primary objectives of Leg 90 were related to paleoceanographic history, rather than basement problems, a site was chosen in an area of thicker (600 m) sediment cover, but still close to Site 207.

Site 592 consists of one hole cored continuously with the HPC from 0-234.9 m sub-bottom and then with the XCB from 234.9-388.5 m sub-bottom (Fig. 11). Although the hole was cored continuously, recovery is not complete and decreases below 240 m sub-bottom (middle Miocene) in the rotary-cored sequence. The core quality is generally excellent.

The recovered section consists of a single lithostratigraphic unit that varies from foraminifer-bearing nannofossil ooze (chalk) to nannofossil ooze (chalk) (Fig. 11). The section ranges in age from the Quaternary to middle late Eocene (42 m.y. ago). A paleomagnetic polarity stratigraphy has been identified down to the late Gauss Chron (2.5 m.y.). The lower part of the section consists of 83.5 m of Paleogene ooze and chalk ranging in age from the late Eocene to the early Oligocene (35 m.y.). The regional unconformity of the southwest Pacific separates the lower Oligocene sediments from immediately overlying middle lower Miocene sediments 18.5 m.y. old. Calcareous nannofossils are the dominant component (about 75%) throughout the entire sediment sequence. Foraminifers vary from less than 5 to 25%. Beds containing numerous 1-4 cm-sized molluscan (*Ostrea*) fragments occur in the early Oligocene (Section 592-34-3). Noncarbonate components occur only in trace abundances: volcanic glass, pyrite, and clay minerals occur throughout the sequence, whereas quartz, feldspar, and heavy minerals are found only occasionally. Biogenic opal is absent except for the late Quaternary and the Eocene, where radiolarians and sponge spicules occur in trace amounts.

The induration of the sediment varies from a soft ooze at the top of the sequence to a firm ooze near 250 m (earliest middle Miocene), to a chalk near 273.3 m (early Miocene) sub-bottom. The early Oligocene sediment from 305.8-250.0 m, below the regional unconformity, is an ooze. The lower part of this sequence, near 334.4 m, is marked by a chert nodule within a 15-cm thick layer of lithified limestone. The ooze grades downward between 350 and 369 m into a firm recrystallized chalk containing a high abundance of micrite (5-25%) (latest Eocene).

The section has been divided into five subunits: Subunit IA represents a veneer (0 to 0.3 m) of pale orange to pinkish gray foraminifer-bearing nannofossil ooze within the oxidized zone near the seafloor. Subunits IB to IE are differentiated by degree of lithification. There is good planktonic foraminifer preservation in the Neogene and Oligocene, but the benthic foraminifers and the nannofossils are well preserved only in the late Neogene and Oligocene. Radiolarians are present in small amounts only in the Eocene. The biostratigraphic sequences seem to be complete except for that part which is missing in the regional unconformity. Sedimentation rates range from lowest values (7 m/m.y.) in the late Eocene to highest

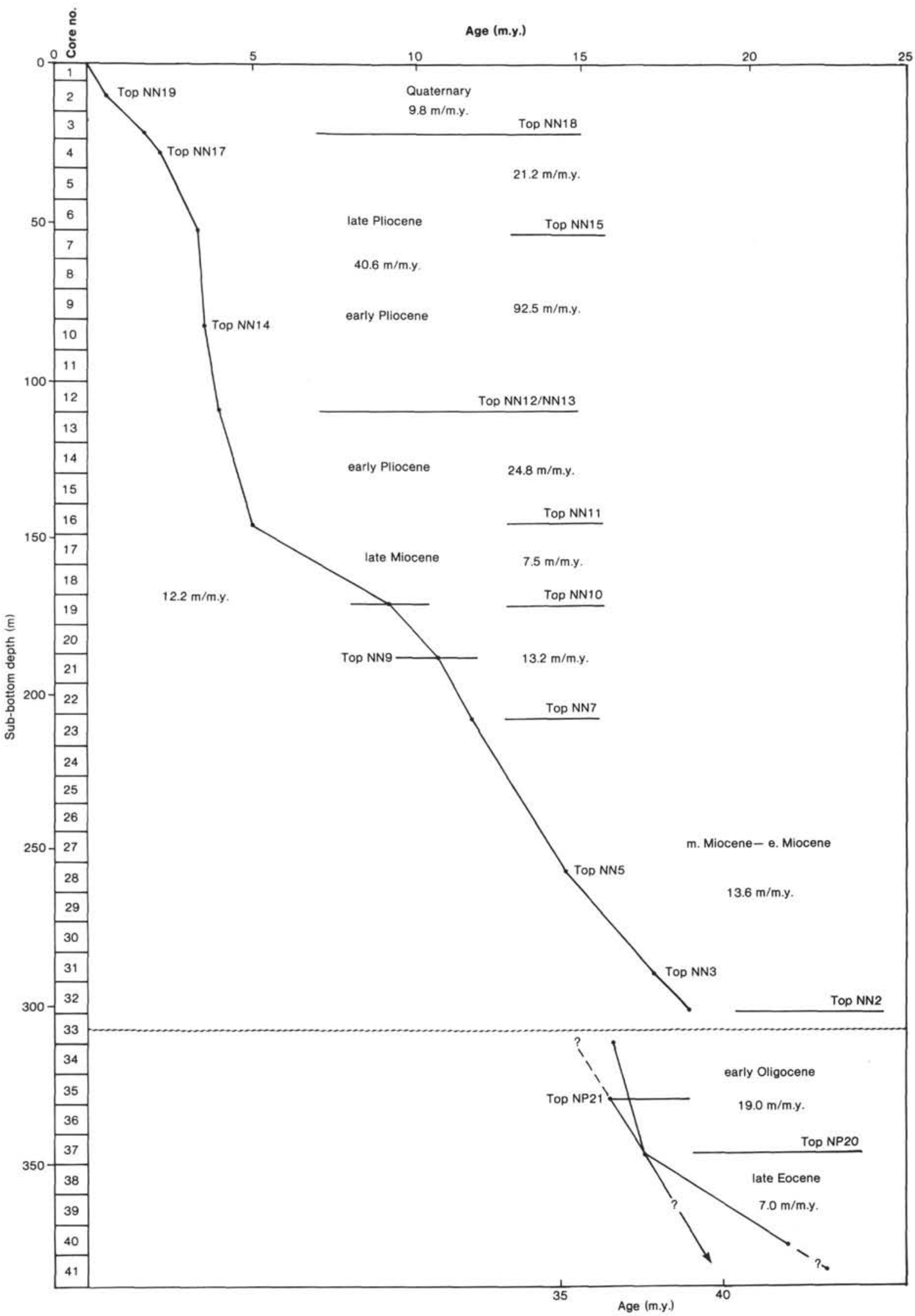

Figure 10. Sedimentation rates and datum levels in Site 592.

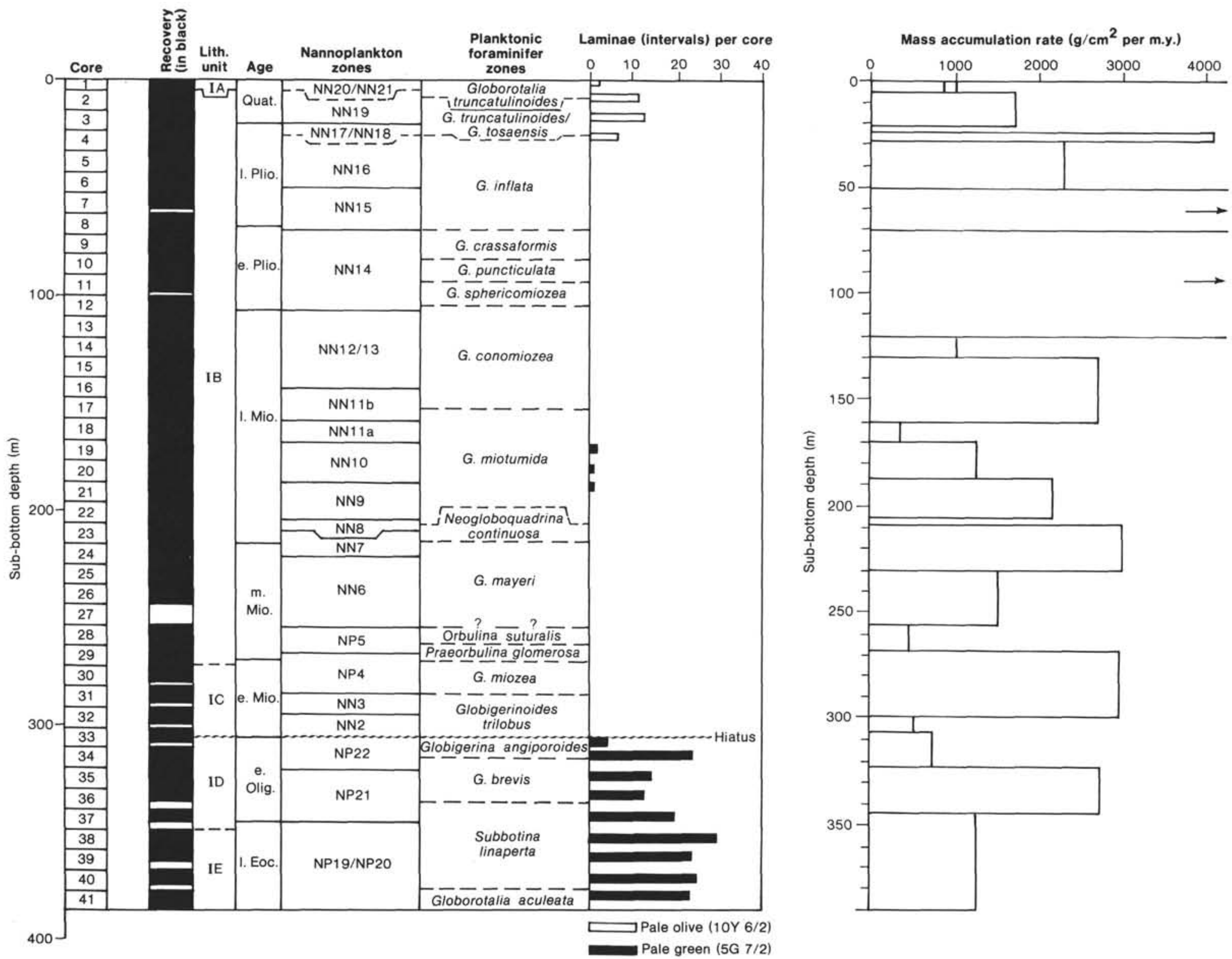

Figure 11. Summary lithology, biostratigraphy, and mass accumulation rates for Site 592. Also shown are ash and altered ash layers.

values (92.5 m/m.y.) in the late early Pliocene. In general, sedimentation rates are much lower at Site 592 than in sites both to the north and south.

Of particular interest at this site is a fine, complete boundary section between the Eocene and the Oligocene in Cores 592-36 and 592-37. The hiatus present in all other South Pacific sites except Site 277 in the subantarctic area south of New Zealand is not found at Site 592. A distinct lithologic change occurs near the level of extinction of *Globigerinatheka index*, which is the foraminifer marker for the boundary in south temperate latitudes. The underlying upper Eocene is represented by nannofossil chalks containing siliceous microfossils such as radiolarians and sponge spicules, whereas the Oligocene is represented by surprisingly soft nannofossil ooze lacking biosiliceous materials.

The extinction of *G. index* is noted in Section 592-36-3 between 90 and 64 cm. According to the nannoplankton record, the boundary at the extinction of *Discoaster saipanensis* is in Section 592-37-2, between 5–6 and 33–34 cm. A similar sequence of extinctions for the two taxa was recovered at DSDP Site 277, drilled south of New Zealand (Kennett, Houtz, et al., 1975).

The hiatus separating the early Oligocene from the early Miocene (at 592-33-3, 70 cm) is of considerable interest because it represents the regional unconformity that occurs throughout much of the Tasman Sea (Burns, Andrews, et al., 1973; Kennett et al., 1972). The range which this hiatus represents differs depending upon whether evidence supplied by planktonic foraminifers or calcareous nannofossils is used.

In terms of planktonic foraminiferal zones the unconformity is between the lower part of the *Globigerinoides trilobus* Zone and the upper part of the *Globigerina angiporoides* Zone. The uppermost samples below the unconformity contain both *Globorotalia munda* and *Chiloguembelina cubensis, Globorotaloides testarugosa,* and *Globigerina ampliapertura,* which suggest that this is in the upper part of the *G. angiporoides* Zone. The extinction of *C. cubensis* slightly later in the late Oligocene has been dated by Berggren (1972) at about 30 m.y. ago.

The lowermost lower Miocene above the unconformity is within the *Globigerinoides trilobus* Zone, above the local extinction of *Catapsydrax dissimilis*. An estimated age for this part of the zone is about 18–19 m.y. (Berggren et al., in press). Thus the planktonic foraminifers suggest an age range for the hiatus of about 13 m.y. (i.e., between 31–32 and 18–19 m.y. ago). The calcareous nannofossils, on the other hand suggest a range of 15.5 m.y. (between NP22 at 35 m.y. ago and NN2 at 19.5 m.y. ago).

A few pale olive intervals in the upper (Quaternary) and middle parts (early late Miocene) and some grayish green to pale green pockets in the lower part (Paleogene) of the sediment sequence are marked by more common volcanic glass. These intervals may represent episodes of increased volcanic explosivity in the source regions.

Paleoenvironmental History of Site 592

The middle to late Cenozoic sedimentary section at Site 592 represents deposition in a relatively simple pelagic environment near the southern end of Lord Howe Rise. Deposition was in middle bathyal depths that seemed to change little during the Cenozoic. The biogenic sedimentary material is by far dominated by calcareous nannofossils with an admixture of foraminifers. Terrigenous sediments are insignificant in this isolated setting and are restricted to eolian clay and volcanic ash which is either disseminated or occurs as distinct layers. Siliceous biogenic material is almost absent except in the Eocene, where it forms a noticeable fraction. Temperate faunas and floras dominate throughout, with little warm-water influence.

There may have been mild current activity on the seafloor at Site 592 during much of the Cenozoic, since the section is relatively thin and the seismic profiles show a marked thinning of the sequence toward the crest of the Rise at this latitude. Maximum thickness here is only 200 m.

During the late Eocene, calcareous oozes were deposited with trace amounts of radiolarians, sponge spicules, and reworked material. Numerous altered volcanic ash layers indicate a high amount of explosive volcanism in the region. The benthic foraminifers show a high degree of endemism, including forms such as *Vaginulinopsis hochstetteri, Cibicidoides molestus,* and *Rotaliatina sulcigera.*

Deposition continued uninterrupted across the Eocene/Oligocene boundary (foraminifers indicate it to be in 592-36-3, between 90 and 64 cm). There is no sign of any hiatus. Important planktonic microfossils become extinct at or close to the boundary. The extinction of the important marker species *Discoaster saipanensis* occurs slightly earlier (Section 592-37-2) than *Globigerinatheka index* (592-36-3). Siliceous microfossils disappear from the sediments at the same level as the extinction of *G. index.* The replacement of oozes lacking biosiliceous components by those containing such components is very common in the oceanic sedimentary record. This is tied to a major drop of about 2000 m in the calcite compensation depth at the Eocene/Oligocene boundary and related geochemical changes, seemingly at all depths, in the ocean basins. A number of changes in the benthic foraminifers occurred at this time, including the disappearance of *Vaginulinopsis.* Species that become common at the boundary include the spinose stilostomellids, *Valvulineria* sp., *Sphaeroidina bulloides, Cibicidoides lobatulus,* and the bolivinids. Others that become less common are the more ornate cibicidids with limbate sutures.

The change in sedimentation that occurred at the boundary provided a distinctly different diagenetic potential which eventually led to the formation of chalk for the Eocene sediments, whereas those of earliest Oligocene age remained very soft ooze. Sedimentation rates increased to 19 m/m.y. in the early Oligocene, probably as a result of increased productivity and preservation. The early Oligocene assemblages are typically temperate and exhibit low diversity, which is related to cool oceanic temperatures. *Ostrea* (oyster) beds were laid down during one brief interval. Explosive volcanicity continued actively, as in the late Eocene. Early Oligocene benthic foraminifers remained much the same as those of the late Eocene except for larger proportions of *Anomali-*

noides semiteres, Cibicidoides io, Cibicides lobatulus, and the striate bolivinids.

During the middle Cenozoic, bottom currents intensified in the region and created a major hiatus (592-33-3, 70 cm) between lower Oligocene and lower Miocene sediments. This represents a break in sedimentation of 14 to 15.15 m.y. The hiatus represents an extension of the major, regional hiatus of the southwest Pacific (Burns, Andrews, et al., 1973; Kennett et al, 1972). The ages of the major event or events that created the erosion are not known clearly but they are centered in the early to middle Oligocene. Erosion in some areas seems to have commenced at the Eocene/Oligocene boundary and to have continued into the early Miocene. At Site 592, within the Oligocene–early Miocene, erosion did not cut back as far as the Eocene/Oligocene boundary, which was preserved. Kennett et al. (1972) have speculated that the Tasman Sea–Coral Sea area was a major conduit for northward-moving bottom waters until the late Oligocene, at about the time that deep circum-Antarctic circulation began and bottom-water flow was diverted away from the Lord Howe Rise region.

Sedimentation recommenced at Site 592 about 19 m.y. ago in the late early Miocene. By this time, explosive volcanism had virtually disappeared from the immediate region, judging by a near absence of altered volcanic ash layers, except for a few minor, pale green layers in the early late Miocene. Although there was much volcanism in New Zealand during the Neogene, Site 592 is located upwind, with less opportunity for volcanic ash deposition. Sedimentation rates through the early and middle Miocene remained much the same as they had been in the early Oligocene, about 13 m/m.y. However, by the latest Miocene they were reduced to 7.5 m/m.y.

The Neogene benthic foraminifers develop much less endemic characteristics. Most species are known from the broader oceanic sphere. The early Miocene assemblages exhibit increased percentages of robulinids, and during the late Miocene there is a marked increase in *Bolivina anastomosa*. The latest Miocene exhibits an increase in the abundance of miliolids and the spectacular benthic form *Anomalina semipunctata* first appears. These events occur earlier at Site 592 than in sites to the north.

The Pliocene is again marked by much higher sedimentation rates, the highest for this section during the Cenozoic. Early early Pliocene rates are 24.8 m/m.y. Late early Pliocene rates are a remarkable 92.5 m/m.y. and late Pliocene, 21 m/m.y. Volcanic ash layers are absent from the Pliocene sediments.

During the late Pliocene at the *Globorotalia crassaformis/G. inflata* turnover, which is considered to be the time of change to glacial conditions, the faunas change in two ways. First, *Cibicides lobatulus* increases dramatically in abundance and dominates all faunas through the remainder of the Pliocene and Quaternary. The numbers of other cibicidids and of the bolivinids increase markedly also. In addition, there is an increase in the proportion of uvigerinids, and a change in the types of uvigerinids from a *Uvigerina hispida–U. hispido-costata* assemblage below, to one dominated by the *U. perigrina* plexus, including forms tending to *U. mediterranea,* and in one sample, *U. spinulosa*. These morphotypes were not seen at the more northerly sites.

The *U. peregrina* plexus then disappears during the *G. tosaensis* interval, when miliolids again become more common in the benthic faunas; it reappears in the Quaternary (Cores 592-2-1).

The Quaternary, as in a number of other sites, is marked by much lower sedimentation rates of nearly 10 m/m.y. This is perhaps due to increased winnowing which is related to stimulated oceanic circulation. Several distinct, pale olive ash layers probably represent major volcanic events in New Zealand to the east. The Quaternary record terminates with a late Quaternary (0 to 0.3 m) pale orange to pinkish gray foraminifer-bearing nannofossil ooze. This represents the zone of oxidation at the sediment/water interface that occurs at almost all of the sites cored during Leg 90.

REFERENCES

Berggren, W. A., 1972. A Cenozoic time-scale: some implications for regional geology and paleobiography. *Lethaia*, 5:195.

Berggren, W. A., Kent, D. V., and Van Couvering, J. A., in press. Neogene geochronology and chronostratigraphy. *In* Snelling, N. J. (Ed.), *Geochronology and the Geologic Time Scale.* Geol. Soc. London, Spec. Pap.

Burns, R. E., Andrews, J. E., et al., 1973. *Init. Repts. DSDP*, 21: Washington (U.S. Govt. Printing Office).

Chen, P. H., 1975. Antarctic radiolaria. *In* Hayes, D. E., Frakes, L. A., et al., *Init. Repts. DSDP*, 28: Washington (U.S. Govt. Printing Office), 437–514.

Foreman, H. P., 1973. Radiolaria of Leg 10 with systematics and ranges for the families Amphicyndacidae, Artostrobiidae and Theoperidae. *In* Worzel, J. L., Bryant, W., et al., *Init. Repts. DSDP*, 10: Washington (U.S. Govt. Printing Office), 407–474.

Jenkins, D. G., 1974. Initiation of the proto circum-Antarctic current. *Nature*, 252:371.

Kennett, J. P., Burns, R. E., Andrews, J. E., Churkin, M., Jr., Davies, T. A., Dumitricâ, P., Edwards, A. R., Galehouse, J. S., Packham, G. H., and van der Lingen, G. J., 1972. Australian–Antarctic continental drift, paleocirculation changes and Oligocene deep-sea erosion. *Nature* (*Phys. Sci.*), 239(91):51–55.

Kennett, J. P., Houtz, R. E., et al., 1975. *Init. Repts. DSDP*, 29: Washington (U.S. Govt. Printing Office),

Mammerickx, J. L., Chase, T. E., Smith, S. M., and Taylor, I. L., 1974. *Bathymetry of the South Pacific*. IMR Technical Reports, Scripps Institution of Oceanography, La Jolla California.

Maurasse, F., and Glass, B., 1976. Radiolarian stratigraphy and North American microtektites in Caribbean RC9-58: Implications concerning late Eocene radiolarian chronology and the age of the Eocene/Oligocene boundary. *Publ. VII Conf. Géol. Caraibes (30 Juin au 12 Juillet 1974):* Cayenne, pp. 205–212.

Petrushevskaya, M. G., 1971. Radiolarians of the ocean: reports on the Soviet expeditions. *Explorations of the Fauna of the Seas* (Vol. 17): Leningrad (Izd. Nauka).

________, 1975. Cenozoic radiolarians of the Antarctic, Leg 29, DSDP. *In* Kennett, J. P., Houtz, R. E., et al., *Init. Repts. DSDP,* 29: Washington (U.S. Govt. Printing Office), 541–674.

Riedel, W. R., 1967. Some new families of Radiolaria. *Proc. Geol. Soc. London*, 1640:148–149.

Riedel, W. R., and Sanfilippo, A., 1971. Cenozoic Radiolaria from the western tropical Pacific, DSDP Leg 7. *In* Winterer, E. L., Riedel, W. R., et al., *Init. Repts. DSDP*, 7, Pt. 2: Washington (U.S. Govt. Printing Office),1529–1672.

Riedel, W. R., and Sanfilippo, A., 1977. Cainozoic Radiolaria. *In* Ramsey, A. T. S (Ed.), *Oceanic Micropaleontology* (Vol. 2): London (Academic Press), 847–912.

Saunders, J., Perch-Nielsen, K., Sanfilippo, A., and Riedel, W. R., in press. Biostratigraphy of the Eocene to early Oligocene sections at Bathcliff Barbados. *Micropaleontology.*

Date of Acceptance: 1 December 1983

SITE 592 HOLE CORE 1 CORED INTERVAL 0.0–4.5 m

TIME – ROCK UNIT: Quaternary | BIOSTRATIGRAPHIC ZONE: NN21; *G. truncatulinoides* NN21 / NN20 | FOSSIL CHARACTER: FORAMINIFERS, NANNOFOSSILS, RADIOLARIANS, DIATOMS (A, A, A; A, A) | SECTION: 1, 2, 3, CC | METERS: 0.5, 1.0 | GRAPHIC LITHOLOGY | DRILLING DISTURBANCE | SEDIMENTARY STRUCTURES | SAMPLES

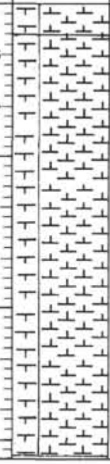

10YR 8/2 to 5YR 8/1
10Y 6/2
10Y 6/2 mottles
10Y 6/2
10Y 6/2 } N8
N7
10Y 6/2
10Y 6/2 + N7
10Y 6/2
10Y 6/2
N8
10Y 6/2
10Y 6/2
10Y 6/2
10Y 6/2 + N5 py.
10Y 6/2
N8

LITHOLOGIC DESCRIPTION

FORAMINIFER-BEARING (20%) NANNOFOSSIL OOZE, very pale orange (10YR 8/2) to pinkish gray (5YR 8/1) soft, massive, oxidized subunit.

FORAMINIFER-BEARING (5–20%) NANNOFOSSIL OOZE, alternating subdominant pale olive (10Y 6/2) and dominant light gray (N7) to very light gray (N8) units, soft, massive with occasional pale olive (10Y 6/2) burrow mottles and medium gray (N5) pyrite streaks, diffuse contacts with host ooze.

SMEAR SLIDE SUMMARY:

	1, 8	1, 55	2, 22	2, 79
	D	D	D	D
Texture:				
Silt	A	A	A	A
Clay	D	D	D	D
Composition:				
Quartz	T	–	–	–
Volcanic glass	T–	–	T	–
Foraminifers	C	C	C	C
Calc. nannofossils	D	D	D	D
Diatoms	T	–	–	–
Radiolarians	T	–	T	–
Sponge spicules	T	–	–	–
Other	T	–	T	T

SITE 592 HOLE CORE 2 CORED INTERVAL 4.5–14.1 m

TIME – ROCK UNIT: Quaternary | BIOSTRATIGRAPHIC ZONE: NN19; *G. truncatulinoides/G. tosaensis*; *G. truncatulinoides/G. tosaensis* NN19 | FOSSIL CHARACTER: FORAMINIFERS, NANNOFOSSILS, RADIOLARIANS, DIATOMS (A; A; A; A; A, A) | SECTION: 1, 2, 3, 4, 5, 6, 7, CC | METERS: 0.5, 1.0 | GRAPHIC LITHOLOGY | DRILLING DISTURBANCE | SEDIMENTARY STRUCTURES | SAMPLES

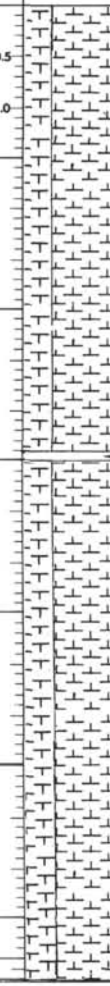

10Y 6/2
10Y 6/2
N8
10Y 6/2
N8
10Y 6/2
N8–N9
N8
10Y 6/2
N7–N8
10Y 6/2
N7
N7–8
10Y 6/2
N6 N8
IW
10Y 6/2
N9
N8
10Y 6/2
N8
10Y 8/2
N8
10Y 6/2
N8
N6
N8
N9
N8
10Y 8/2
N8

LITHOLOGIC DESCRIPTION

FORAMINIFER-BEARING NANNOFOSSIL OOZE, soft, very light gray (N8) and white (N9) to pale olive (10Y 6/2), contacts gradational, iron sulfide blebs and streaks (N6); in the pale olive parts more volcanic ash (1–5%); white (N9) part in Section 6 ← NANNOFOSSIL OOZE.

SMEAR SLIDE SUMMARY:

	2, 35	2, 103	6, 122
	D	D	D
Composition:			
Volcanic glass	T	R	R
Pyrite	–	T	T
Foraminifers	C	C	R
Calc. nannofossils	A	A	A
Other	–	–	C

SITE 592 HOLE CORE 3 CORED INTERVAL 14.1–23.7 m

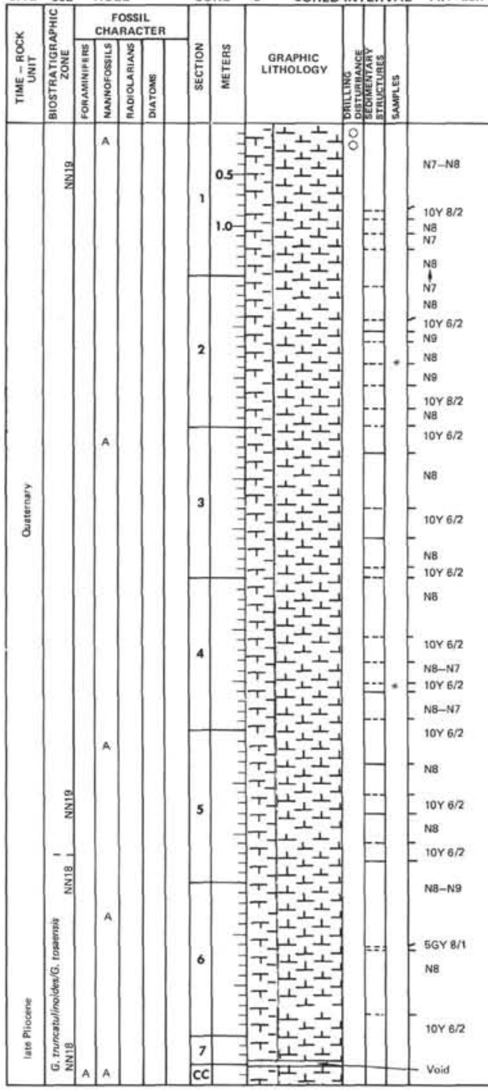

LITHOLOGIC DESCRIPTION

FORAMINIFER-BEARING NANNOFOSSIL OOZE, soft, alternating very light gray (N8) to light gray (N7) and pale greenish yellow (10Y 8/2) to pale olive (10Y 6/2), dark spots (N6), some burrows (10Y 6/2).

SMEAR SLIDE SUMMARY:

	2, 85	4, 106
	D	D
Composition:		
Volcanic glass	T	T
Pyrite	T	T
Foraminifers	C	C
Calc. nannofossils	A	A

SITE 592 HOLE CORE 4 CORED INTERVAL 23.7–33.3 m

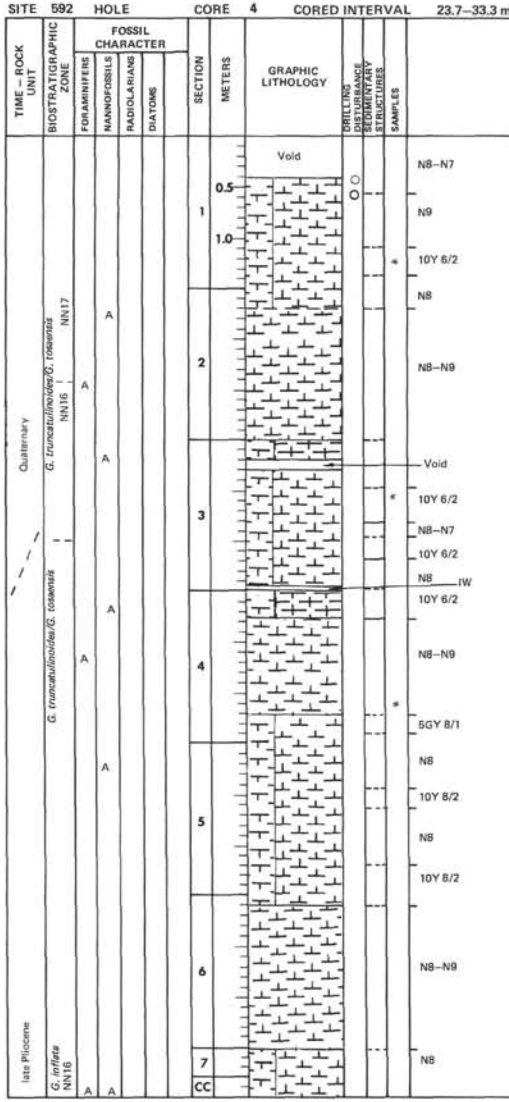

LITHOLOGIC DESCRIPTION

FORAMINIFER-BEARING NANNOFOSSIL OOZE, soft, very light gray (N8) to pale greenish yellow (10Y 8/2) and pale olive (10Y 6/2), dark spots and streaks (N6), some burrows (10Y 6/2); whitish (N9) parts less forams ← NANNOFOSSIL OOZE.

SMEAR SLIDE SUMMARY:

	1, 125	3, 56	4, 108
	D	D	D
Composition:			
Feldspar	T	–	–
Heavy minerals	T	T	T
Volcanic glass	T	T	T
Pyrite	T	T	–
Foraminifers	C	C	R
Calc. nannofossils	A	A	A

SITE 592 HOLE CORE 5 CORED INTERVAL 33.3–42.9 m

TIME – ROCK UNIT: late Pliocene

BIOSTRATIGRAPHIC ZONE: NN16; *G. inflata* NN16

FOSSIL CHARACTER: FORAMINIFERS | NANNOFOSSILS | RADIOLARIANS | DIATOMS — Nannofossils: A (Section 3), A (Section 6); Foraminifers A, Nannofossils A (CC)

SECTION: 1, 2, 3, 4, 5, 6, 7, CC

METERS: 0.5, 1.0

GRAPHIC LITHOLOGY | DRILLING DISTURBANCE | SEDIMENTARY STRUCTURES | SAMPLES

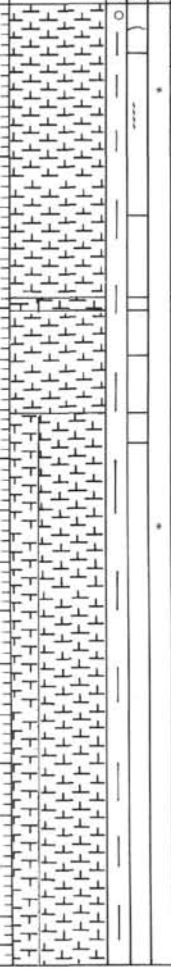

LITHOLOGIC DESCRIPTION

NANNOFOSSIL OOZE, soft, very light gray (N8) to white (N9), dark (N6) streaks, some pale olive (10Y 6/2) burrows.

FORAMINIFER-BEARING NANNOFOSSIL OOZE, soft, homogeneous, light greenish gray (5GY 7/1) some pale olive (10Y 6/2) burrows.

SMEAR SLIDE SUMMARY:

	1, 82 D	4, 64 D
Composition:		
Volcanic glass	R	T
Pyrite	T	T
Foraminifers	R	C
Calc. nannofossils	D	A

SITE 592 HOLE CORE 6 CORED INTERVAL 42.9–52.5 m

TIME – ROCK UNIT: late Pliocene

BIOSTRATIGRAPHIC ZONE: NN16; *G. inflata* NN15

FOSSIL CHARACTER: FORAMINIFERS | NANNOFOSSILS | RADIOLARIANS | DIATOMS — Nannofossils: A (Section 3); Foraminifers A, Nannofossils A (CC)

SECTION: 1, 2, 3, 4, 5, 6, 7, CC

METERS: 0.5, 1.0

GRAPHIC LITHOLOGY | DRILLING DISTURBANCE | SEDIMENTARY STRUCTURES | SAMPLES

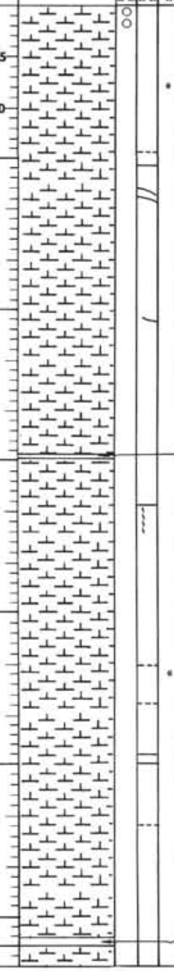

LITHOLOGIC DESCRIPTION

NANNOFOSSIL OOZE, soft, very light gray (N8) to light greenish gray (5GY 8/1), homogeneous. Some dark streaks (N7).

SMEAR SLIDE SUMMARY:

	1, 80 D	5, 60 D
Composition:		
Volcanic glass	T	T
Pyrite	T	T
Foraminifers	R	R
Calc. nannofossils	D	D

SITE 592 HOLE CORE 7 CORED INTERVAL 52.5–62.1 m

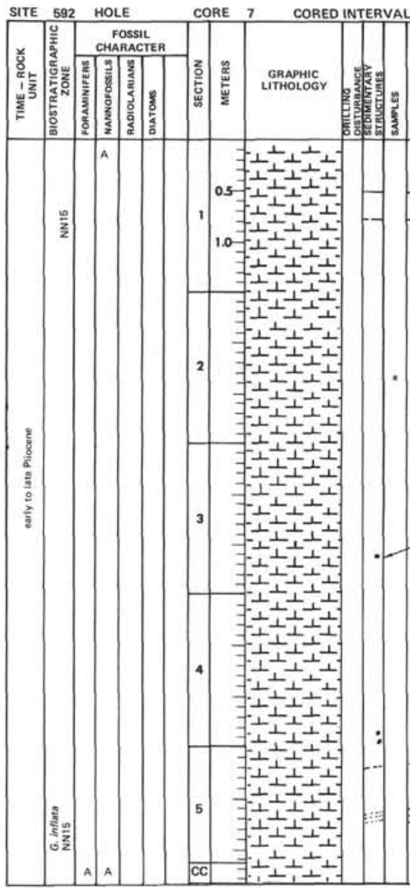

LITHOLOGIC DESCRIPTION

NANNOFOSSIL OOZE, soft, very light gray (N8), homogeneous, some dark (N7–N6) spots and streaks.

SMEAR SLIDE SUMMARY:

	2, 86
	D
Composition:	
Volcanic glass	R
Pyrite	T
Foraminifers	R
Calc. nannofossils	A

SITE 592 HOLE CORE 8 CORED INTERVAL 62.1–71.7 m

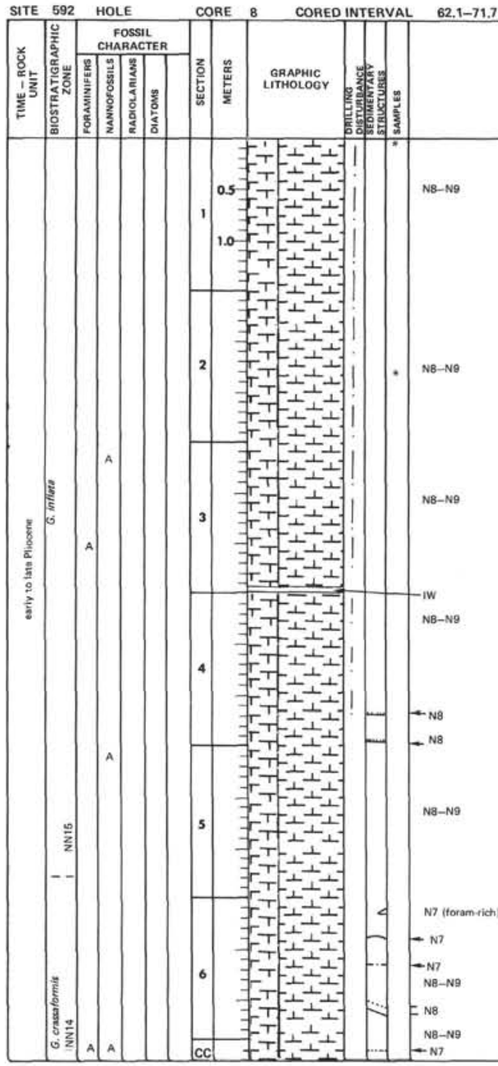

LITHOLOGIC DESCRIPTION

FORAMINIFER-BEARING NANNOFOSSIL OOZE, soft, white (N9) to very light gray (N8), homogeneous, some dark (N6–N7) spots and streaks.

SMEAR SLIDE SUMMARY:

	2, 81	1, 0[a]
	D	M
Composition:		
Quartz	–	T
Heavy minerals	T	–
Clay	–	A
Volcanic glass	T	C
Foraminifers	C	–
Calc. nannofossils	A	–

[a]insoluble residue

SITE 592 HOLE CORE 9 CORED INTERVAL 71.7–81.3 m

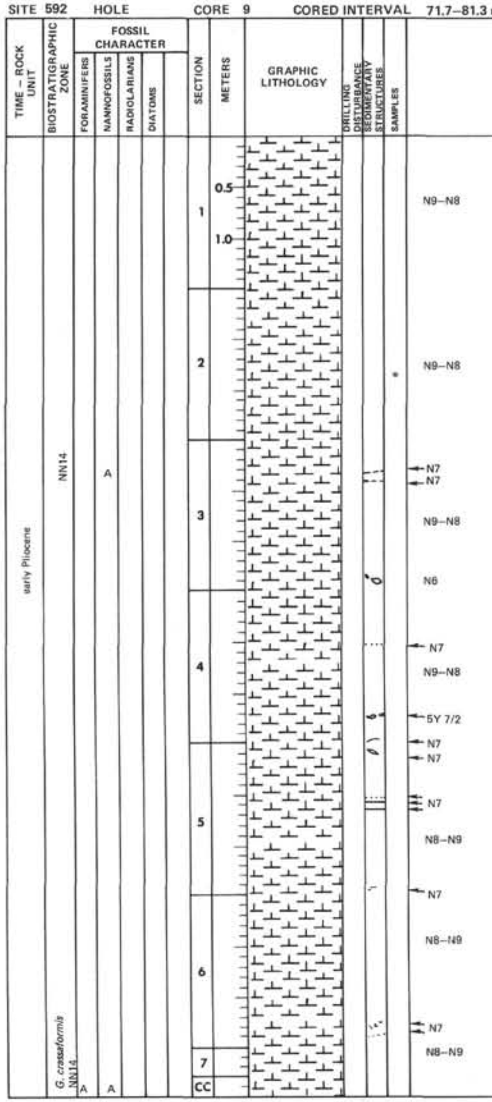

LITHOLOGIC DESCRIPTION

NANNOFOSSIL OOZE, soft, white (N9) to very light gray (N8), homogeneous, dark (N7–N6) spots and streaks rare.

SMEAR SLIDE SUMMARY:

	2, 80
	D
Composition:	
Volcanic glass	T
Foraminifers	R
Calc. nannofossils	D

SITE 592 HOLE CORE 10 CORED INTERVAL 81.3–90.9 m

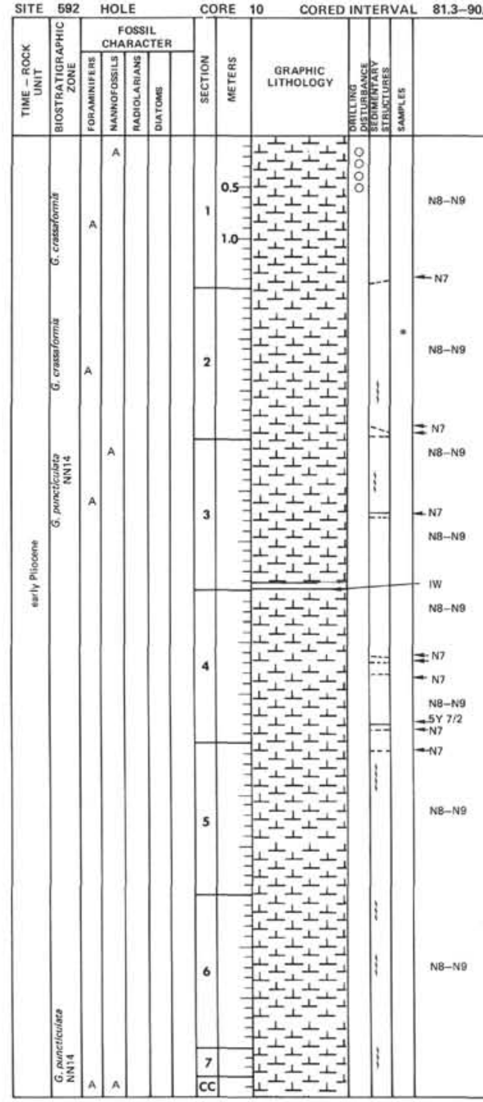

LITHOLOGIC DESCRIPTION

NANNOFOSSIL OOZE, soft, white (N9) to very light gray (N8), homogeneous, dark (N6–N7) spots and streaks very rare; bioturbation very rare.

SMEAR SLIDE SUMMARY:

	2, 51
	D
Composition:	
Volcanic glass	T
Pyrite	T
Foraminifers	R
Calc. nannofossils	D

SITE 592 HOLE CORE 11 CORED INTERVAL 90.9–100.5 m

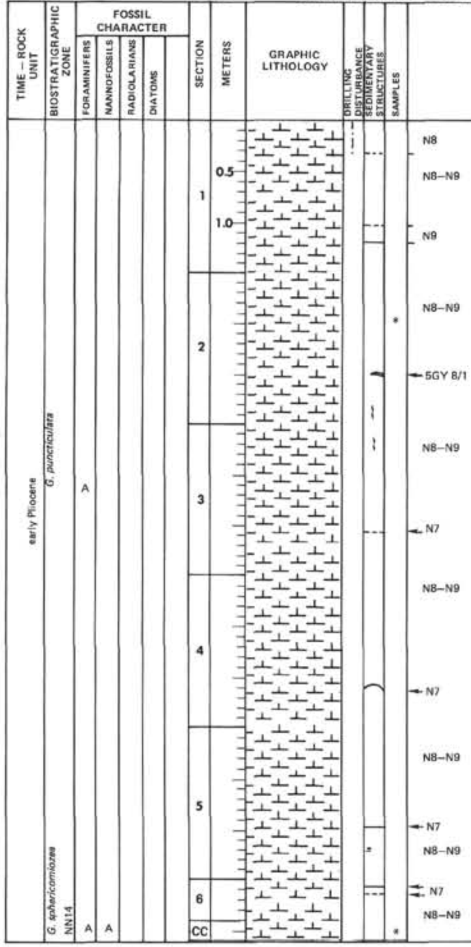

LITHOLOGIC DESCRIPTION

NANNOFOSSIL OOZE, soft, white (N9) to very light gray (N8), homogeneous, dark (N7–N6) spots and streaks rare.

SMEAR SLIDE SUMMARY:

	2, 50	CC[a]
	D	M
Composition:		
Quartz	–	T
Feldspar	–	T
Heavy minerals	–	T
Clay	–	A
Volcanic glass	T	R
Pyrite	–	R
Palagonite	T	–
Foraminifers	R	–
Calc. nannofossils	D	–

[a]insoluble residue

SITE 592 HOLE CORE 12 CORED INTERVAL 100.5–110.1 m

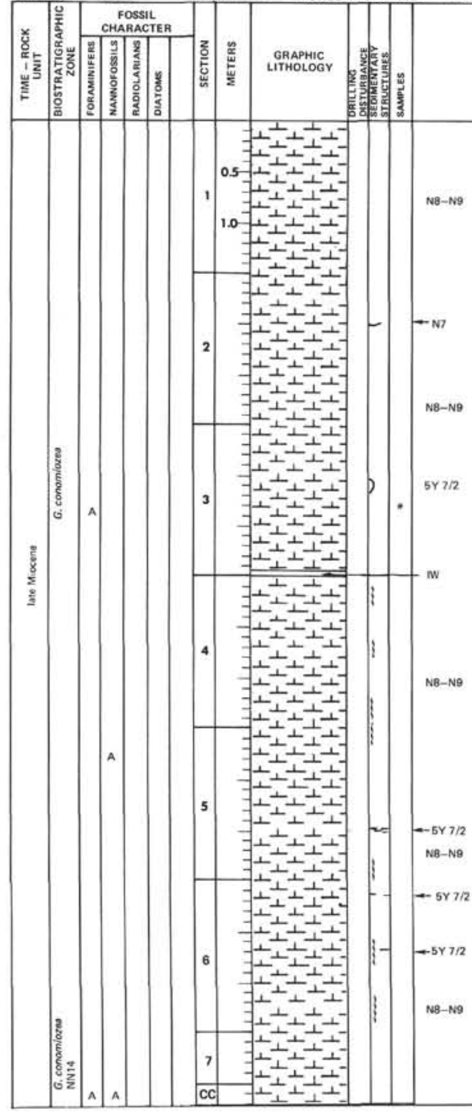

LITHOLOGIC DESCRIPTION

NANNOFOSSIL OOZE, soft, white (N9) to very light gray (N8), homogeneous, Section 4 to bottom, yellow gray (5Y 7/2) burrow mottles.

SMEAR SLIDE SUMMARY:

	3, 82
	D
Composition:	
Volcanic glass	T
Pyrite	T
Foraminifers	R
Calc. nannofossils	D

SITE 592 HOLE CORE 13 CORED INTERVAL 110.1–119.7 m

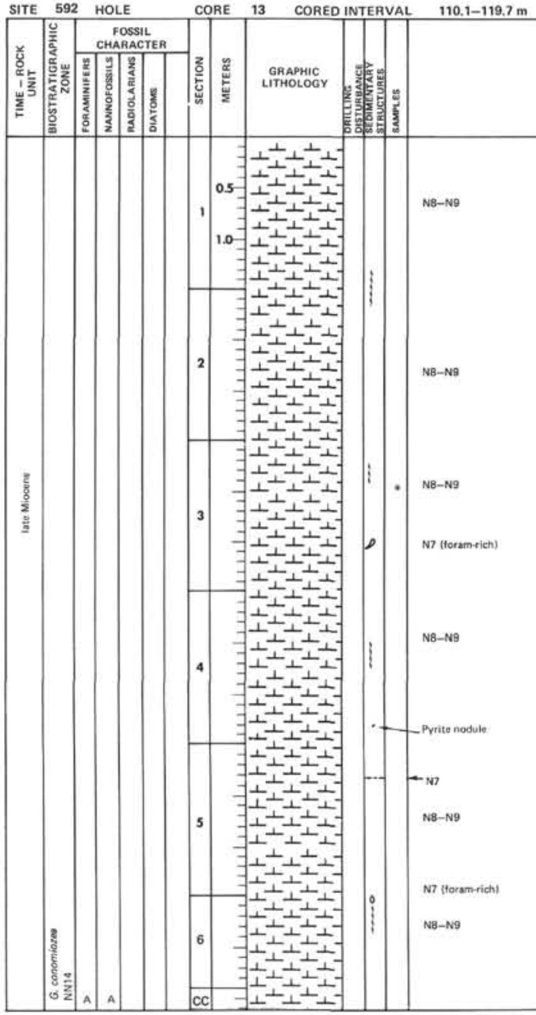

LITHOLOGIC DESCRIPTION

NANNOFOSSIL OOZE, soft, white (N9) to very light gray (N8), homogeneous. Some yellowish gray (5Y 7/2) mottles (burrows). Dark (N7–N6) spots rare.

SMEAR SLIDE SUMMARY:

	3, 45
	D
Composition:	
Volcanic glass	T
Pyrite	T
Foraminifers	R
Calc. nannofossils	D

SITE 592 HOLE CORE 14 CORED INTERVAL 119.7–129.3 m

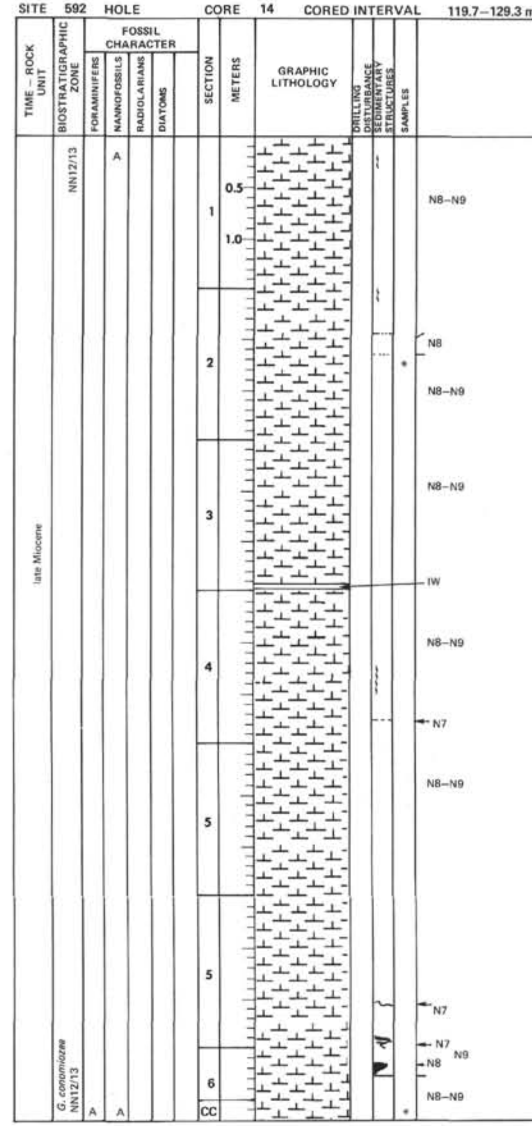

LITHOLOGIC DESCRIPTION

NANNOFOSSIL OOZE, soft, white (N9) to very light gray (N8), homogeneous. Some yellowish gray (5Y 7/2) mottles. Dark (N7–N6) spots rare.

SMEAR SLIDE SUMMARY:

	2, 80	CC[a]
	D	M
Composition:		
Quartz	–	T
Feldspar	–	T
Heavy minerals	–	T
Clay	–	A
Volcanic glass	T	T
Pyrite	–	R
Foraminifers	R	–
Calc. nannofossils	D	–

[a]insoluble residue

SITE 592 HOLE CORE 15 CORED INTERVAL 129.3–138.9 m

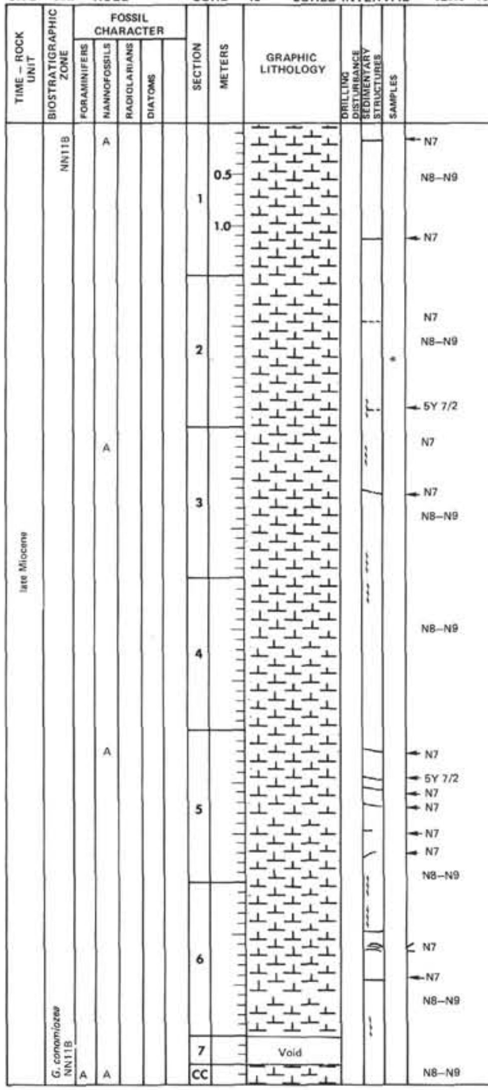

LITHOLOGIC DESCRIPTION

NANNOFOSSIL OOZE, soft, white (N9) to very light gray (N8), homogeneous, dark (N7–N6) spots. Some yellowish gray (5Y 7/2) mottles (burrows).

SMEAR SLIDE SUMMARY:

	2, 80
	D
Composition:	
Volcanic glass	T
Foraminifers	R
Calc. nannofossils	D

SITE 592 HOLE CORE 16 CORED INTERVAL 138.9–148.5 m

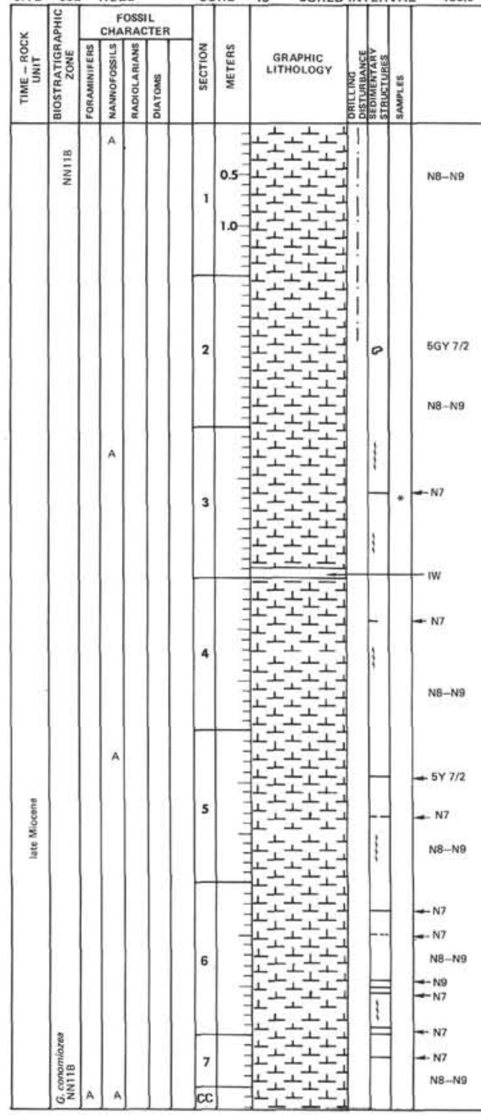

LITHOLOGIC DESCRIPTION

NANNOFOSSIL OOZE, soft, white (N9) to very light gray (N8), homogeneous, dark (N6–N7) and yellowish gray (5Y 7/2) spots ← burrows.

SMEAR SLIDE SUMMARY:

	3, 69
	D
Composition:	
Volcanic glass	T
Foraminifers	R
Calc. nannofossils	D

SITE 592 HOLE CORE 17 CORED INTERVAL 148.5–158.1 m

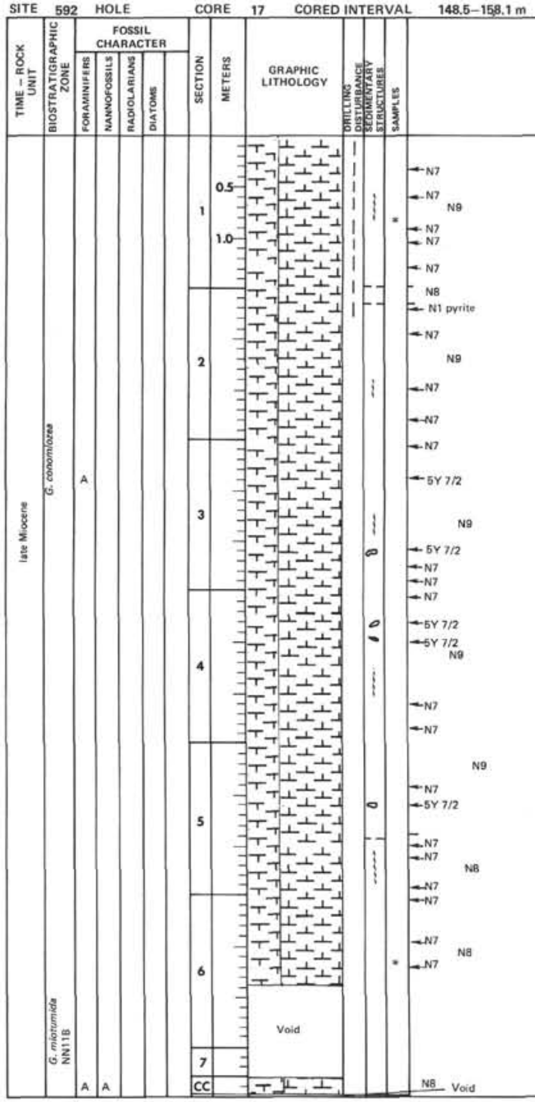

LITHOLOGIC DESCRIPTION

FORAMINIFER-BEARING (5–10%) NANNOFOSSIL OOZE, soft, white (N9) to very light gray (N8), with occasional light gray (N7) streaks, blebs and halos of pyritized ooze, as well as rare yellowish gray (5Y 7/2) burrow mottles, all with diffuse boundaries.

SMEAR SLIDE SUMMARY:

	1, 81	6, 68
	D	D
Texture:		
Silt	C	C
Clay	D	D
Composition:		
Volcanic glass	–	T
Foraminifers	C	C
Calc. nannofossils	D	D
Radiolarians	T	–

SITE 592 HOLE CORE 18 CORED INTERVAL 158.1–167.7 m

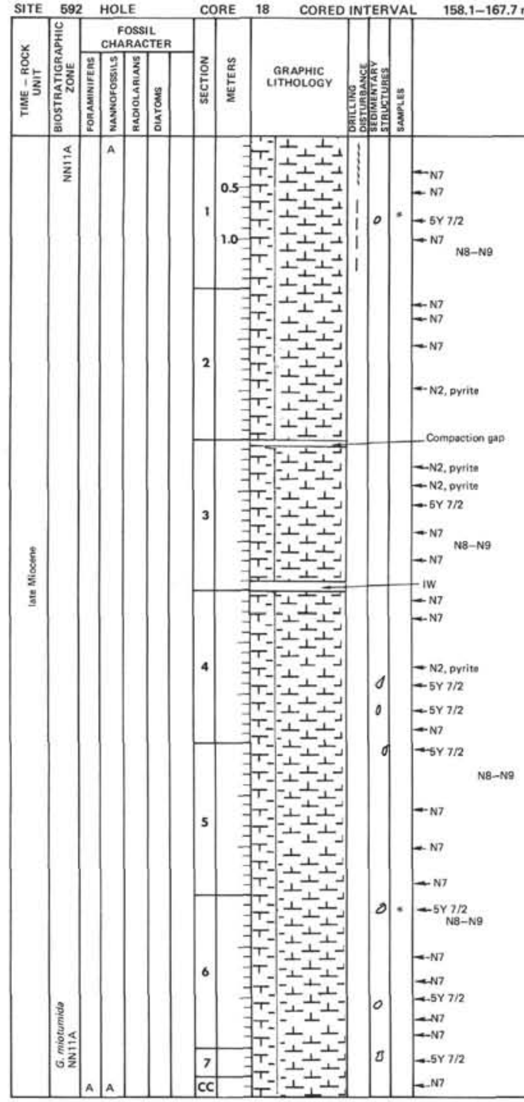

LITHOLOGIC DESCRIPTION

FORAMINIFER-BEARING (≥ 5%) NANNOFOSSIL OOZE, soft, white (N9) to very light gray (N8), massive with occasional yellowish gray (5Y 7/2) burrow mottles and pyritized (N7 to 5P 4/2) blebs and streaks, all having diffuse contacts with host ooze. Yellowish gray burrows contain more foraminifers (10–15%).

SMEAR SLIDE SUMMARY:

	1, 80	6, 18
	D	M
Texture:		
Silt	C	C
Clay	D	D
Composition:		
Volcanic glass	–	T
Pyrite	–	T
Foraminifers	C	C
Calc. nannofossils	D	D

SITE 592 HOLE CORE 19 CORED INTERVAL 167.7–177.3 m

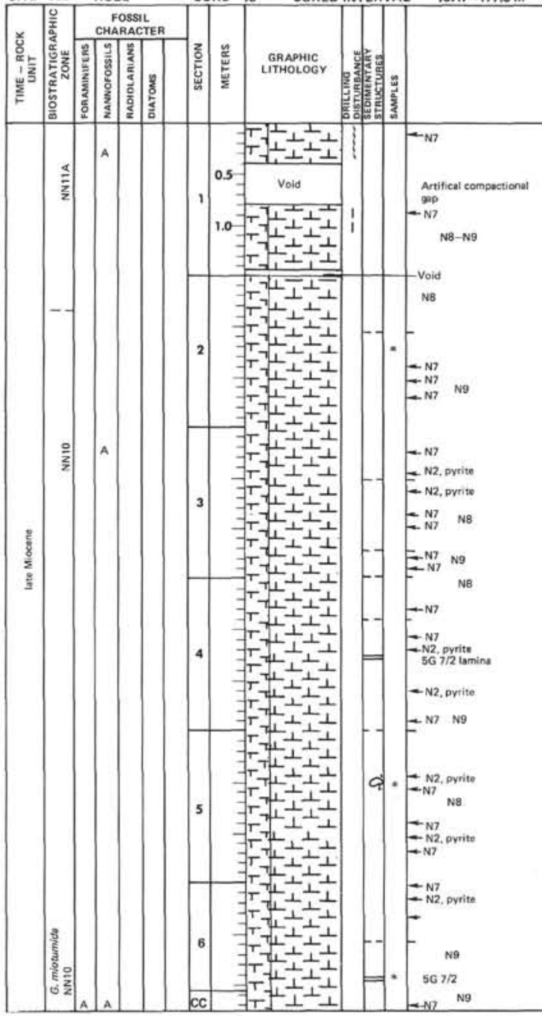

LITHOLOGIC DESCRIPTION

FORAMINIFER-BEARING (>5%) NANNOFOSSIL OOZE, soft, white (N9) to very light gray (N8), massive with light gray (N7) pyritized blebs and streaks. Rare pale green (5G 7/2) laminae.

SMEAR SLIDE SUMMARY:

	2, 77	5, 56	6, 85
	D	D	M
Texture:			
Silt	C	C	C
Clay	D	D	D
Composition:			
Volcanic glass	–	–	T
Foraminifers	C	C	C
Calc. nannofossils	D	D	D

SITE 592 HOLE CORE 20 CORED INTERVAL 177.3–186.9 m

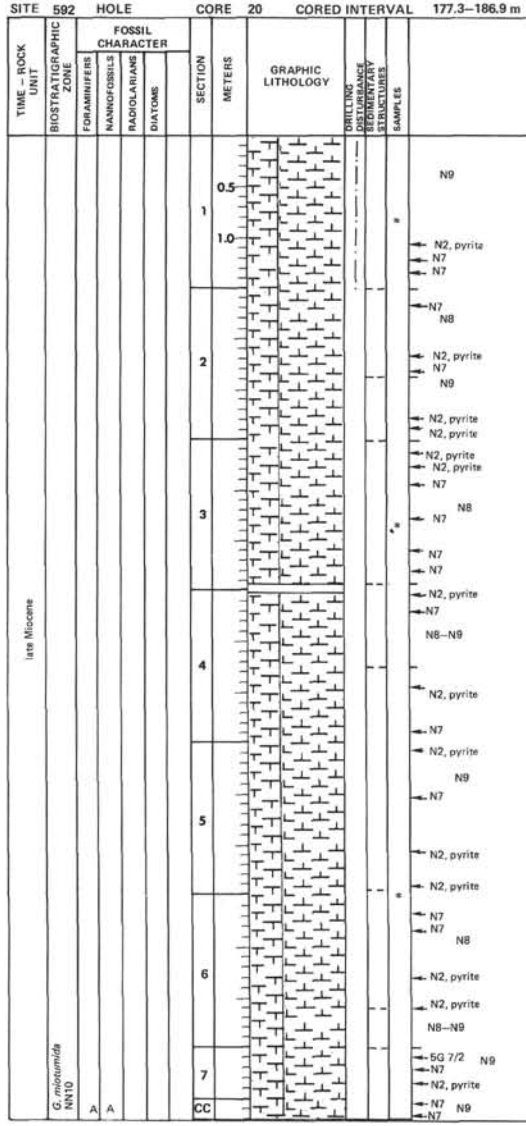

LITHOLOGIC DESCRIPTION

NANNOFOSSIL OOZE TO FORAMINIFER-BEARING (5–20%) NANNOFOSSIL OOZE, soft, white (N9) to very light gray (N8), massive with occasional light gray (N7) pyritized streaks and blebs. Irregular alternation of N8 and N9 color units with N8 enriched (5–20%) in foraminifers, all boundaries gradational. Pale green lamina in Section 7.

SMEAR SLIDE SUMMARY:

	1, 82	3, 81
	D	D
Texture:		
Silt	R	C
Clay	D	D
Composition:		
Volcanic glass	T	T
Foraminifers	R	C
Calc. nannofossils	D	D

SITE 592 HOLE CORE 21 CORED INTERVAL 186.9–196.5 m

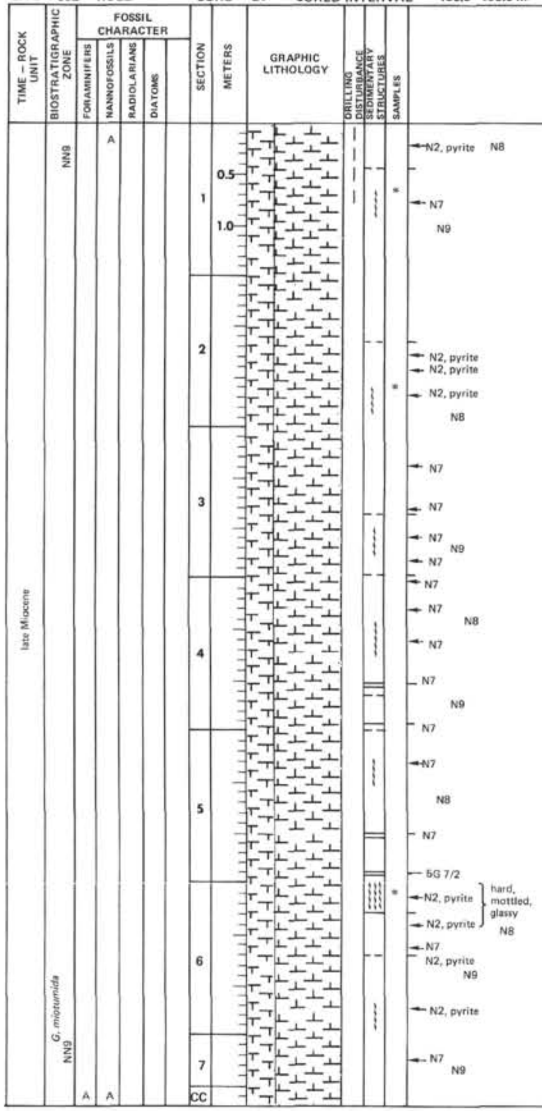

LITHOLOGIC DESCRIPTION

FORAMINIFER-BEARING (5–10%) NANNOFOSSIL OOZE TO (RARELY) FORAMINIFER (25–30%) NANNOFOSSIL OOZE, soft, white (N9) to very light gray (N8) in alternating units, the former with 10% foraminifers and the latter with 10–30% foraminifers, pyritized light gray (N7) blebs, streaks, and laminae scattered throughout. Pale green (5G 7/2) lamina in Section 5 with underlying 40 cm indurated, burrow mottled and containing scattered volcanic glass and pyrite.

SMEAR SLIDE SUMMARY:

	1, 68	2, 112	6, 15
	D	D	M
Texture:			
Silt	C	A	C
Clay	D	A	D
Composition:			
Volcanic glass	–	–	R
Pyrite	–	T	–
Foraminifers	C	A	C
Calc. nannofossils	D	A	D

SITE 592 HOLE CORE 22 CORED INTERVAL 196.5–206.1 m

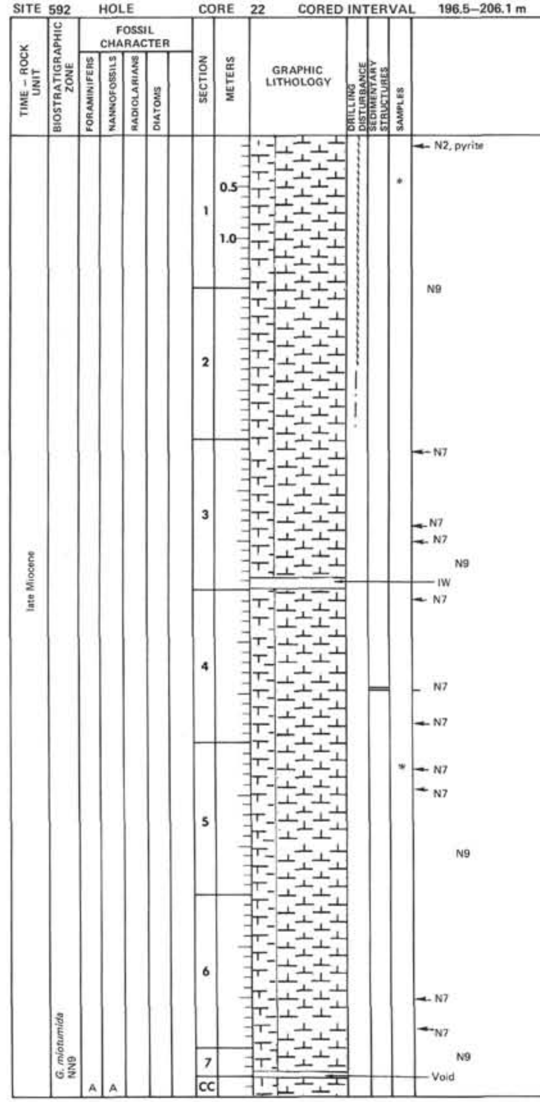

LITHOLOGIC DESCRIPTION

FORAMINIFER-BEARING (5–10%) NANNOFOSSIL OOZE, soft, predominantly white (N9) with rare very light gray (N8) shades, massive with rare light gray (N7) pyritized blebs. Featureless core compared to those above.

SMEAR SLIDE SUMMARY:

	1, 47	5, 23
	D	D
Texture:		
Silt	C	C
Clay	D	D
Composition:		
Volcanic glass	T	T
Foraminifers	C	C
Calc. nannofossils	D	D

SITE 592 HOLE CORE 23 CORED INTERVAL 206.1–215.7 m

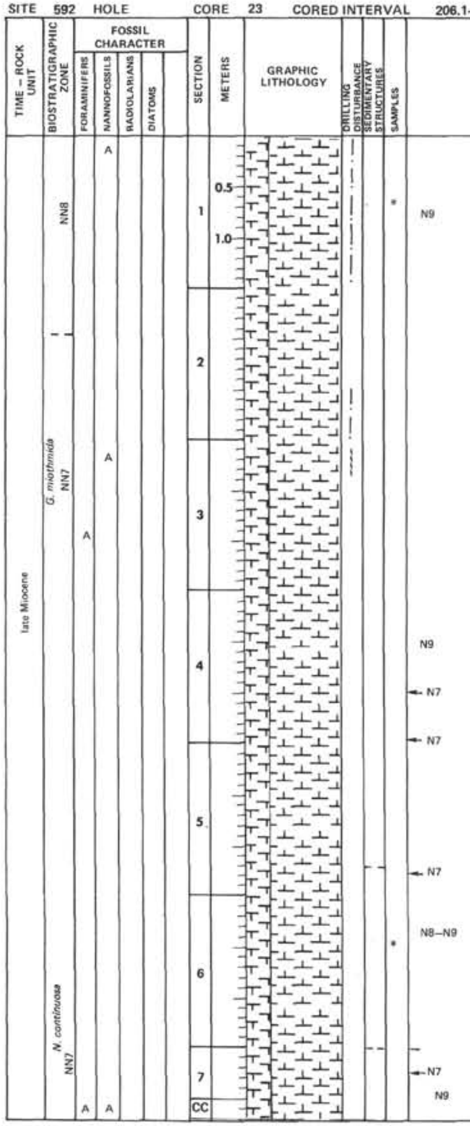

LITHOLOGIC DESCRIPTION

FORAMINIFER-BEARING (5–10%) NANNOFOSSIL OOZE, soft but firm, predominantly white (N9) with shades of N8 in some portions, massive with very rare light gray (N7) pyritized blebs. Featureless core overall.

SMEAR SLIDE SUMMARY:

	1, 84	6, 45
	D	D
Texture:		
Silt	C	C
Clay	D	D
Composition:		
Volcanic glass	T	T
Pyrite	T	T
Foraminifers	C	C
Calc. nannofossils	D	D

SITE 592 HOLE CORE 24 CORED INTERVAL 215.7–225.3 m

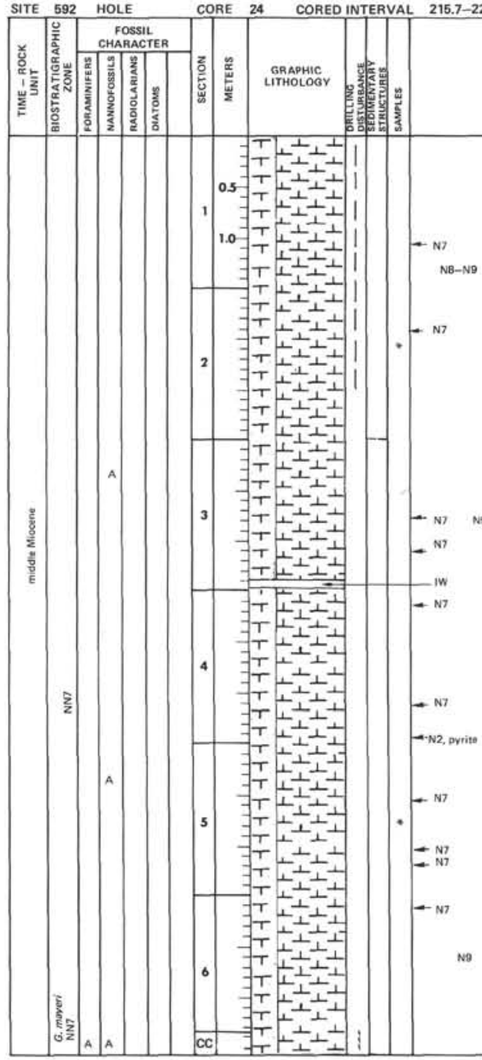

LITHOLOGIC DESCRIPTION

FORAMINIFER-BEARING (~ 5%) NANNOFOSSIL OOZE, soft but firm, predominantly white (N9) with shades of very light gray (N8) in Sections 1 and 2, massive with rare light gray (N7) pyritized blebs and streaks.

SMEAR SLIDE SUMMARY:

	2, 72	5, 75
	D	D
Texture:		
Silt	C	C
Clay	D	D
Composition:		
Volcanic glass	T	T
Pyrite	T	–
Foraminifers	C	C
Calc. nannofossils	D	D

SITE 592 HOLE CORE 25 CORED INTERVAL 225.3–234.9 m

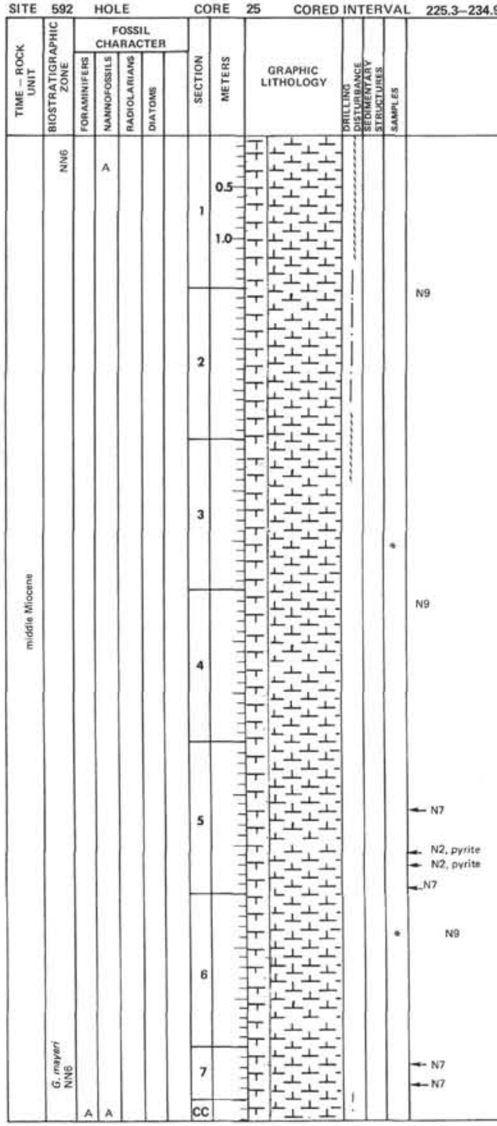

LITHOLOGIC DESCRIPTION

FORAMINIFER-BEARING (5–10%) NANNOFOSSIL OOZE, soft, white (N9), massive with very rare light gray (N7) pyritized blebs.

SMEAR SLIDE SUMMARY:

	3, 107	6, 40
	D	D
Texture:		
Silt	C	C
Clay	D	D
Composition:		
Volcanic glass	T	T
Foraminifers	C	C
Calc. nannofossils	D	D

SITE 592 HOLE CORE 26 CORED INTERVAL 234.9–244.5 m

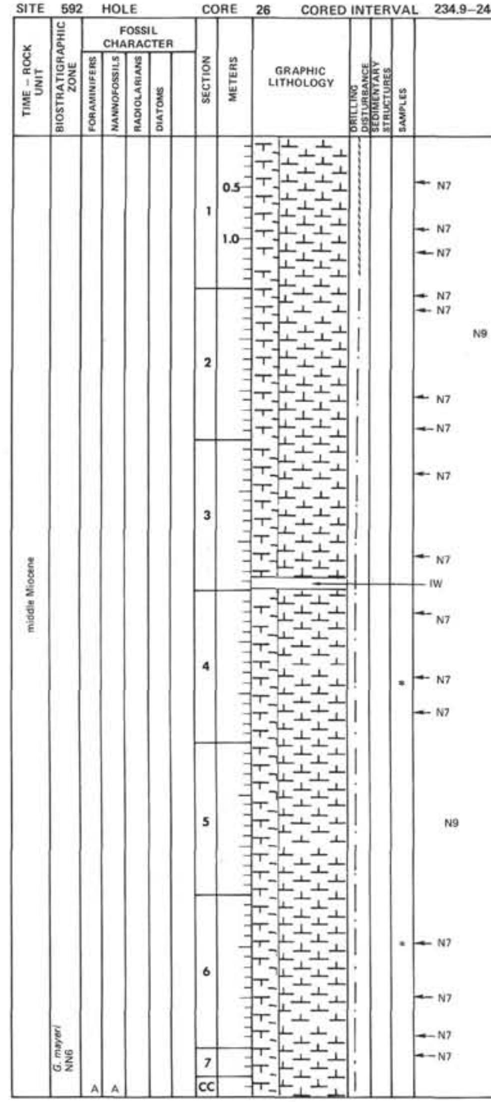

LITHOLOGIC DESCRIPTION

FORAMINIFER-BEARING (~5%) NANNOFOSSIL OOZE, soft, white, massive with rare light gray (N7) pyritized blebs which are streaked out to varying degree by coring disturbance.

SMEAR SLIDE SUMMARY:

	4, 88	6, 95
	D	M
Texture:		
Silt	R	C
Clay	D	D
Composition:		
Volcanic glass	T	T
Pyrite	T	T
Foraminifers	R	C
Calc. nannofossils	D	D

SITE 592 HOLE CORE 28 CORED INTERVAL 254.1–263.7 m

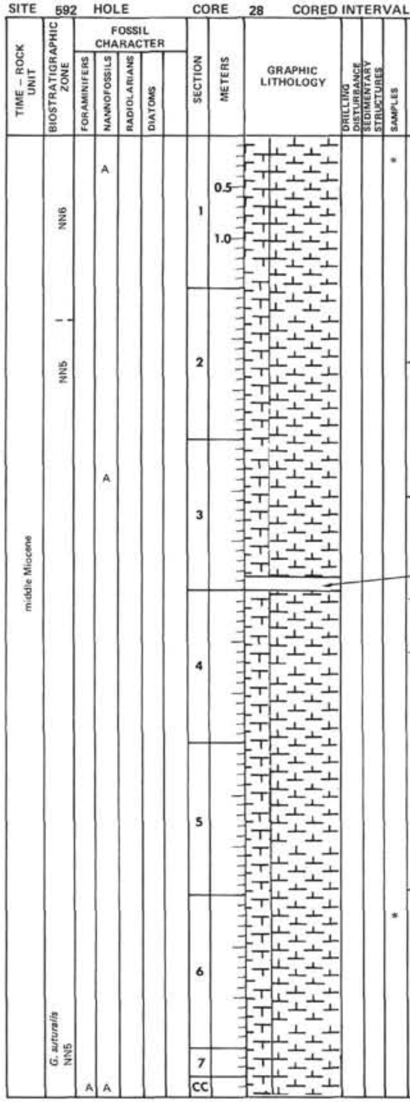

LITHOLOGIC DESCRIPTION

FORAMINIFER-BEARING (5–10%) NANNOFOSSIL OOZE, soft, with occasional firmer biscuits, white (N9) to bluish white (5B 9/1), entirely massive except for very rare light gray (N7) and grayish black (N2) pyritized burrows and blebs more intensely white than above cores and uniformity makes evaluation of possible coring disturbance difficult.

SMEAR SLIDE SUMMARY:

	1, 26	6, 20
	D	D
Texture:		
Silt	C	C
Clay	D	D
Composition:		
Volcanic glass	T	T
Foraminifers	C	C
Calc. nannofossils	D	D

SITE 592 HOLE CORE 29 CORED INTERVAL 263.7–273.3 m

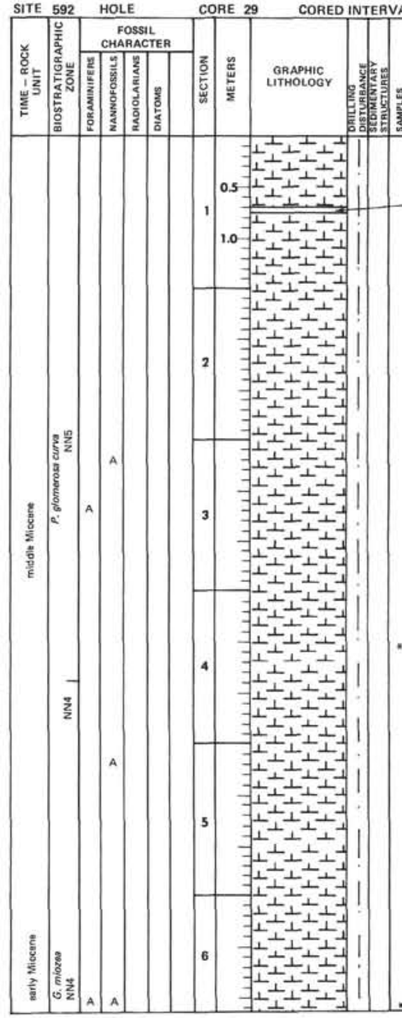

LITHOLOGIC DESCRIPTION

NANNOFOSSIL OOZE, soft to firm, white (N9), homogeneous.

Drilling disturbance:

Broken in biscuits

SMEAR SLIDE SUMMARY:

	4, 67	6, 115[a]
	D	
Composition:		
Quartz	–	T
Feldspar	–	T
Heavy minerals	–	T
Clay	–	A
Volcanic glass	T	C
Pyrite	–	T
Foraminifers	R	–
Calc. nannofossils	D	–
Radiolarians	T	–

[a]insoluble residue

SITE 592 HOLE CORE 30 CORED INTERVAL 273.3–282.9 m

TIME – ROCK UNIT	BIOSTRATIGRAPHIC ZONE	FORAMINIFERS	NANNOFOSSILS	RADIOLARIANS	DIATOMS	SECTION	METERS	GRAPHIC LITHOLOGY	DRILLING DISTURBANCE	SEDIMENTARY STRUCTURES	SAMPLES	LITHOLOGIC DESCRIPTION
early Miocene	G. miozea NN4	A	A			1, 2, 3, 4, 5, 6, CC	0.5, 1.0				*	

N9

N8–N9

N9

N9–N7

N9

N8–N9

FORAMINIFER-BEARING NANNOFOSSIL CHALK (soft→) firm, white (N9) to very light gray (N8), homogeneous. Bioturbation in the lower part.

SMEAR SLIDE SUMMARY:

	3, 56
	D
Composition:	
Volcanic glass	T
Micrite	C
Foraminifers	C
Calc. nannofossils	A

SITE 592 HOLE CORE 31 CORED INTERVAL 282.9–292.5 m

TIME – ROCK UNIT	BIOSTRATIGRAPHIC ZONE	FORAMINIFERS	NANNOFOSSILS	RADIOLARIANS	DIATOMS	SECTION	METERS	GRAPHIC LITHOLOGY	DRILLING DISTURBANCE	SEDIMENTARY STRUCTURES	SAMPLES	LITHOLOGIC DESCRIPTION
early Miocene	NN4 G. miozea; NN3; G. trilobus NN3	A; A	A; A; A			1, 2, 3, 4, 5, 6, CC	0.5, 1.0				*	

N9

N8

N9

N8–N9

IW

N8–N9 to 5GY 8/1

Celestite(?)

N8–N9 to 5GY 8/1

N9–5GY 8/1

NANNOFOSSIL CHALK, firm, white (N9) and very light gray to light greenish gray (5GY 8/1), some bioturbation. Top of the core (0–100 cm) very disturbed by drilling.

SMEAR SLIDE SUMMARY:

	4, 68
	D
Composition:	
Volcanic glass	T
Micrite	C
Foraminifers	R
Calc. nannofossils	A

SITE 592 HOLE CORE 32 CORED INTERVAL 292.5–302.1 m

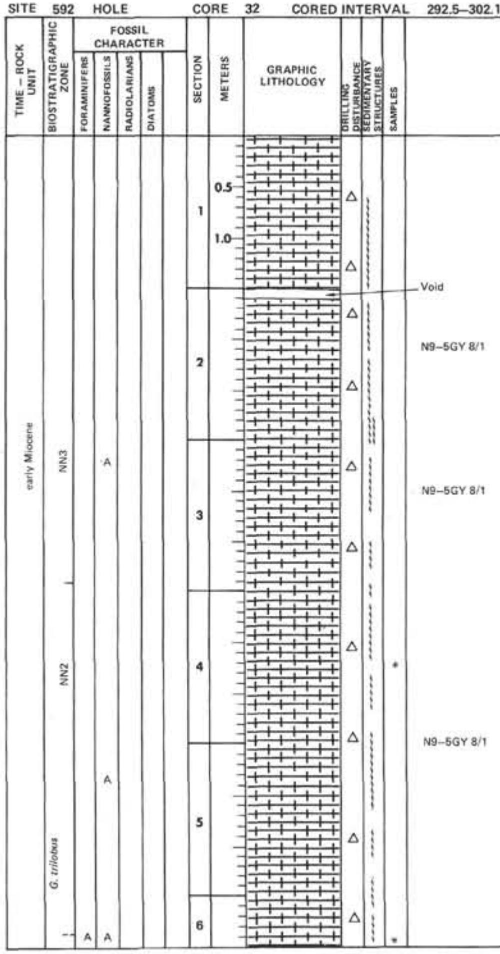

LITHOLOGIC DESCRIPTION

NANNOFOSSIL CHALK, firm, white (N9) to very light greenish gray (5GY 8/1), moderately bioturbated.

SMEAR SLIDE SUMMARY:

	4, 71	6, 50[a]
	D	M
Composition:		
Feldspar	–	T
Heavy minerals	–	T
Clay	–	A
Volcanic glass	T	T
Pyrite	–	T
Micrite	C	–
Foraminifers	R	–
Calc. nannofossils	A	–
Undefined	–	C

[a]insoluble residue

SITE 592 HOLE CORE 33 CORED INTERVAL 302.1–311.7 m

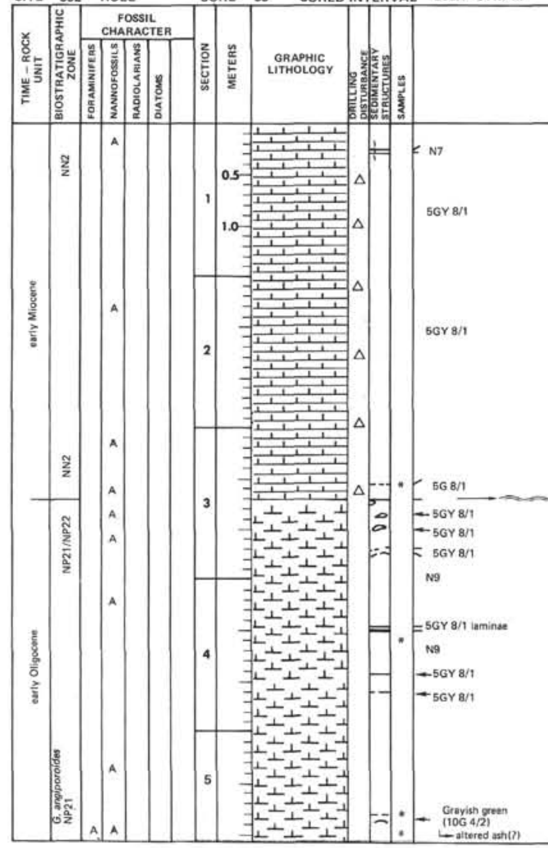

LITHOLOGIC DESCRIPTION

NANNOFOSSIL CHALK, firm, light greenish gray (5GY 8/1 to 5G 8/1), some bioturbation in the upper part. Sharp boundary near 70 cm in Section 3: below soft, white (N9), sometimes light greenish gray (5GY 8/1) laminae
└NANNOFOSSIL OOZE.

SMEAR SLIDE SUMMARY:

	3, 60	4, 60	5, 77	CC[a]
	D	D	M	M
Composition:				
Quartz	–	–	–	T
Feldspar	T	–	–	T
Heavy minerals	–	–	T	–
Volcanic glass	T	–	D	T
Pyrite	T	–	–	–
Zeolites	–	–	–	D
Micrite	C	–	–	–
Foraminifers	R	R	R	–
Calc. nannofossils	A	D	A	–

[a]insoluble residue

SITE 592 HOLE CORE 34 CORED INTERVAL 311.7–321.3 m

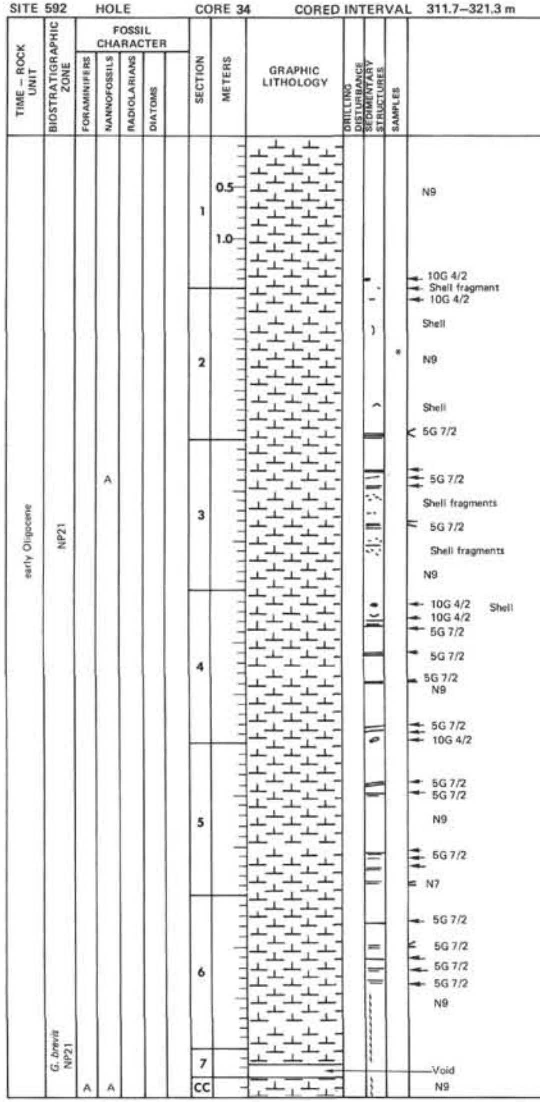

LITHOLOGIC DESCRIPTION

NANNOFOSSIL OOZE, soft, white (N9), thin pale green (5G 7/2) laminae and grayish green (10G 7/2) pockets ⟵volcanic glass (smear slide); Sections 1–4 shell fragments (oysters), 1–4 cm size; bioturbation in Sections 6 and 7 (beautiful *Zoophycos, Planolites*).

SMEAR SLIDE SUMMARY:

	2, 66	4, 141
	D	M
Composition:		
Volcanic glass	T	A
Pyrite	–	R
Foraminifers	R	T
Calc. nannofossils	D	A

SITE 592 HOLE CORE 35 CORED INTERVAL 321.3–330.9 m

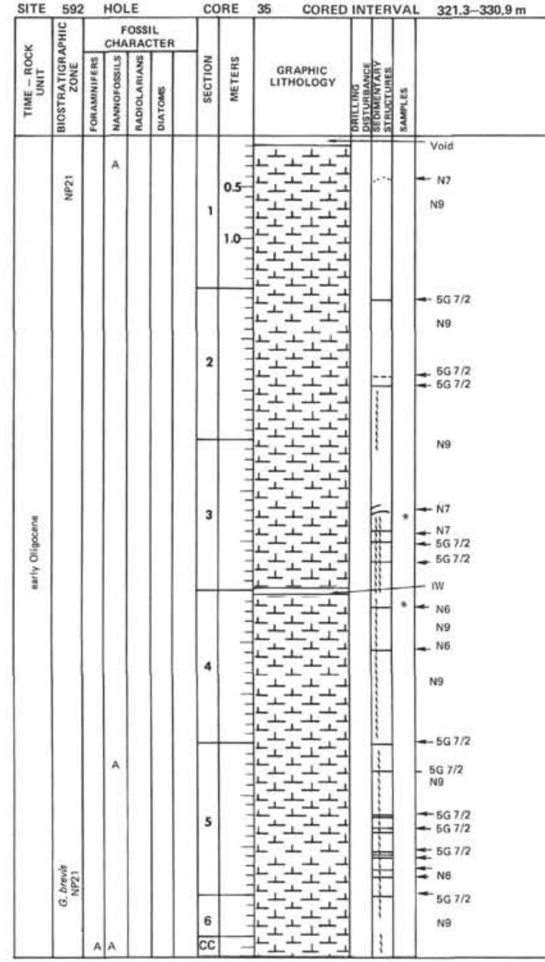

LITHOLOGIC DESCRIPTION

NANNOFOSSIL OOZE, soft, white (N9), upper part homogeneous (Section 1), thin pale green (5G 7/2) laminae, (⟵volcanic ash layers?); moderate bioturbation (beautiful *Zoophycos*).

SMEAR SLIDE SUMMARY:

	3, 78	4, 14
	D	M
Composition:		
Feldspar	T	–
Heavy minerals	–	T
Volcanic glass	T	–
Pyrite	–	C
Foraminifers	R	R
Calc. nannofossils	D	D
Diatoms	T	–

SITE 592 HOLE CORE 36 CORED INTERVAL 330.9–340.5 m

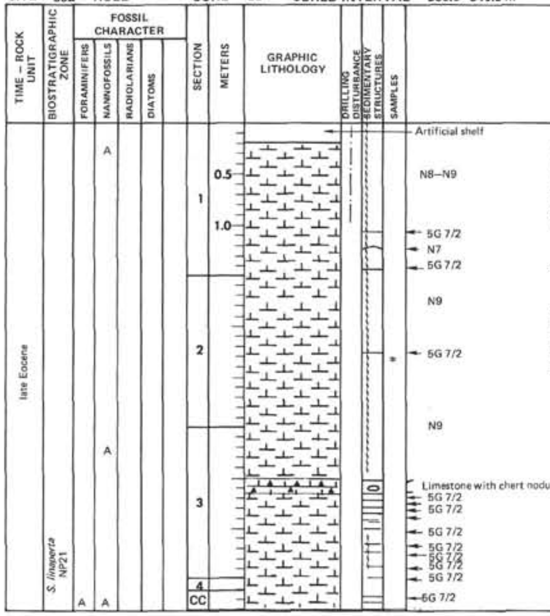

LITHOLOGIC DESCRIPTION

NANNOFOSSIL OOZE, soft, white (N9) to very light gray (N8); thin pale green (5G 7/2) laminae ← volcanic ash layers(?); bioturbation (*Zoophycos*, yellowish gray [5Y 8/1] burrows).

Section 3, 50–63 cm: lithified, limestone, chert nodule in the center.

SMEAR SLIDE SUMMARY:

	2, 82
	D
Composition:	
Feldspar	T
Pyrite	T
Foraminifers	R
Calc. nannofossils	D

SITE 592 HOLE CORE 37 CORED INTERVAL 340.5–350.1 m

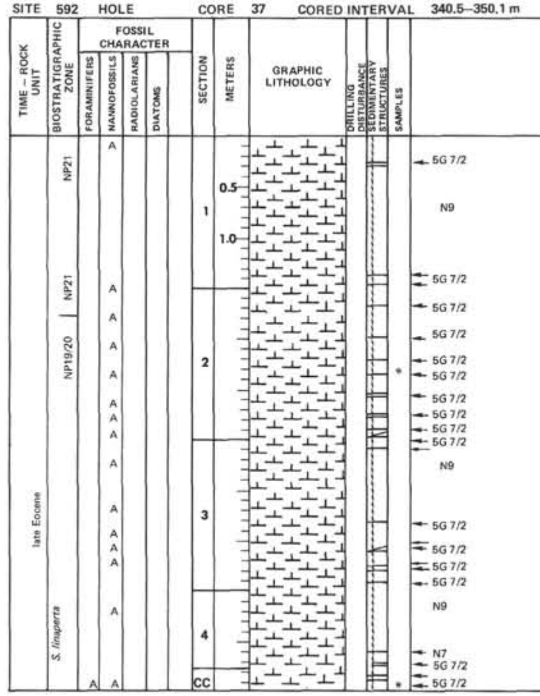

LITHOLOGIC DESCRIPTION

RECRYSTALLIZED NANNOFOSSIL OOZE, soft → firm, white (N9) to very light gray (N8); moderately bioturbated. Burrows (5Y 8/1); thin pale green (5G 7/2) laminae, (volcanic ash layers[?]).

SMEAR SLIDE SUMMARY:

	2, 88	CC[a]
	D	M
Composition:		
Quartz	T	–
Feldspar	T	–
Volcanic glass	–	R
Micrite	C	–
Clay	–	C
Foraminifers	R	–
Calc. nannofossils	D	–
Sponge spicules	T	C
Radiolarians	–	C
Silicoflagellates	–	T

[a]insoluble residue

SITE 592 HOLE CORE 38 CORED INTERVAL 350.1–359.7 m

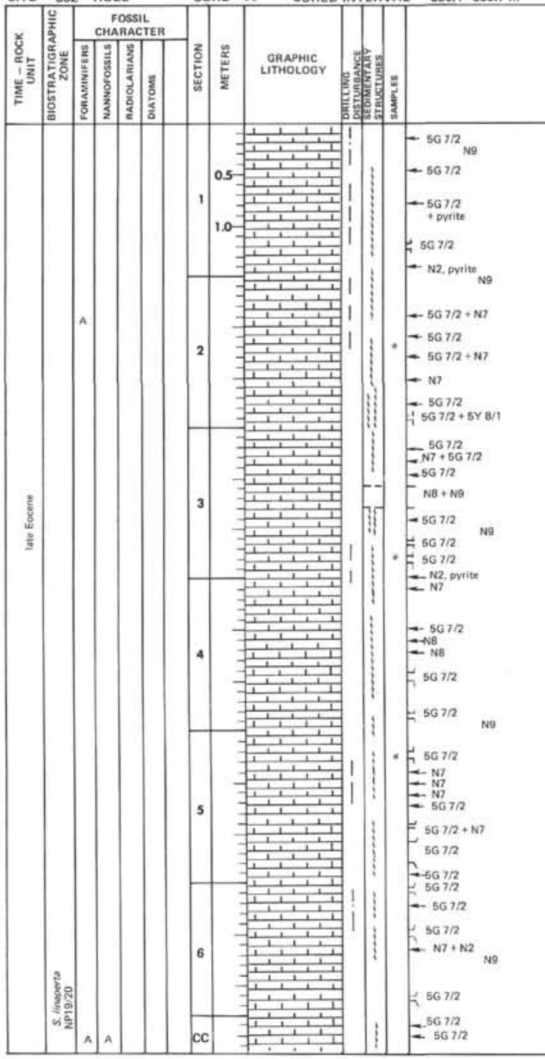

LITHOLOGIC DESCRIPTION

NANNOFOSSIL (OOZE TO) CHALK, soft to firm, white (N9) to rarely very light gray (N8), with many levels of pale green (5G 7/2) color laminations superimposed, as well as less common light gray (N7) and grayish black (N2) pyritized laminae, wisps, halos and blebs. Bioturbation slight to moderate with some *Zoophycos* and *Chondrites*.

SMEAR SLIDE SUMMARY:

	2, 73	5, 32	3, 133
	D	M	D
Texture:			
Silt	R	R	R
Clay	D	D	D
Composition:			
Quartz	–	T	–
Volcanic glass	T	R	T
Carbonate unspec.	C	C	C
Foraminifers	R	R	R
Calc. nannofossils	D	D	D

SITE 592 HOLE CORE 39 CORED INTERVAL 359.7–369.3 m

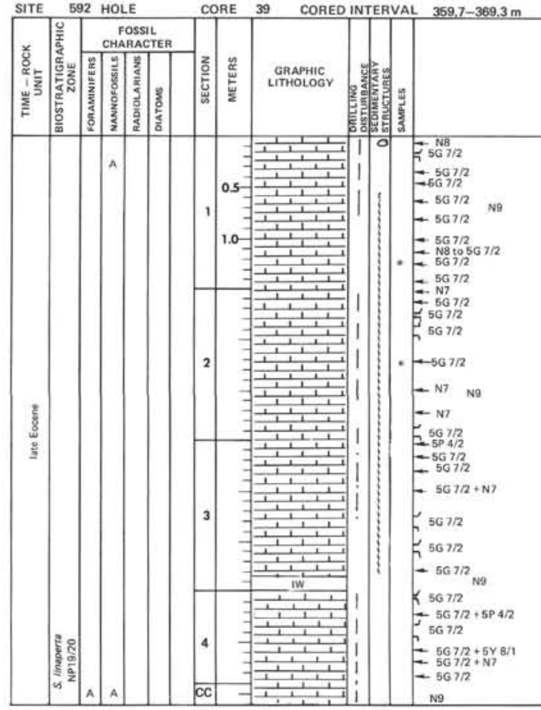

LITHOLOGIC DESCRIPTION

NANNOFOSSIL (OOZE TO) CHALK, firm (softer intervals possibly due to coring), white (N9) with very common superimposed pale gray (5G 7/2) color laminae and less common light gray (N7) and grayish purple (5P 4/2) wisps, laminae and blebs. Slight to moderate bioturbation with *Zoophycos*- and *Planolites*-like burrows evident in yellowish gray (5Y 8/1) tones.

SMEAR SLIDE SUMMARY:

	1, 126	2, 84
	D	M
Texture:		
Silt	R	R
Clay	D	D
Composition:		
Volcanic glass	T	T
Carbonate unspec.	C	C
Foraminifers	R	R
Calc. nannofossils	D	D

SITE 592 HOLE CORE 40 CORED INTERVAL 369.3–378.9 m

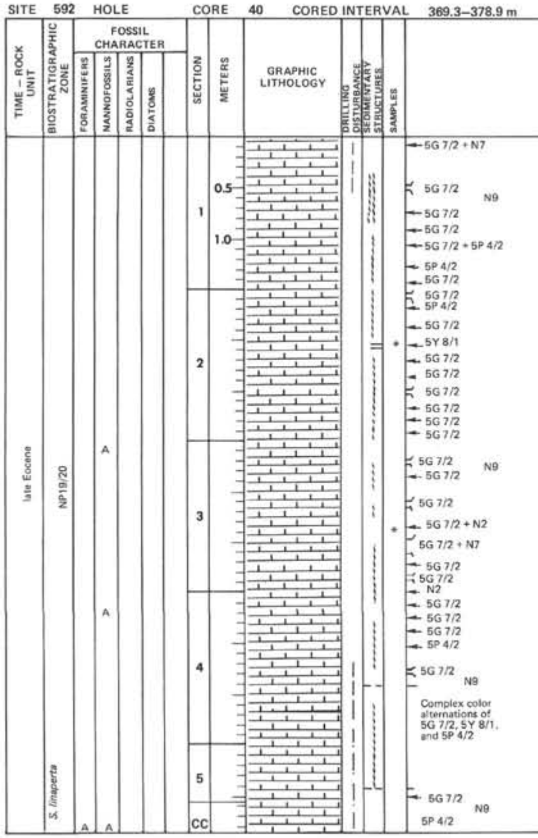

LITHOLOGIC DESCRIPTION

NANNOFOSSIL CHALK, generally firm, white (N9) with prominent color laminations of mainly pale green (5G 7/2) but also grayish purple (5P 4/2) and yellowish gray (5Y 8/1), the same colors occurring as streaks, swirls, and halos. Bioturbation slight to moderate with some *Zoophycos* defined by yellowish gray (5Y 8/1) spreite.

SMEAR SLIDE SUMMARY:

	2, 64	3, 86
	M	D
Texture:		
Silt	R	R
Clay	D	D
Composition:		
Volcanic glass	T	–
Carbonate unspec.	C	C
Foraminifers	R	R
Calc. nannofossils	A	A
Diatoms	T	–
Radiolarians	R	R
Sponge spicules	T	T

SITE 592 HOLE CORE 41 CORED INTERVAL 378.9–388.5 m

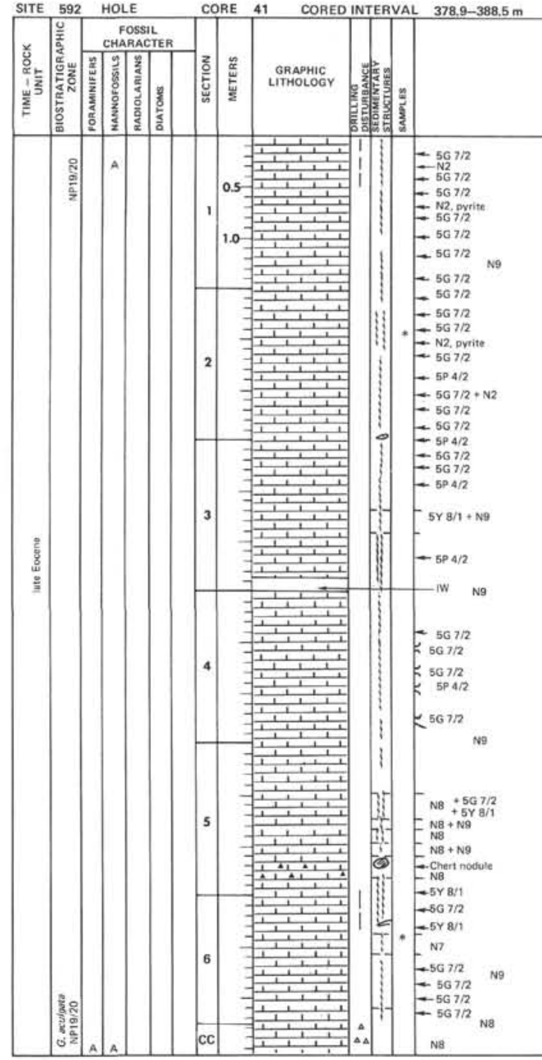

LITHOLOGIC DESCRIPTION

NANNOFOSSIL CHALK, generally firm (some biscuit structures), white (N9) to very light gray (N8) with superimposed color laminations of mainly pale green (5G 7/2) with rare yellowish gray (5Y 8/1) and minor pyritized light gray (N7) to grayish black (N2). Color laminae, streaks and swirls locally complex. Bioturbation slight to moderate with common *Zoophycos*- and some *Chondrites*- and *Planolites*-like burrows.

SMEAR SLIDE SUMMARY:

	6, 37	2, 43
	D	M
Texture:		
Silt	R	R
Clay	D	D
Composition:		
Volcanic glass	T	T
Carbonate unspec.	C	C
Foraminifers	R	R
Calc. nannofossils	D	D
Radiolarians	R	–
Sponge spicules	T	–

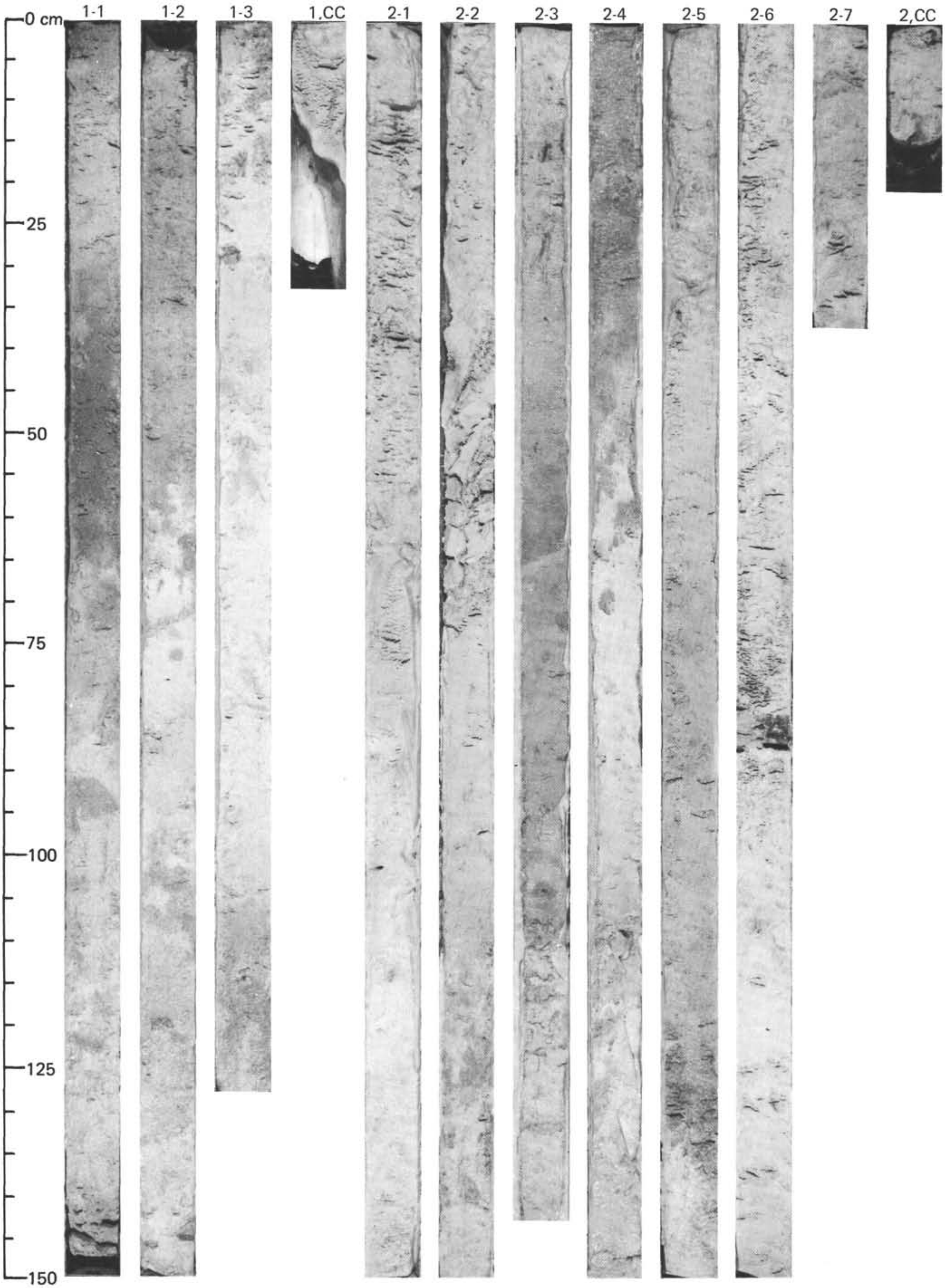
0 cm
25
50
75
100
125
150
1-1
1-2
1-3
1,CC
2-1
2-2
2-3
2-4
2-5
2-6
2-7
2,CC

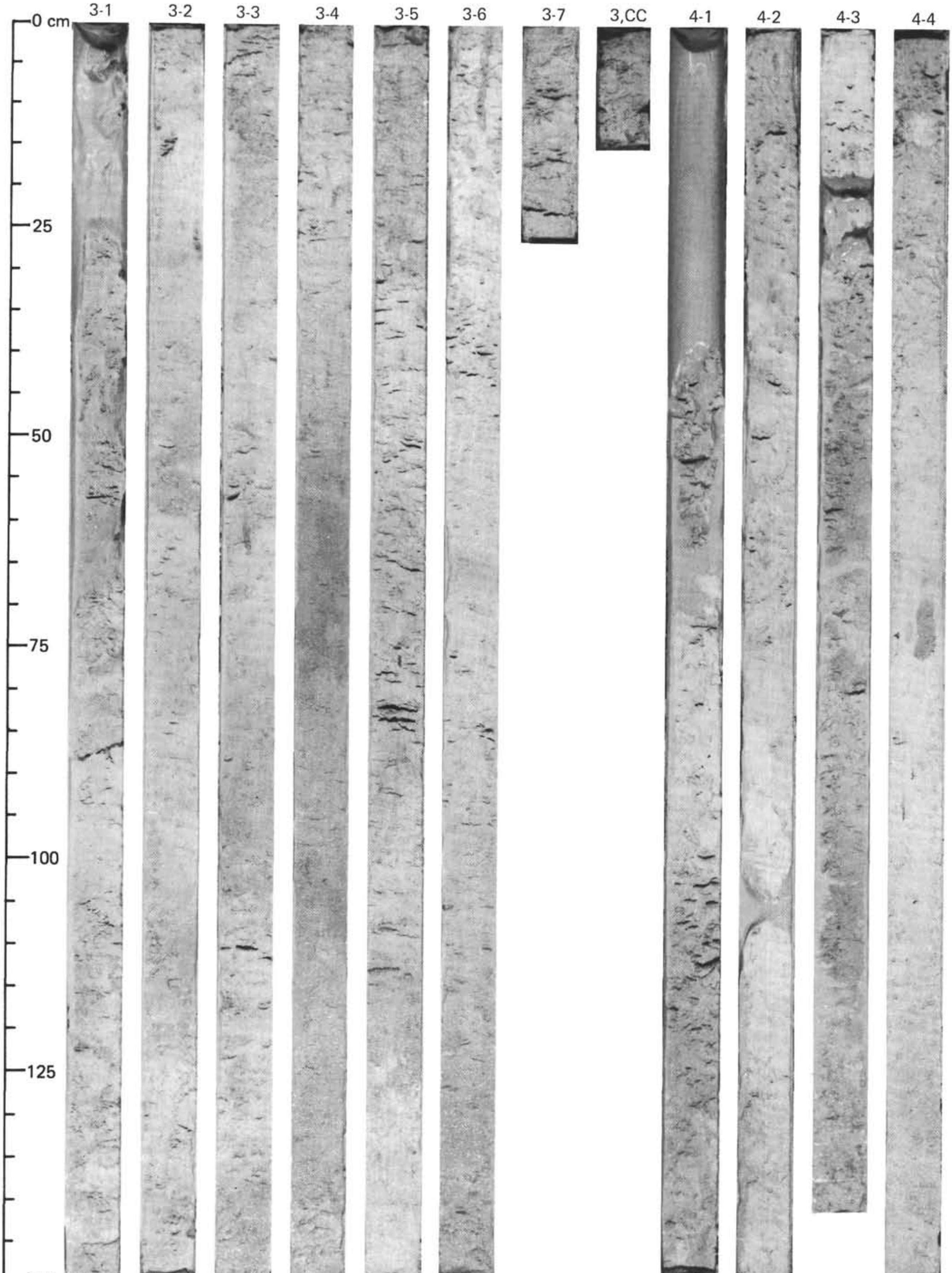
0 cm
25
50
75
100
125
150
3-1
3-2
3-3
3-4
3-5
3-6
3-7
3,CC
4-1
4-2
4-3
4-4

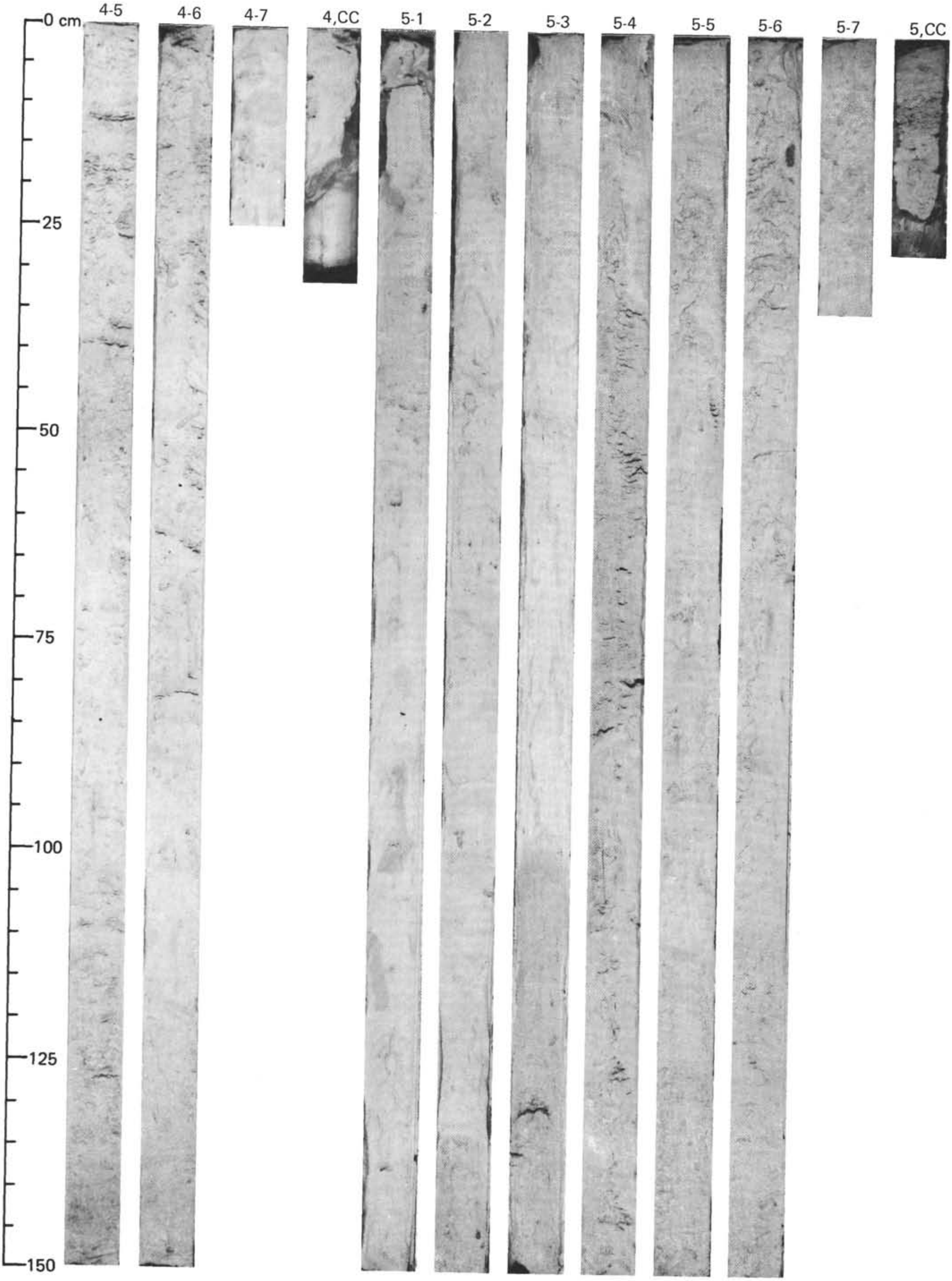
0 cm
25
50
75
100
125
150
4-5
4-6
4-7
4,CC
5-1
5-2
5-3
5-4
5-5
5-6
5-7
5,CC

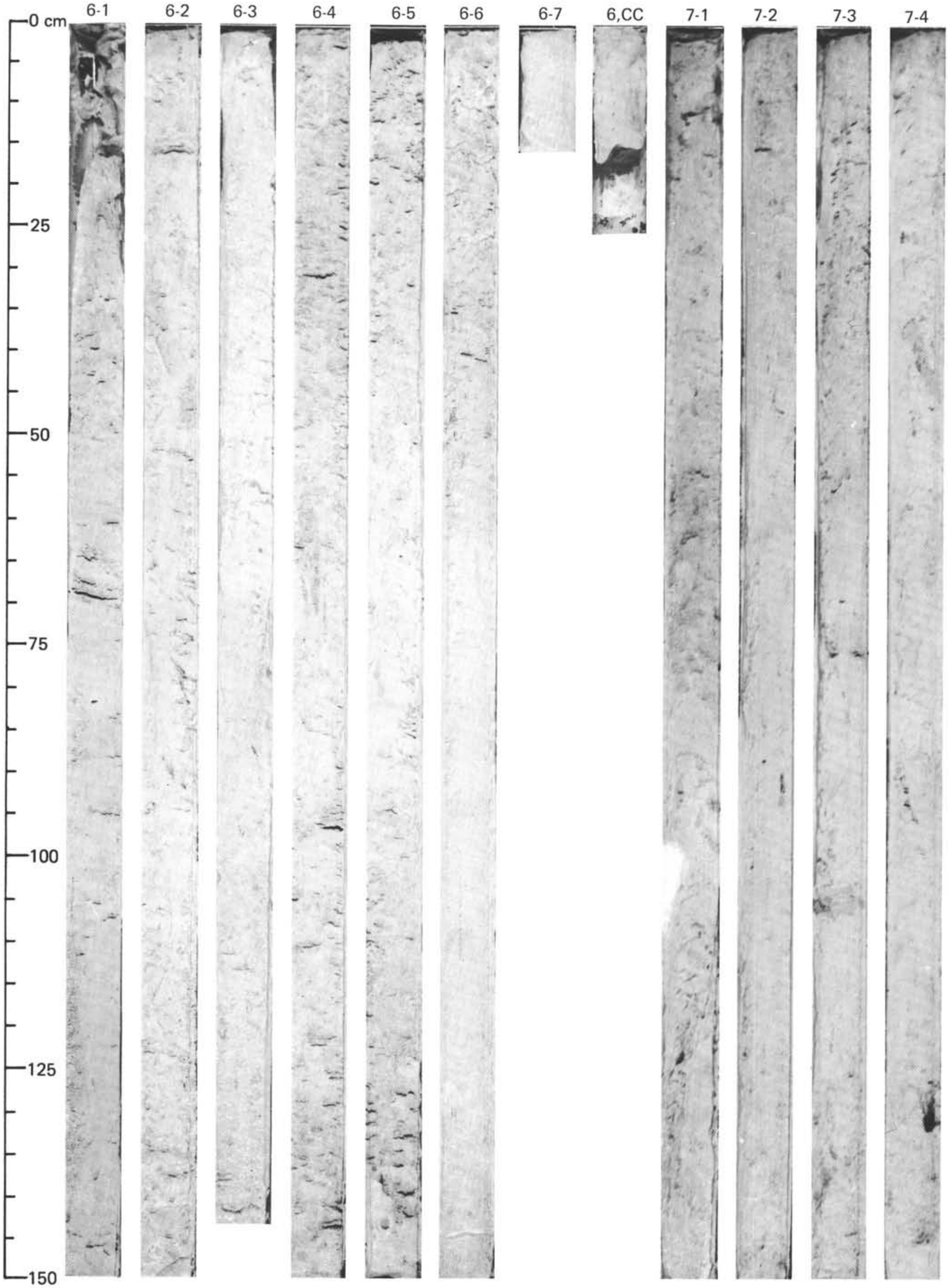
0 cm
25
50
75
100
125
150
6-1
6-2
6-3
6-4
6-5
6-6
6-7
6,CC
7-1
7-2
7-3
7-4

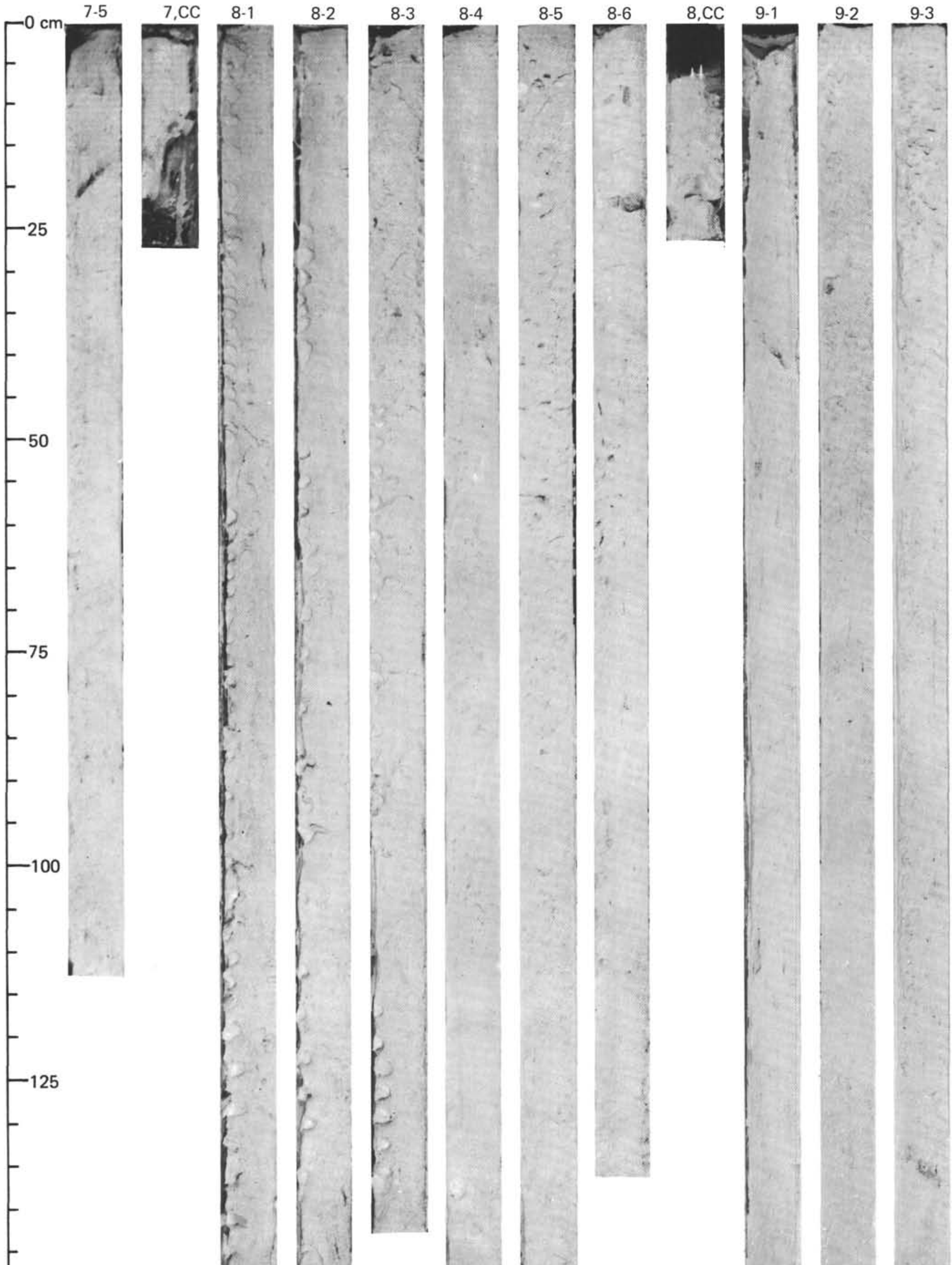
7-5
7,CC
8-1
8-2
8-3
8-4
8-5
8-6
8,CC
9-1
9-2
9-3
0 cm
25
50
75
100
125
150

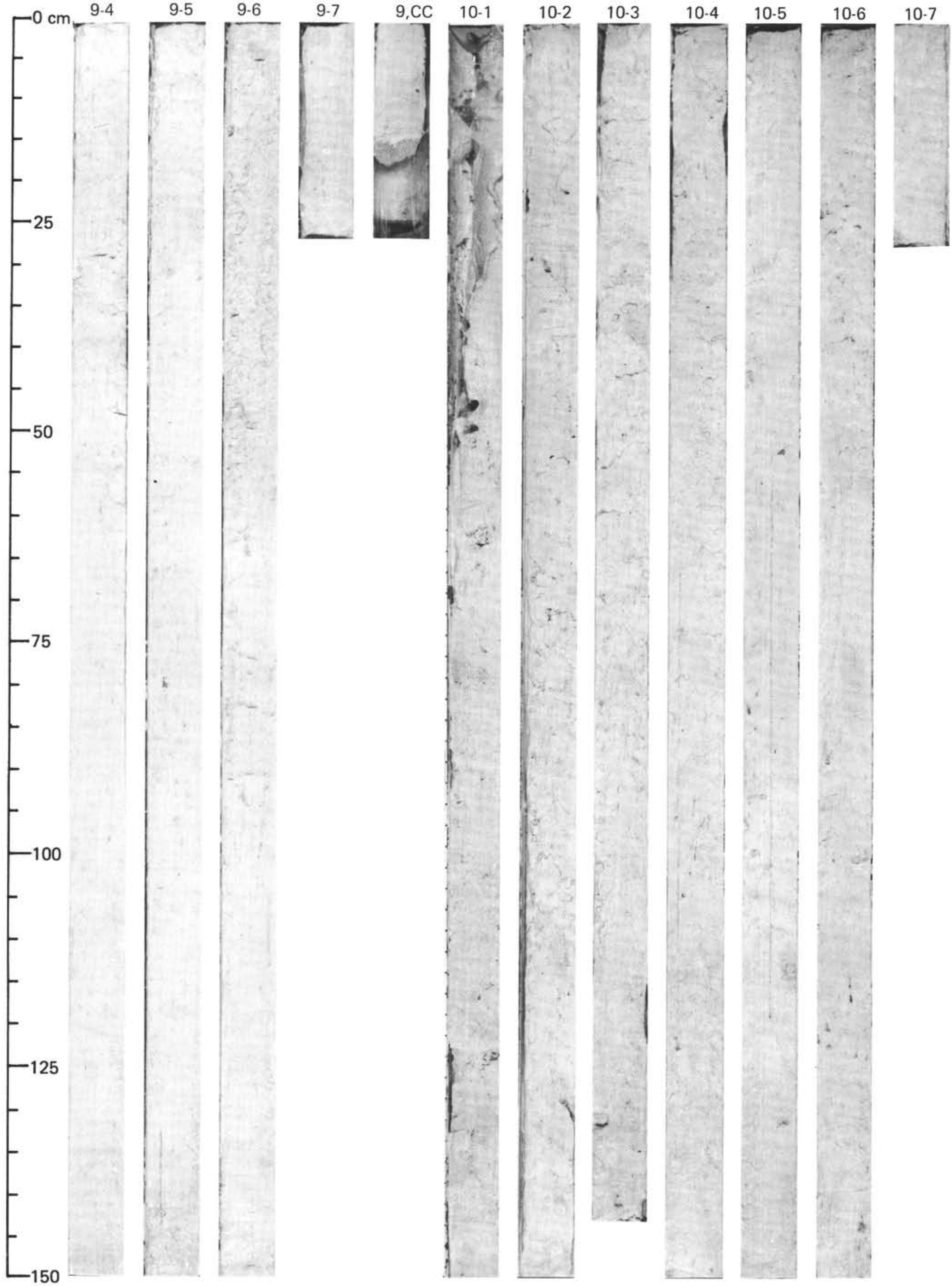
0 cm
25
50
75
100
125
150
9-4
9-5
9-6
9-7
9,CC
10-1
10-2
10-3
10-4
10-5
10-6
10-7

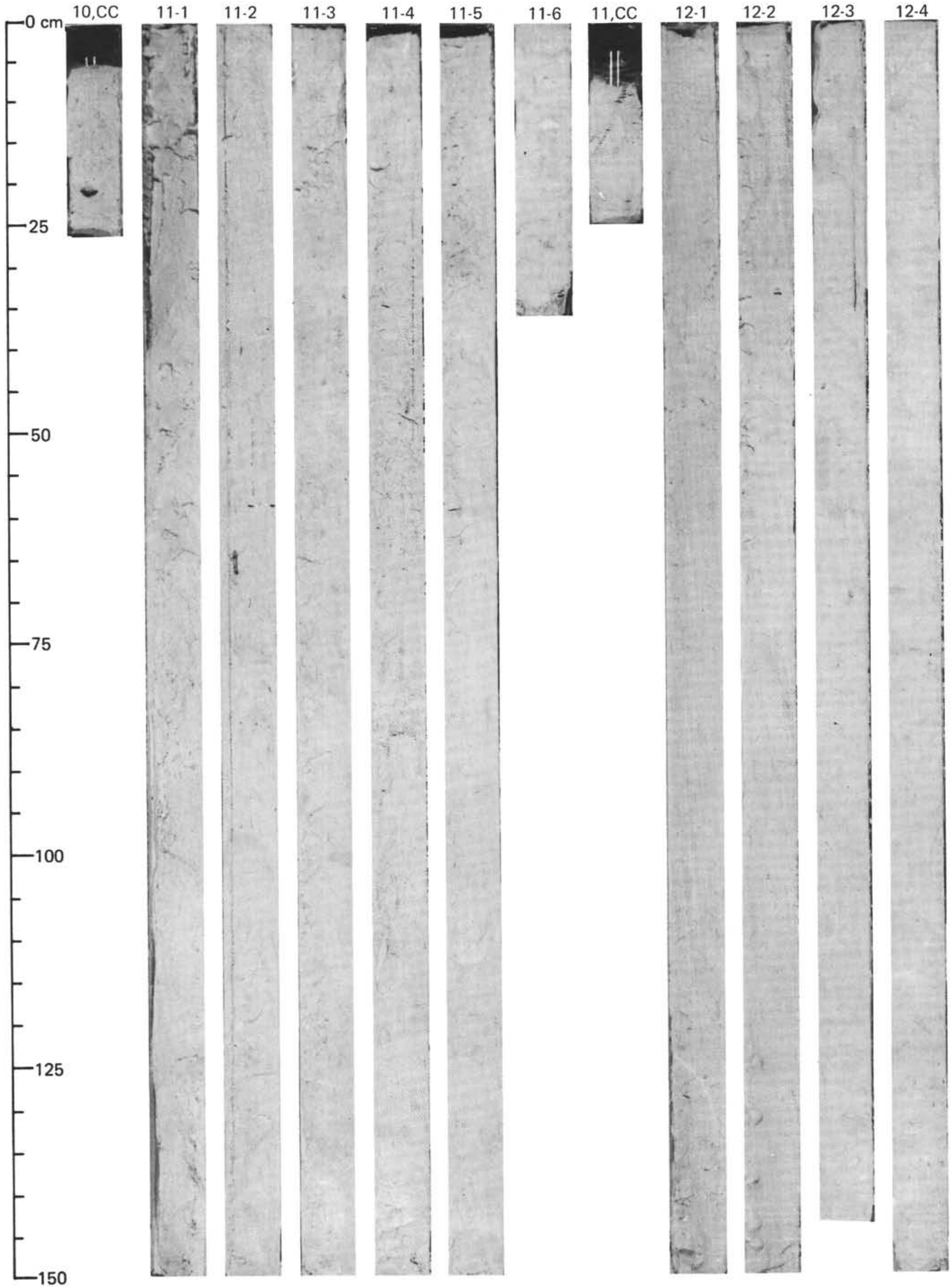
0 cm
25
50
75
100
125
150
10,CC
11-1
11-2
11-3
11-4
11-5
11-6
11,CC
12-1
12-2
12-3
12-4

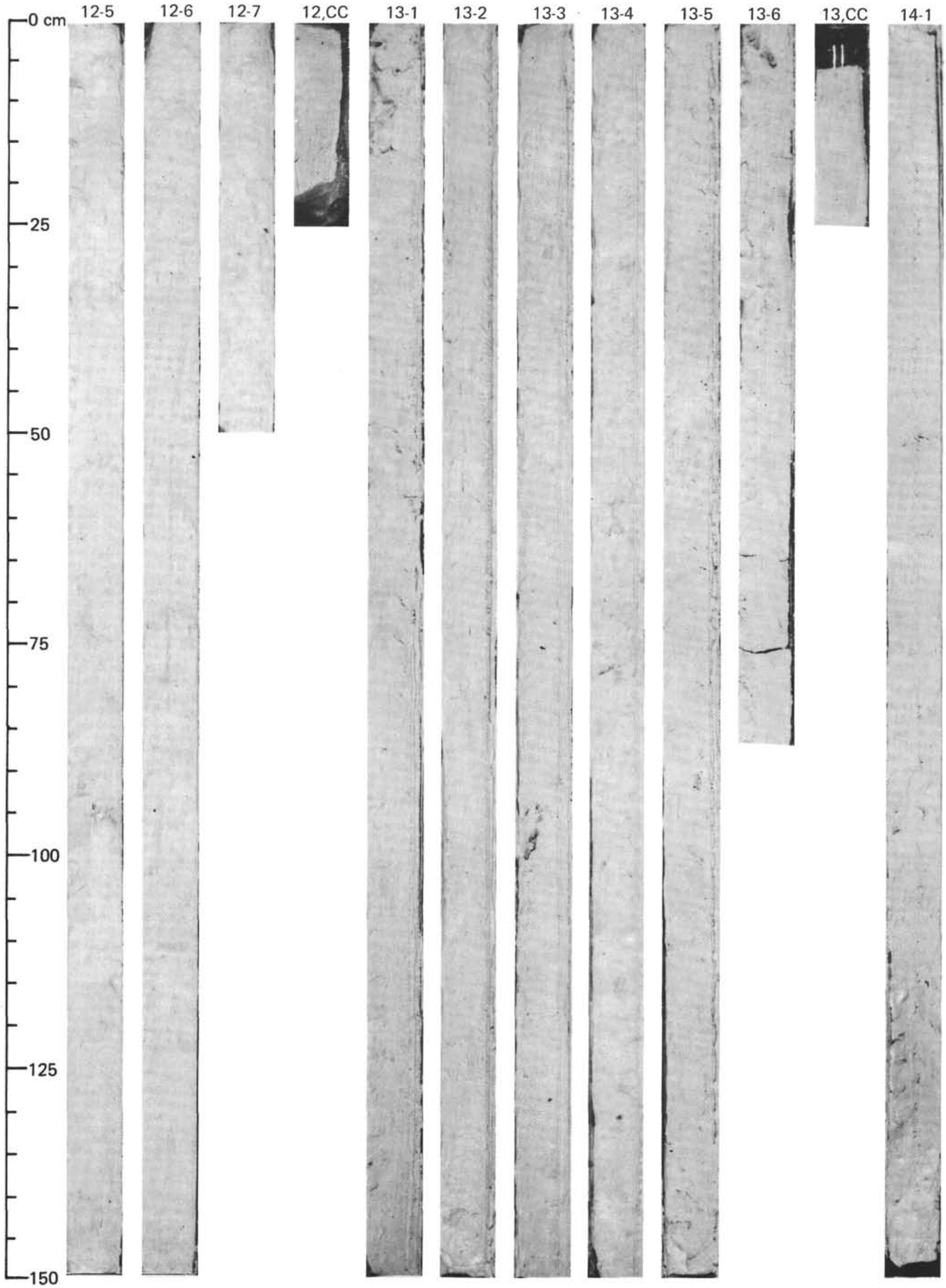
12-5
12-6
12-7
12,CC
13-1
13-2
13-3
13-4
13-5
13-6
13,CC
14-1
0 cm
25
50
75
100
125
150

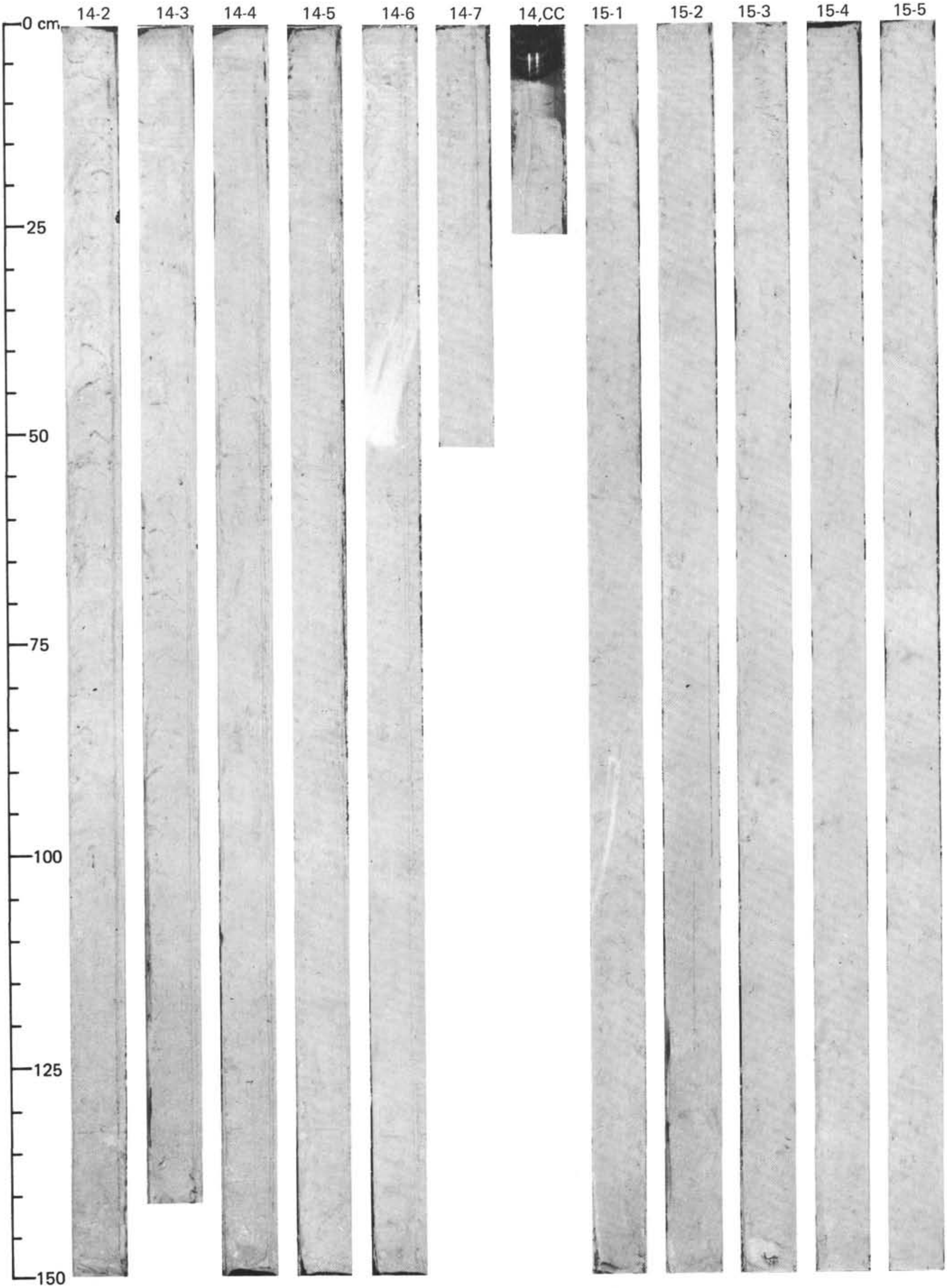
0 cm
25
50
75
100
125
150
14-2
14-3
14-4
14-5
14-6
14-7
14,CC
15-1
15-2
15-3
15-4
15-5

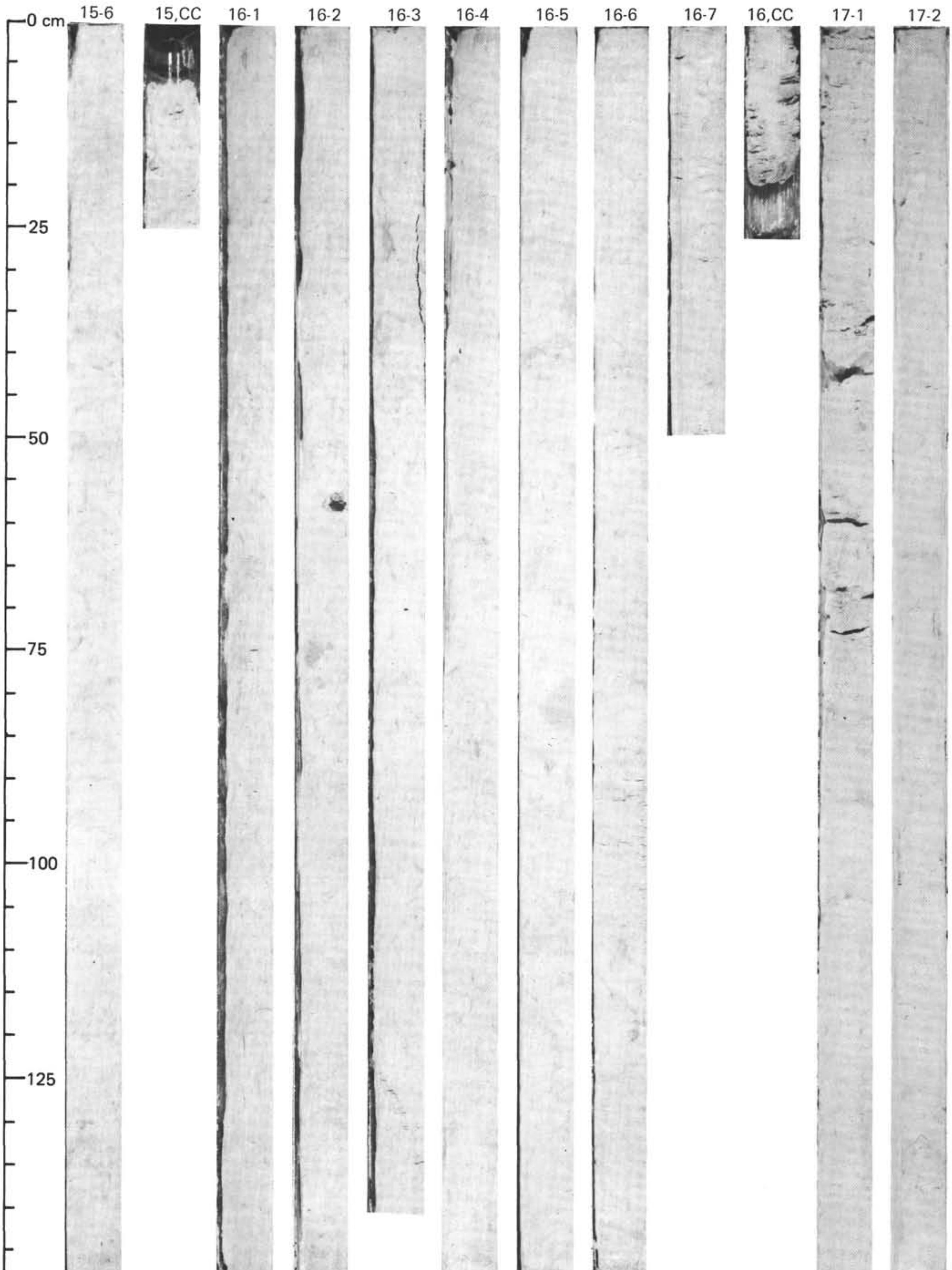
0 cm
25
50
75
100
125
150
15-6
15,CC
16-1
16-2
16-3
16-4
16-5
16-6
16-7
16,CC
17-1
17-2

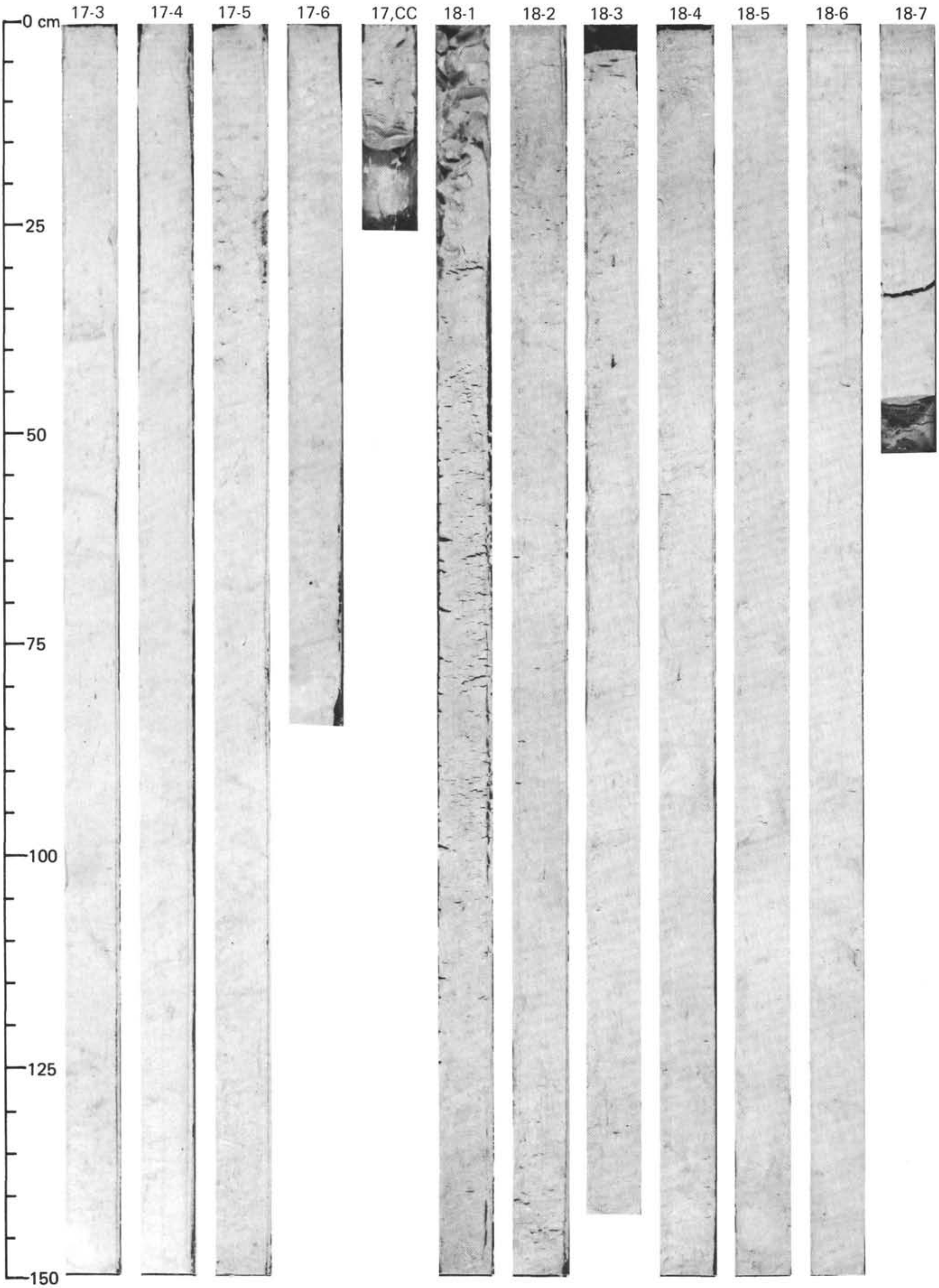
17-3
17-4
17-5
17-6
17,CC
18-1
18-2
18-3
18-4
18-5
18-6
18-7
0 cm
25
50
75
100
125
150

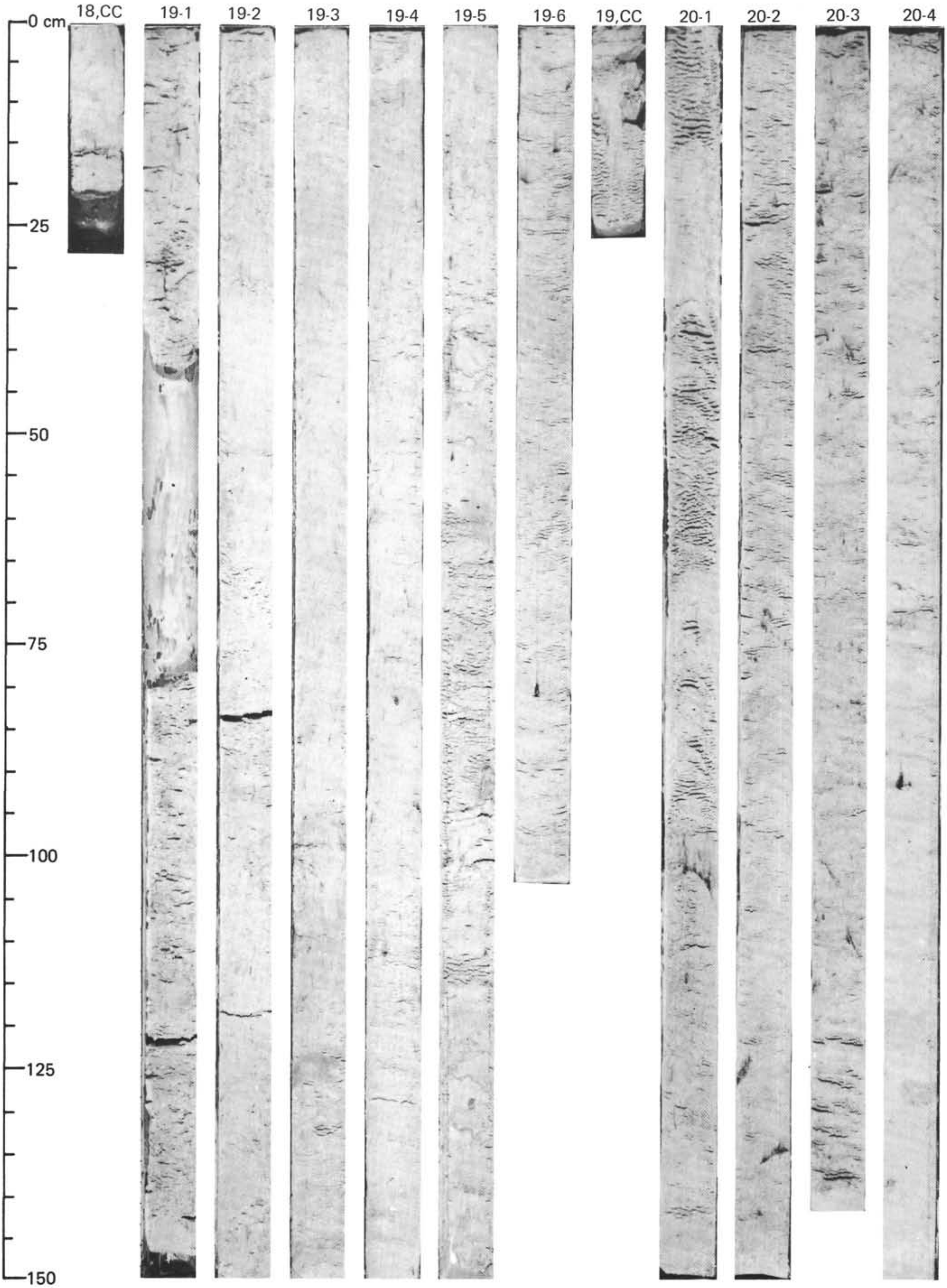
0 cm
25
50
75
100
125
150
18,CC
19-1
19-2
19-3
19-4
19-5
19-6
19,CC
20-1
20-2
20-3
20-4

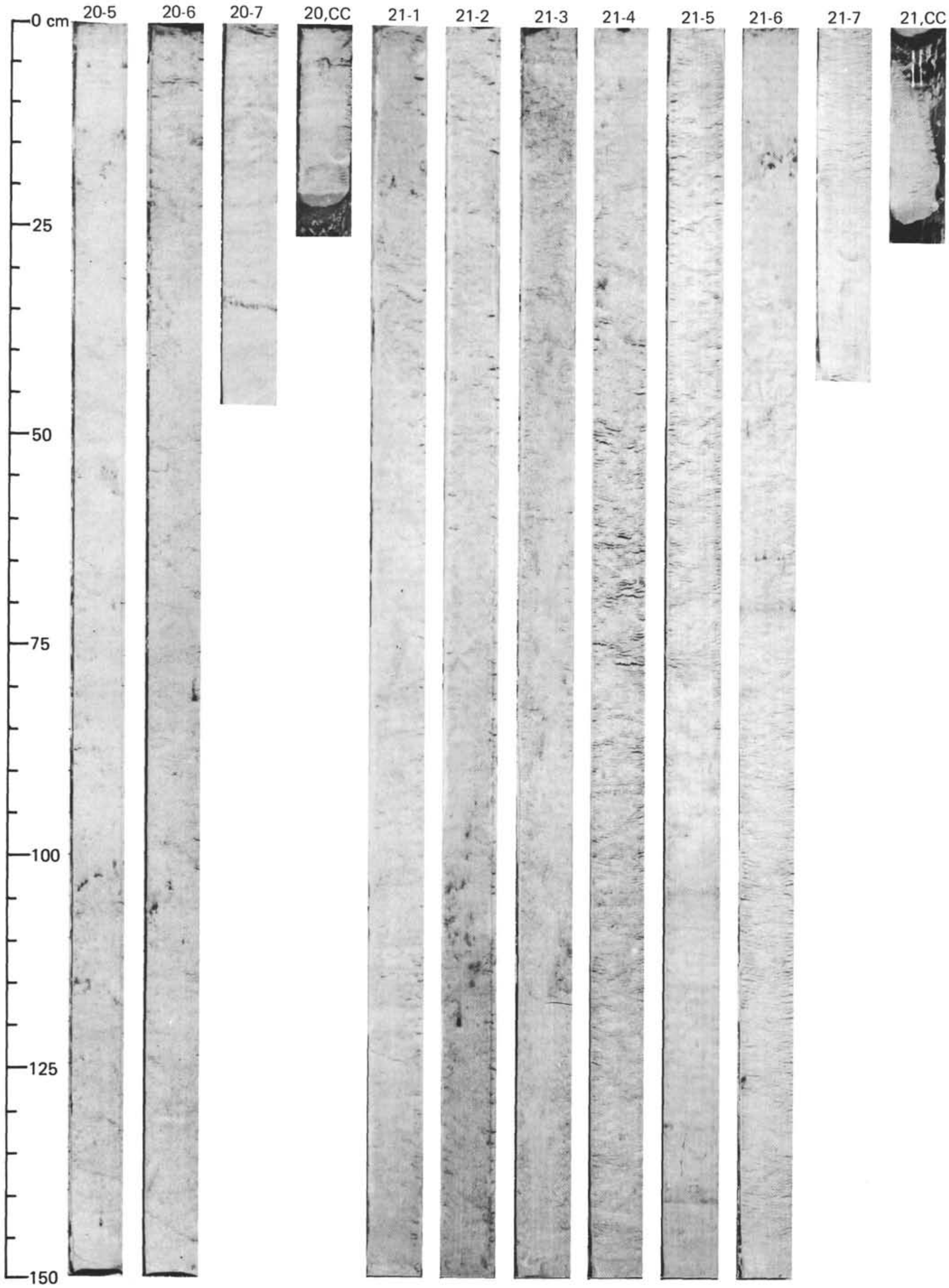
0 cm
25
50
75
100
125
150
20-5
20-6
20-7
20,CC
21-1
21-2
21-3
21-4
21-5
21-6
21-7
21,CC

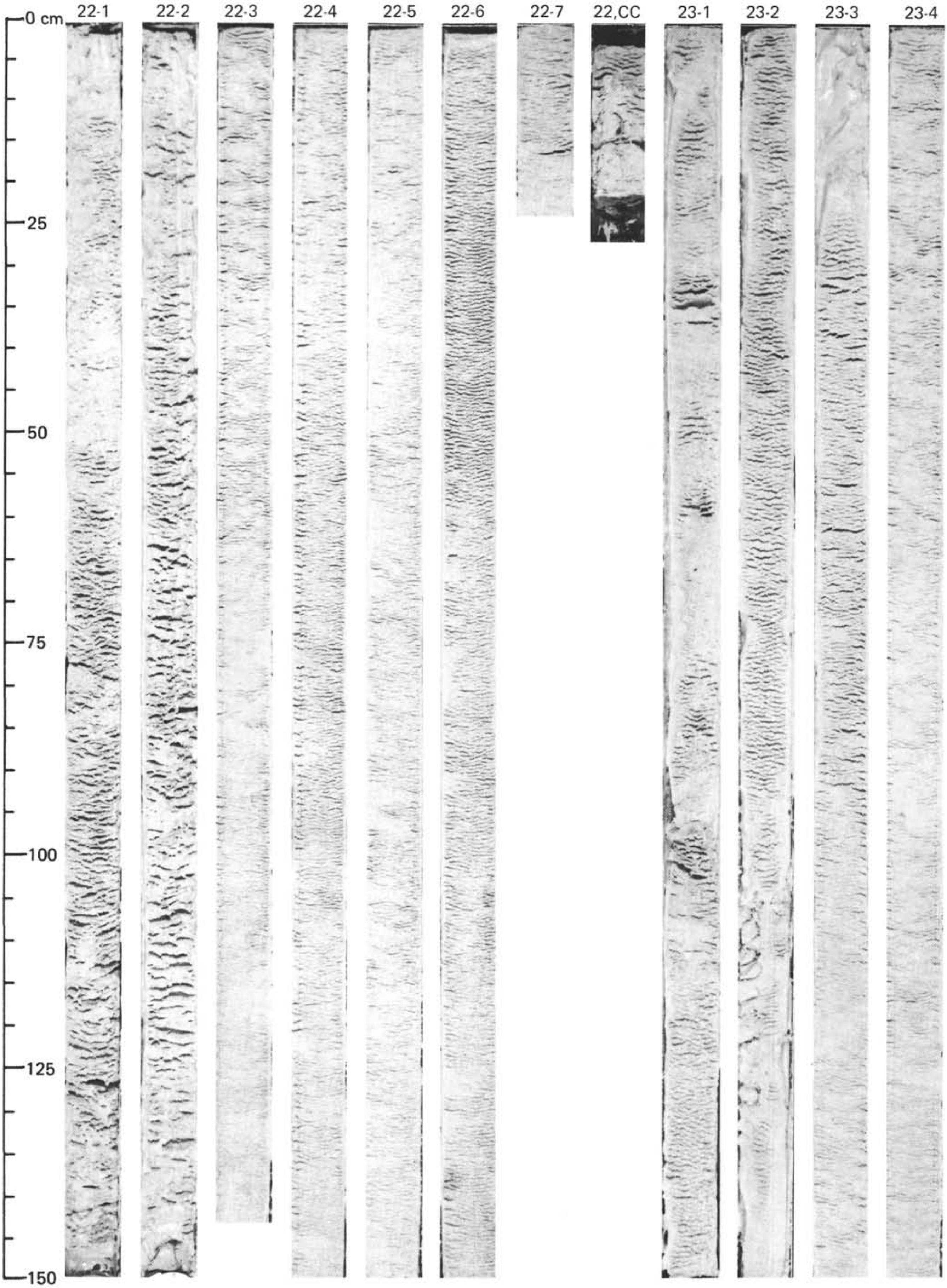
0 cm
25
50
75
100
125
150
22-1
22-2
22-3
22-4
22-5
22-6
22-7
22,CC
23-1
23-2
23-3
23-4

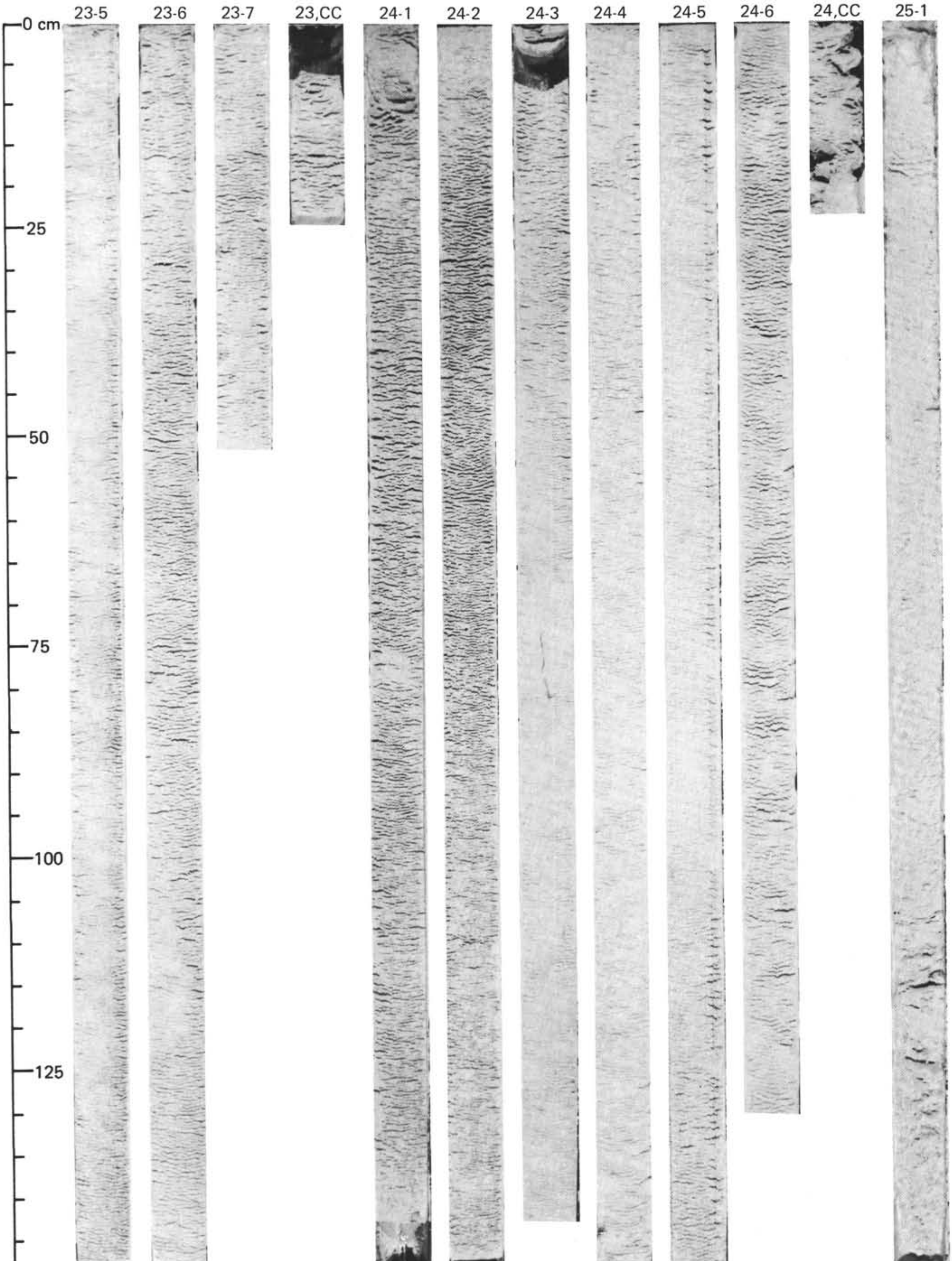
0 cm
25
50
75
100
125
150
23-5
23-6
23-7
23,CC
24-1
24-2
24-3
24-4
24-5
24-6
24,CC
25-1

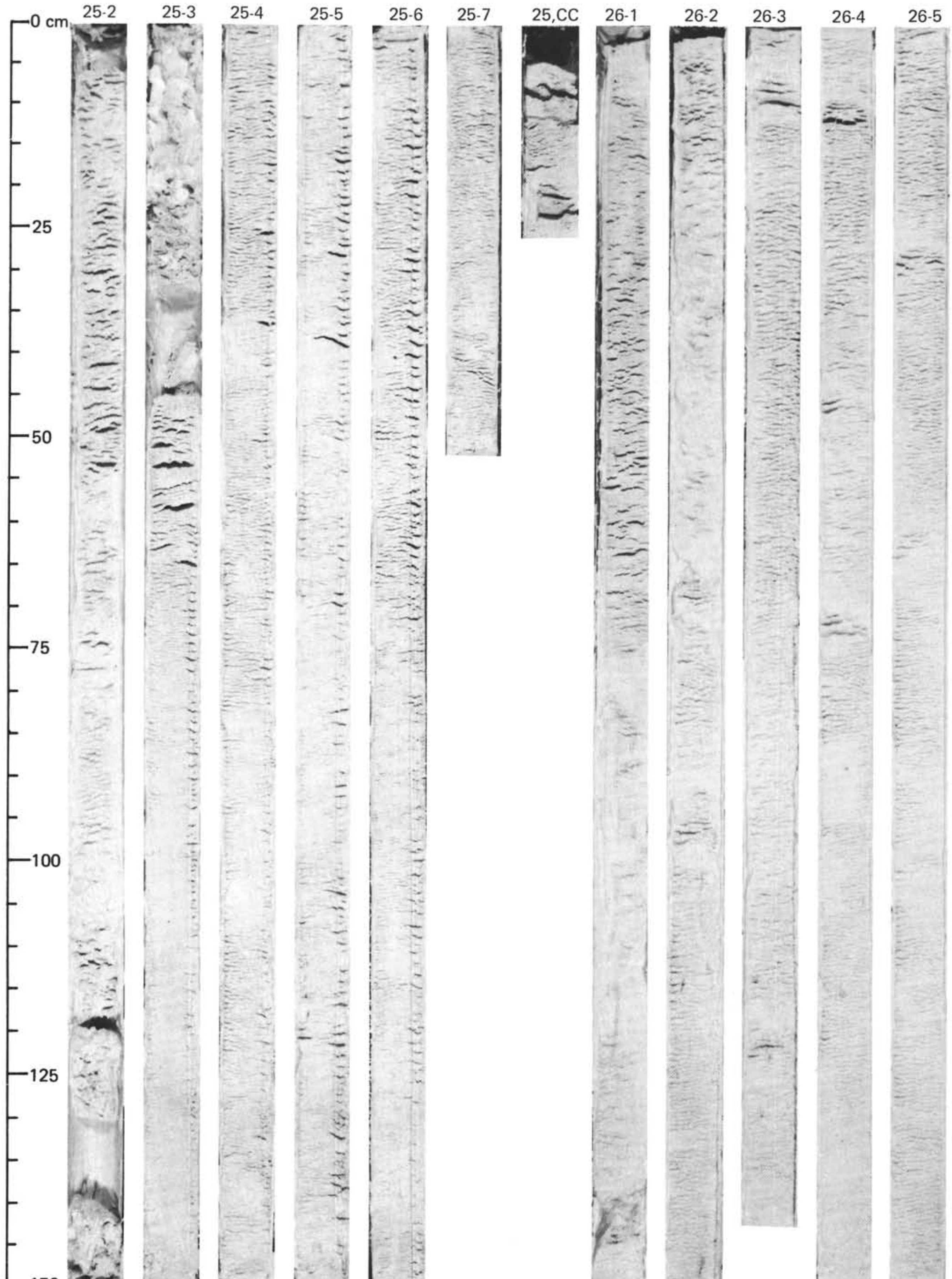
25-2
25-3
25-4
25-5
25-6
25-7
25,CC
26-1
26-2
26-3
26-4
26-5
0 cm
25
50
75
100
125
150

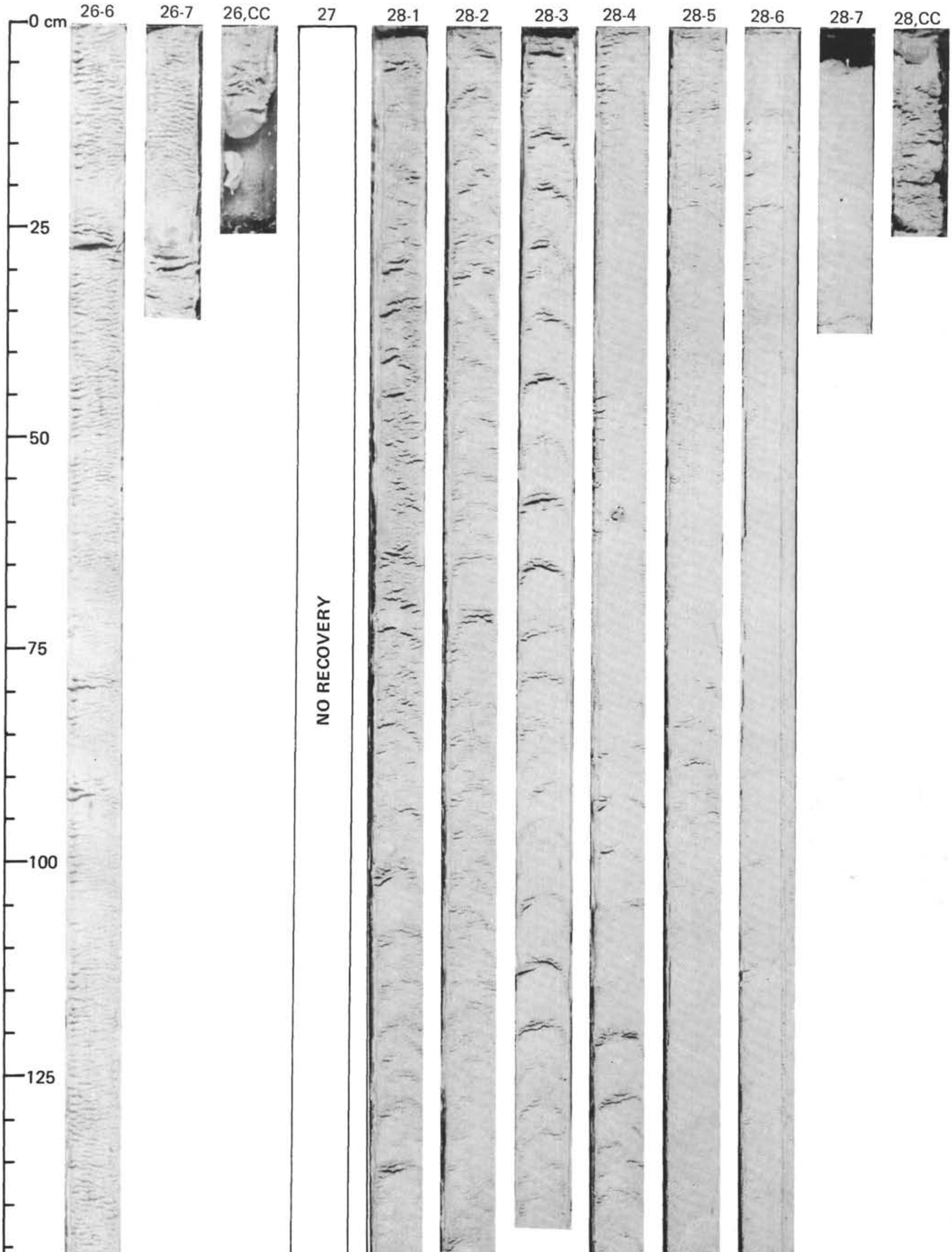
0 cm
25
50
75
100
125
150
26-6
26-7
26,CC
27
28-1
28-2
28-3
28-4
28-5
28-6
28-7
28,CC
NO RECOVERY

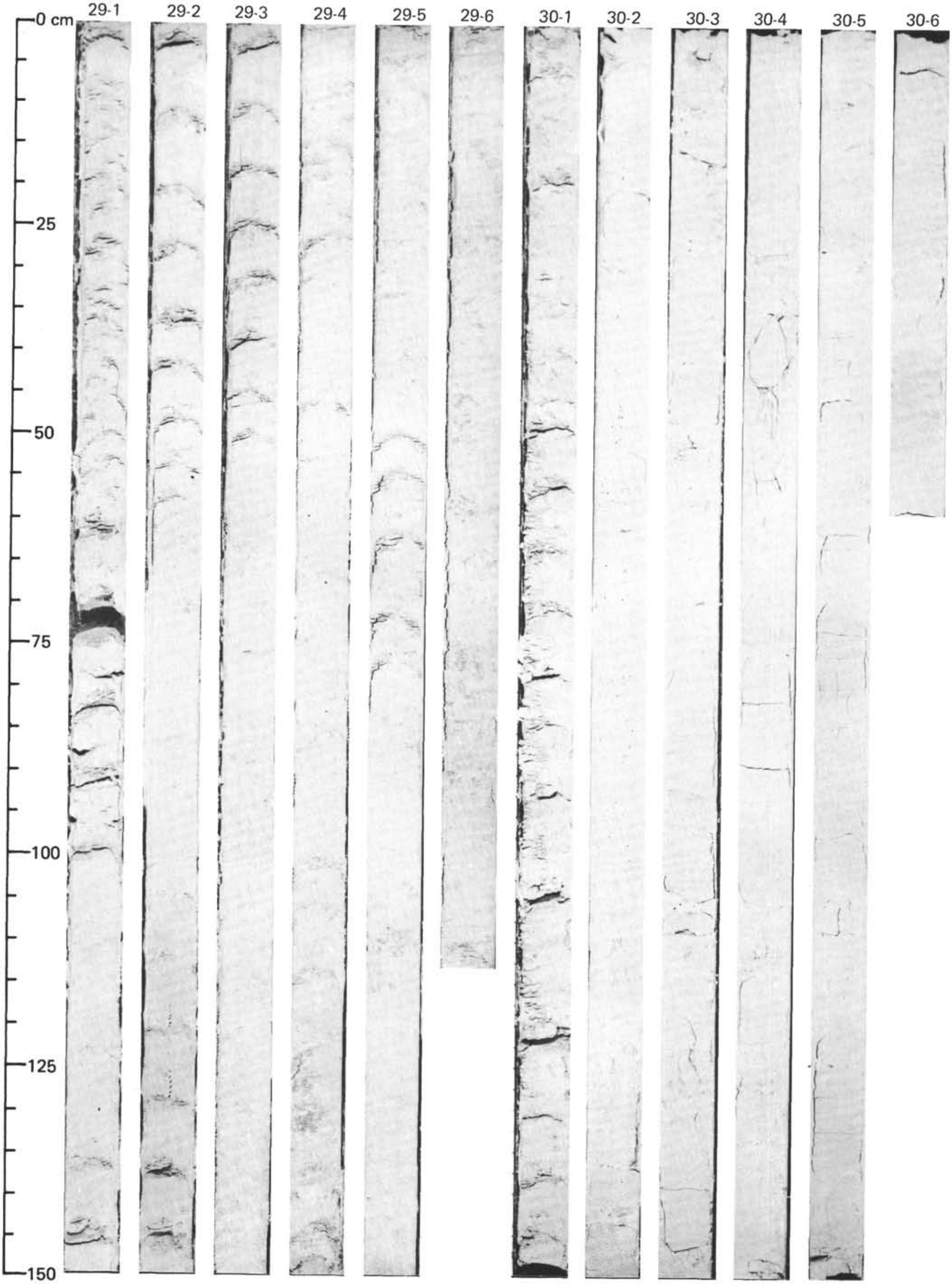
29-1
29-2
29-3
29-4
29-5
29-6
30-1
30-2
30-3
30-4
30-5
30-6
0 cm
25
50
75
100
125
150

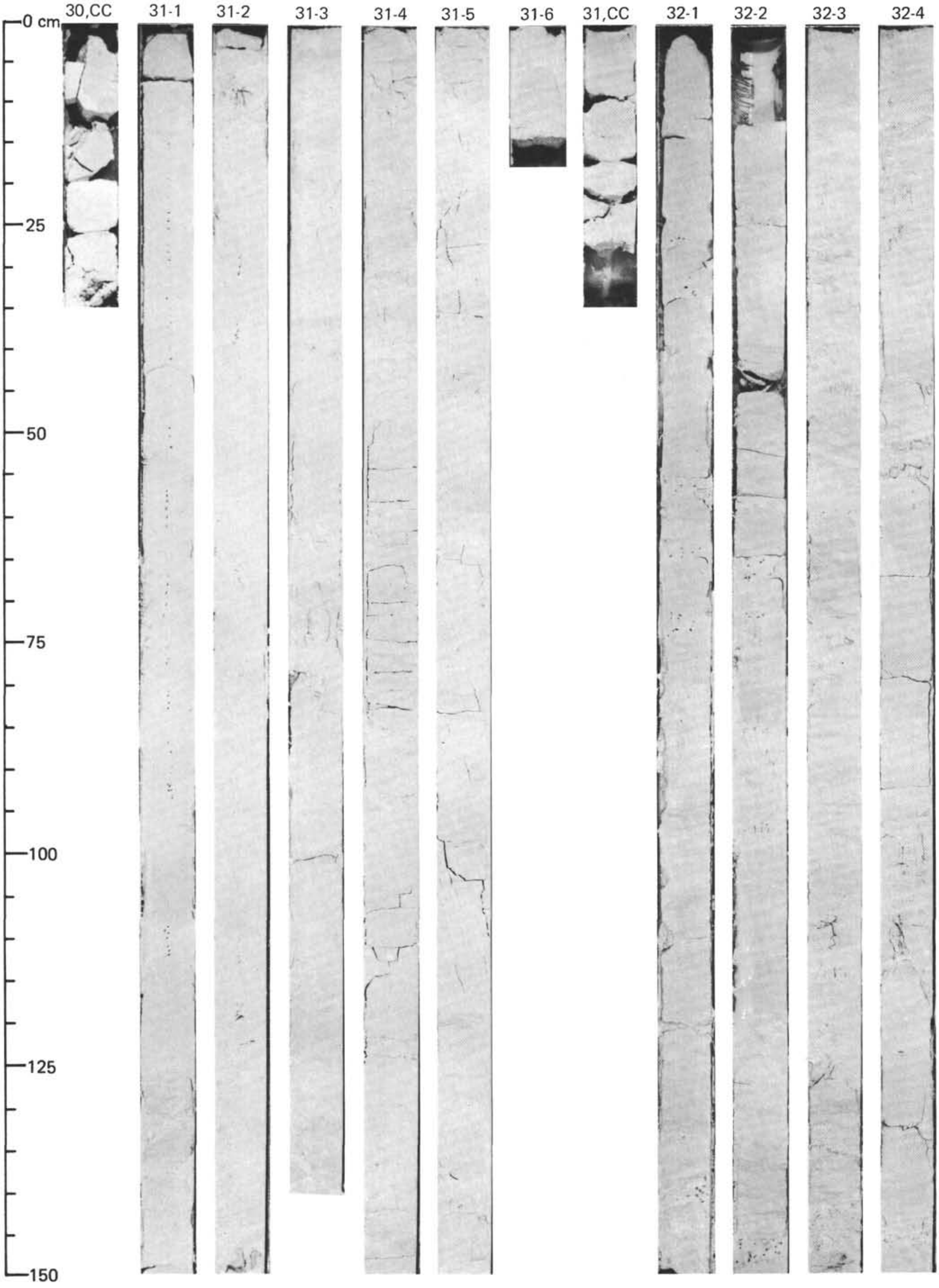

0 cm
25
50
75
100
125
150
30,CC
31-1
31-2
31-3
31-4
31-5
31-6
31,CC
32-1
32-2
32-3
32-4

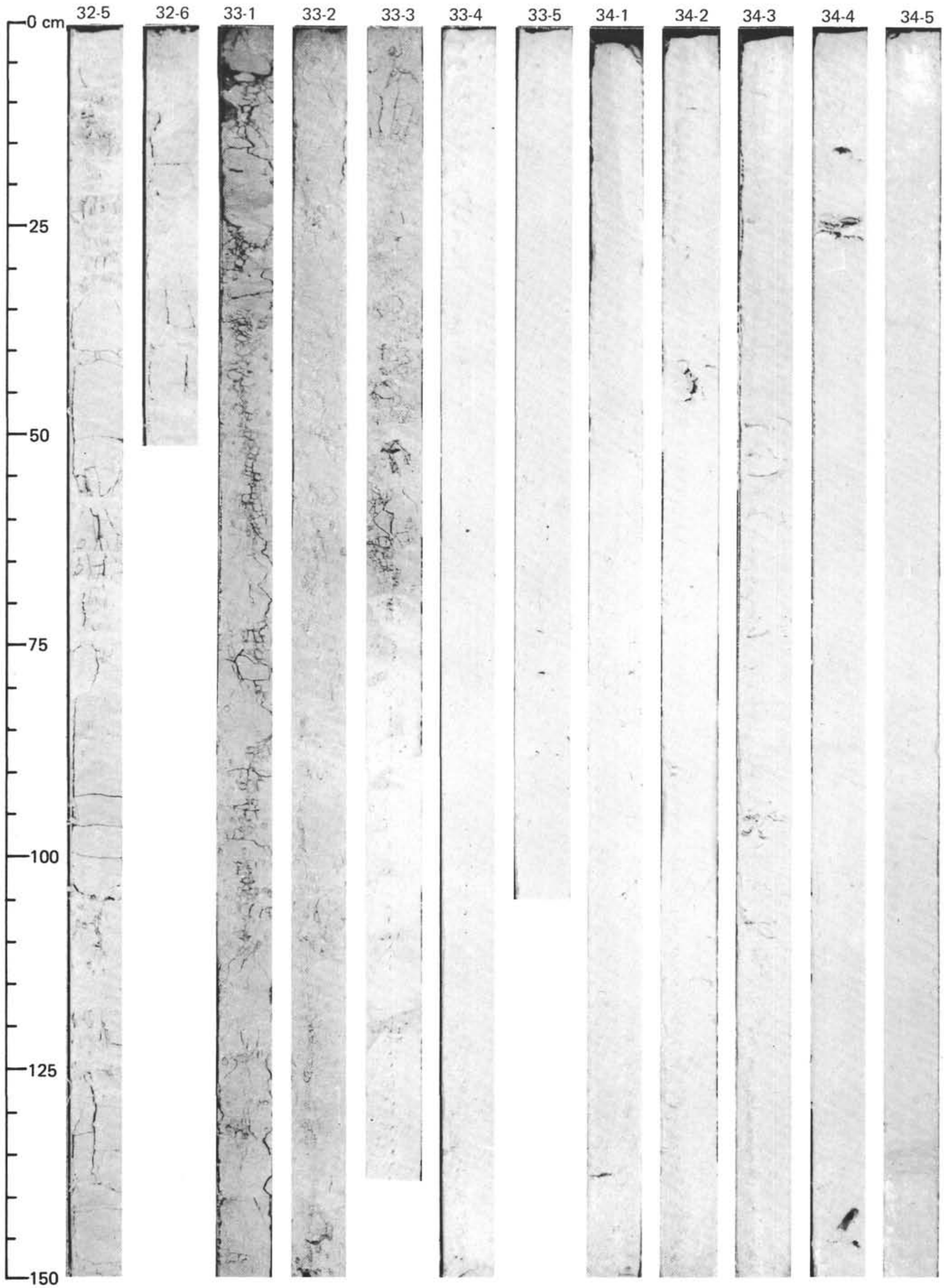
0 cm
25
50
75
100
125
150
32-5
32-6
33-1
33-2
33-3
33-4
33-5
34-1
34-2
34-3
34-4
34-5

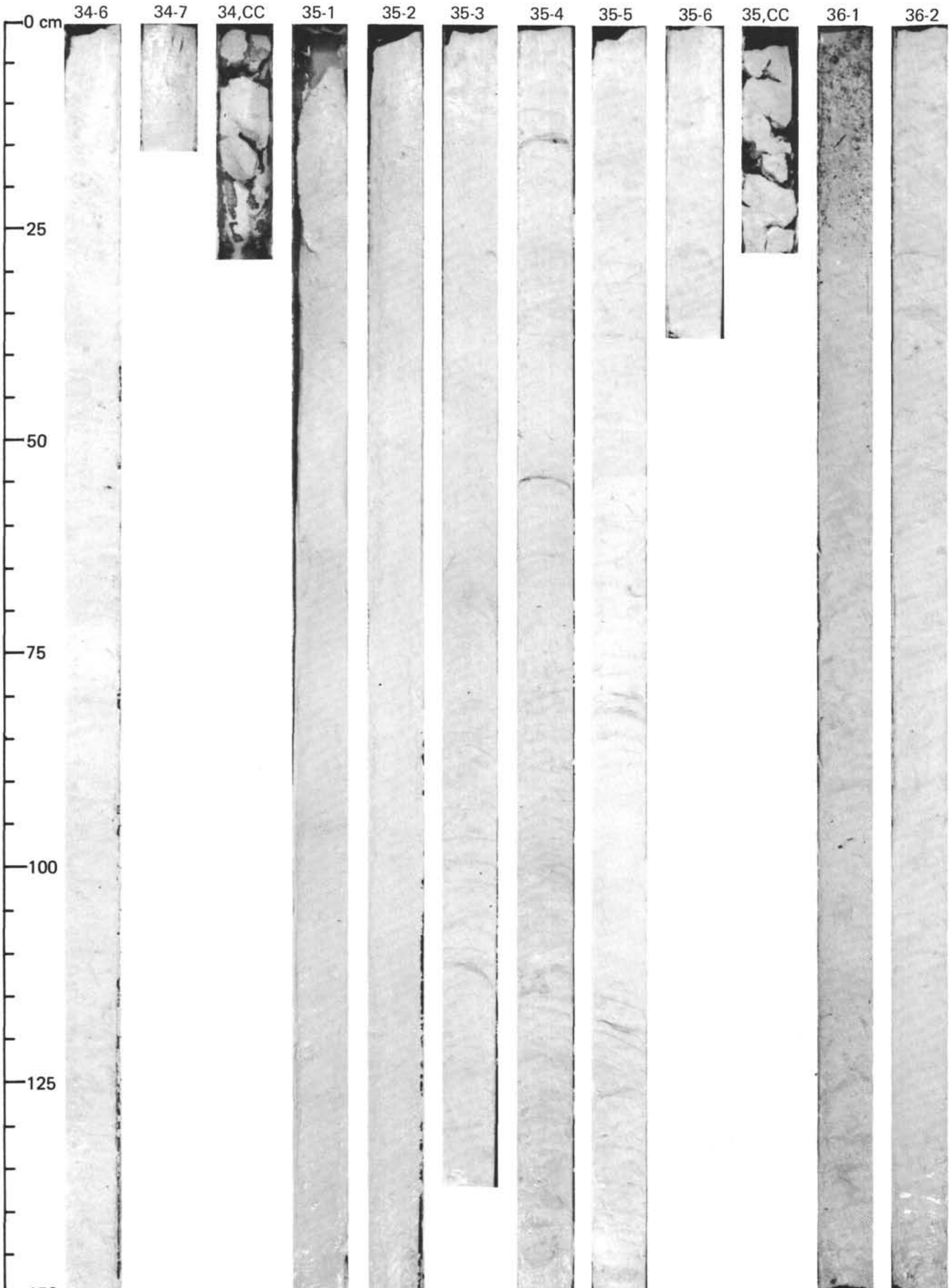
34-6
34-7
34,CC
35-1
35-2
35-3
35-4
35-5
35-6
35,CC
36-1
36-2
0 cm
25
50
75
100
125
150

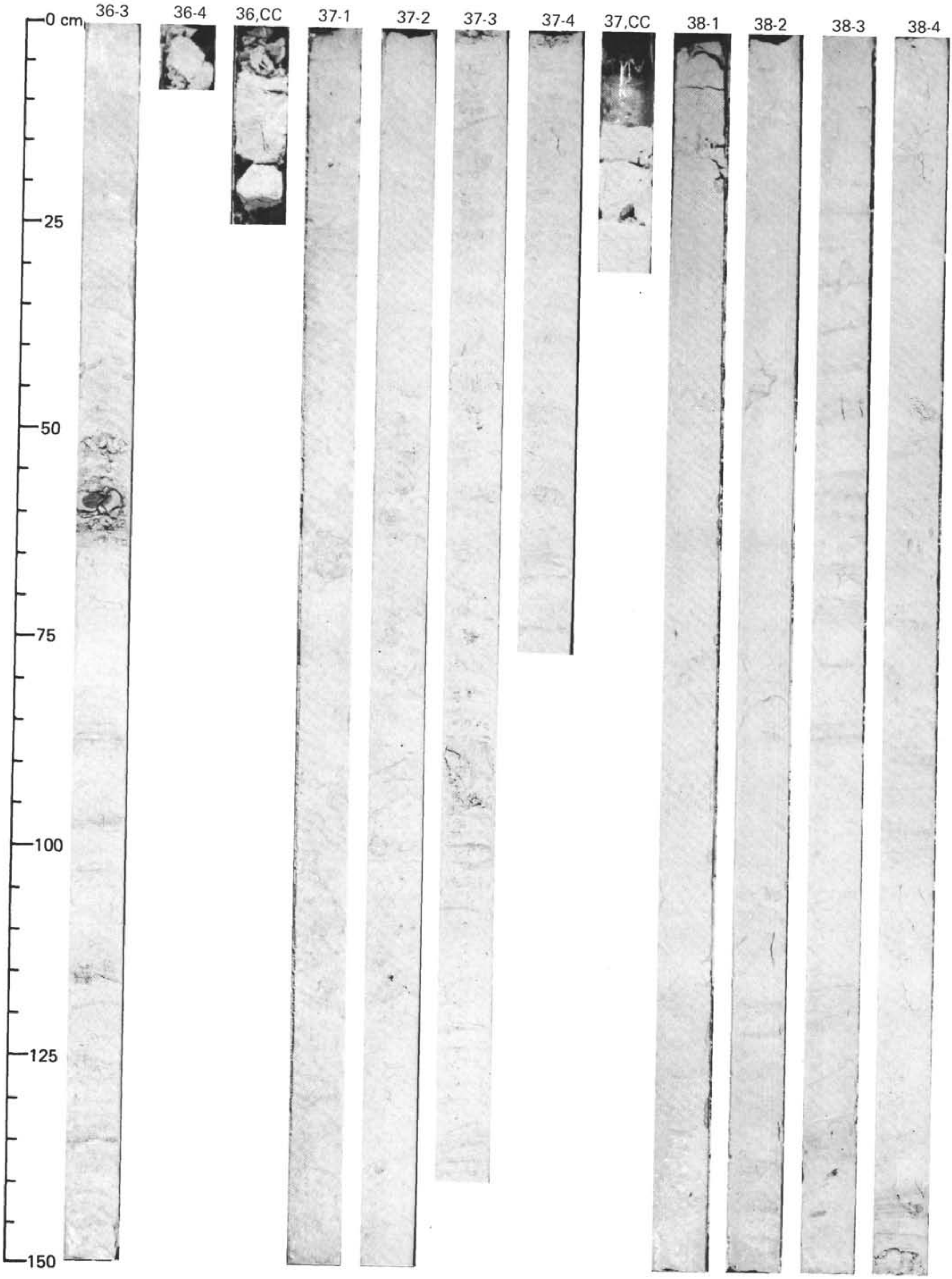
0 cm
25
50
75
100
125
150
36-3
36-4
36,CC
37-1
37-2
37-3
37-4
37,CC
38-1
38-2
38-3
38-4

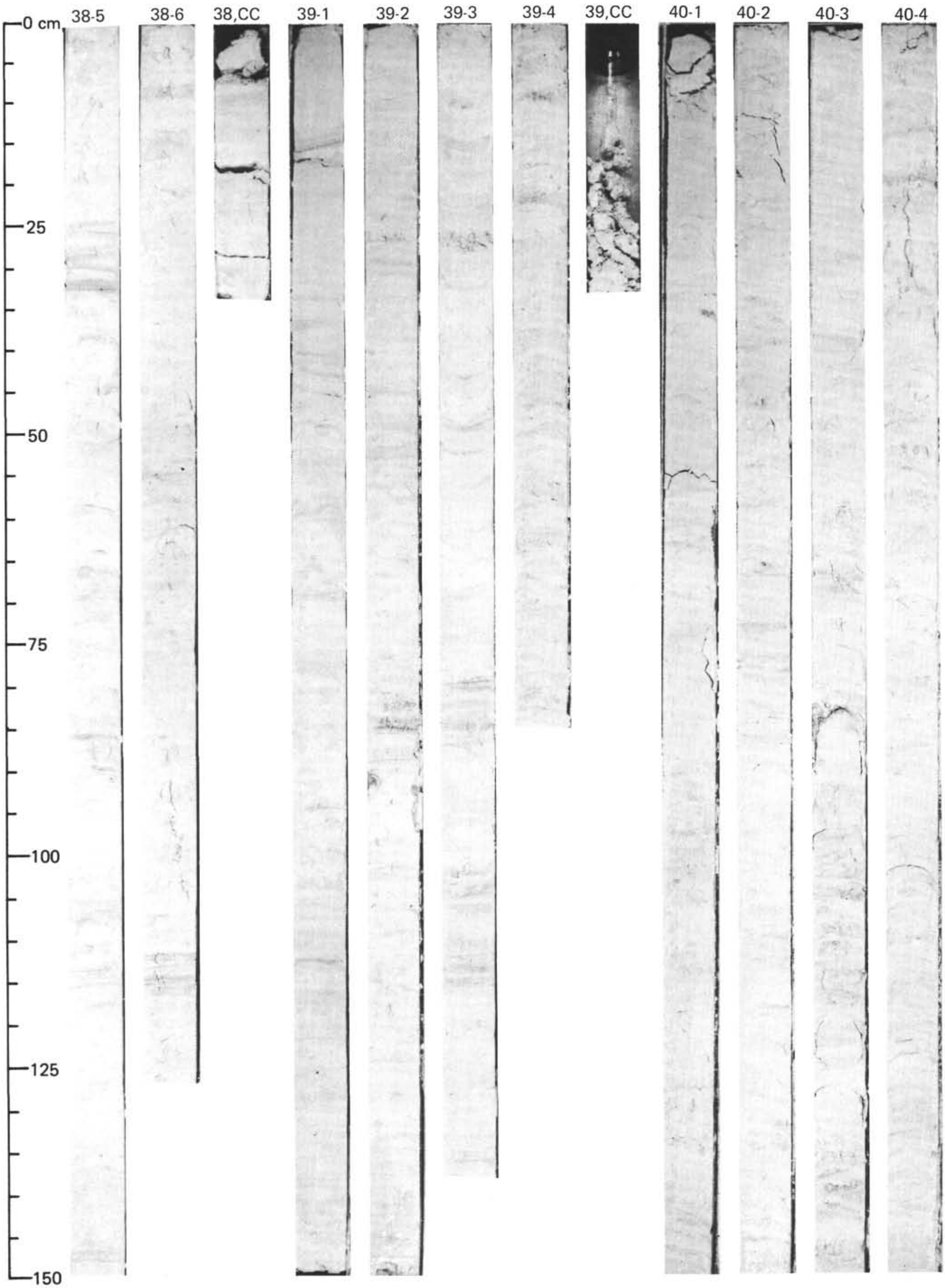
0 cm
25
50
75
100
125
150
38-5
38-6
38,CC
39-1
39-2
39-3
39-4
39,CC
40-1
40-2
40-3
40-4

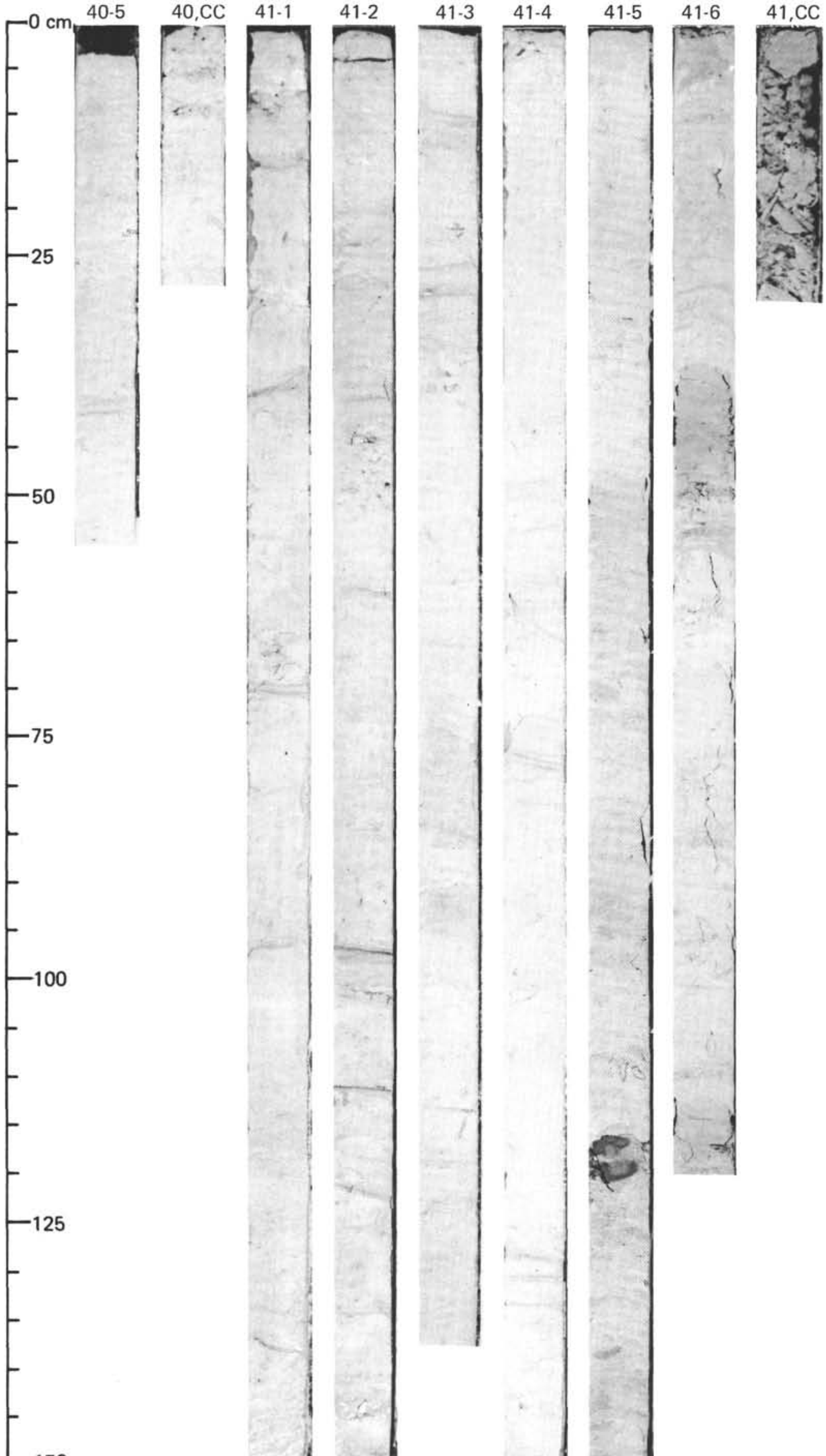
0 cm
25
50
75
100
125
150
40-5
40,CC
41-1
41-2
41-3
41-4
41-5
41-6
41,CC